

## **Sensible and Latent Energy Loading on a Refrigerator During Open Door Conditions**

M. R. Laleman, T. A. Newell, and A. M. Clausing

ACRC TR-20

May 1992

*For additional information:*

Air Conditioning and Refrigeration Center  
University of Illinois  
Mechanical & Industrial Engineering Dept.  
1206 West Green Street  
Urbana, IL 61801  
(217) 333-3115

*Prepared as part of ACRC Project 11  
Sensible and Latent Energy Loading on a  
Refrigerator During Open Door Conditions  
T. A. Newell, Principal Investigator*

*The Air Conditioning and Refrigeration Center was founded in 1988 with a grant from the estate of Richard W. Kritzer, the founder of Peerless of America Inc. A State of Illinois Technology Challenge Grant helped build the laboratory facilities. The ACRC receives continuing support from the Richard W. Kritzer Endowment and the National Science Foundation. The following organizations have also become sponsors of the Center.*

Acustar Division of Chrysler  
Allied-Signal, Inc.  
Amana Refrigeration, Inc.  
Bergstrom Manufacturing Co.  
Caterpillar, Inc.  
E. I. du Pont de Nemours & Co.  
Electric Power Research Institute  
Ford Motor Company  
General Electric Company  
Harrison Division of GM  
ICI Americas, Inc.  
Johnson Controls, Inc.  
Modine Manufacturing Co.  
Peerless of America, Inc.  
Environmental Protection Agency  
U. S. Army CERL  
Whirlpool Corporation

*For additional information:*

*Air Conditioning & Refrigeration Center  
Mechanical & Industrial Engineering Dept.  
University of Illinois  
1206 West Green Street  
Urbana IL 61801*

*217 333 3115*

**SENSIBLE AND LATENT ENERGY LOADING ON A REFRIGERATOR  
DURING OPEN DOOR CONDITIONS**

**Mark Robert Laleman, M.S.**

**Department of Mechanical and Industrial Engineering  
University of Illinois at Urbana-Champaign, 1992**

**Abstract**

This thesis examines the modes of energy loss incurred when the door of a refrigerator is opened. An analysis is done on the fresh food compartment of a 20 cu. ft. refrigerator unit, which is instrumented with aluminum calorimeters. Heat transfer coefficients are determined for the fresh food walls through the lumped capacitance analysis. The open door tests are run under a variety of humidity conditions and compartmental temperatures. The coefficients are separated into latent and sensible values through the heat and mass transfer analogy. Using these coefficients, estimates are made of the total load imposed on the refrigerator for a certain number of door openings. Rayleigh and Nusselt numbers are also calculated and correlated. A shelf is also inserted into the fresh food compartment, and effects on heat transfer coefficients and correlations are discussed.



## Table of Contents

	Page
List of Tables.....	vi
List of Figures.....	vii
1. Introduction.....	1
1.1 Motives for Investigation.....	1
1.2 Project Goals.....	2
2. Literature Review .....	3
3. Experimental Apparatus and Procedure.....	7
3.1 The Transient Calorimeter Model.....	7
3.2 Calorimeter Installation and Testing.....	9
3.3 Governing Equations and Mass Transfer Analogy.....	17
3.4 Data Reduction Procedure.....	22
4. Experimental Results and Analysis .....	30
4.1 Temperature Data .....	30
4.2 Heat Transfer Coefficients.....	35
4.2.1 Empty Compartment Coefficients.....	35
4.2.2 Compartment with One Shelf .....	43
4.3 Energy Calculations .....	51
4.4 Nusselt and Rayleigh Numbers .....	54
5. Conclusions .....	62
References.....	64
Appendix A: Data Reduction Routine.....	64
Appendix B: Data Acquisition and Control System .....	81
Appendix C: Utility Programs.....	83
C.1 ALPT(Aluminum properties subroutine).....	83
C.2 Refrigerator Wall Simulation .....	84
C.3 HT10 Code (one dimensional heat transfer; Fortran) .....	85
Appendix D: Reduced Data Summary Tables .....	95

## List of Tables

Table	Page
3.1 Material properties for calorimeter setup .....	26
4.1 Energy load calculations for daily door opening schedule and various humidity levels.....	53
D.1 Reduced Data from Run 2-No Shelf.....	95
D.2 Reduced Data from Run 3-No Shelf.....	95
D.3 Reduced Data from Run 4-No Shelf.....	96
D.4 Reduced Data from Run 5-No Shelf.....	96
D.5 Reduced Data from Run 6-No Shelf.....	96
D.6 Reduced Data from Run 7-No Shelf.....	97
D.7 Reduced Data from Run 8-No Shelf.....	97
D.8 Reduced Data from Run 9-No Shelf.....	97
D.9 Reduced Data from Run 17-No Shelf-Hot .....	98
D.10 Reduced Data from Run 18-No Shelf-Hot .....	98
D.11 Reduced Data from Run 19-No Shelf.....	98
D.12 Reduced Data from Run 20-No Shelf.....	99
D.13 Reduced Data from Run 21-No Shelf.....	99
D.14 Reduced Data from Run 22-No Shelf.....	99
D.15 Reduced Data from Run 23-No Shelf.....	100
D.16 Reduced Data from Run 24-No Shelf.....	100
D.17 Reduced Data from Run 25-No Shelf.....	100
D.18 Reduced Data from Run 26-No Shelf.....	101
D.19 Reduced Data from Run 27-No Shelf.....	101
D.20 Reduced Data from Run 30-No Shelf.....	101
D.21 Reduced Data from New Run 1-No Shelf.....	102
D.22 Reduced Data from New Run 2-No Shelf.....	102
D.23 Reduced Data from New Run 3-No Shelf.....	102
D.24 Reduced Data from New Run 4-No Shelf.....	103
D.25 Reduced Data from New Run 5-No Shelf.....	103
D.26 Reduced Data from Shelf Run 1.....	103
D.27 Reduced Data from Shelf Run 2.....	104
D.28 Reduced Data from Shelf Run 3.....	104
D.29 Reduced Data from Shelf Run 4.....	104
D.30 Reduced Data from Shelf Run 5.....	105
D.31 Reduced Data from Shelf Run 6.....	105
D.32 Reduced Data from Shelf Run 7.....	105
D.33 Reduced Data for Shelf Unit: All Runs.....	106

## List of Figures

Figure	Page
3.1 Placement of thermocouple bead into aluminum.....	9
3.2 Thermocouple placements and arrangement of calorimeter in frame .....	11
3.3 Fresh food dimensions and typical test setup.....	12
3.4 Wall arrangement and calorimeter numbering.....	15
3.5 Network representation of calorimeter setup for one-dimensional simulation.....	25
3.6 Radiative heat transfer coefficient versus aluminum emissivity.....	27
4.1 Typical temperature data for 180 s run.....	31
4.2 Comparison of thermocouple readings for gradient information.....	32
4.3a Typical temperature distribution for fresh food compartment (without hose modification) .....	33
4.3b Typical temperature distribution for fresh food compartment (without hose modification) .....	34
4.4 Latent fraction of total energy gain versus humidity level.....	36
4.5a Left wall heat transfer coefficients.....	37
4.5b Right wall heat transfer coefficients .....	37
4.5c Rear wall heat transfer coefficients.....	38
4.5d Floor wall heat transfer coefficients.....	38
4.5e Comparison of combined and convective heat transfer coefficients.....	39
4.6 Average plate heat transfer coefficient values for different transfer modes .....	42
4.7 Left wall heat transfer coefficients for hot run.....	43
4.8 Shelf calorimeter arrangement and numbering.....	45
4.9 Results of air flow smoke test for one-shelf tests .....	46
4.10a Left wall coefficients, upper division.....	48
4.10b Left wall coefficients, lower division .....	48
4.10c Rear wall coefficients, upper division .....	49
4.10d Rear wall coefficients, lower division .....	49
4.10e Floor heat transfer coefficients, shelf test .....	50
4.10f Shelf heat transfer coefficients, shelf test .....	50
4.11 Nusselt and Rayleigh number comparison for right wall.....	55
4.12a Left wall: $Nu_L$ versus $Ra_L$ and curve fit .....	57
4.12b Right wall: $Nu_L$ versus $Ra_L$ and curve fit .....	57

## List of Figures (continued)

<b>Figure</b>	<b>Page</b>
4.12c Rear wall: $Nu_L$ versus $Ra_L$ and curve fit .....	58
4.12d Floor: $Nu_L$ versus $Ra_L$ and curve fit .....	58
4.13 Dimensionless heat transfer versus $Ra_L$ : no-shelf.....	60
4.14 Dimensionless heat transfer versus $Ra_L$ : 1-shelf .....	60
B.1 Data acquisition and control system.....	82
C.1 Resistor network for refrigerator wall .....	84

## Nomenclature

A	area ( $m^2$ )
c	specific heat ( $J/kg \cdot K$ )
C	mass concentration ( $kg/m^3$ )
d	thickness (m)
D	binary diffusion coefficient ( $m^2/s$ )
g	acceleration of gravity, $9.81\ m/s^2$
h	heat transfer coefficient ( $W/m^2K$ )
k	thermal capacitance ( $W/m \cdot K$ )
K	kelvin
L	characteristic length
m	mass (kg)
q	heat transfer (W)
R	resistive value ( $K/W$ )
t	time (s)
T	temperature (K)
u	parallel velocity ( $m/s$ )
v	normal velocity ( $m/s$ )
x,y	directional representation

## Greek

$\alpha$	thermal diffusivity ( $m^2/s$ )
$\beta$	volumetric coefficient of thermal expansion ( $K^{-1}$ )
$\beta^*$	volumetric coefficient of expansion with concentration ( $m^3/kg$ )
$\Delta T$	temperature difference (K)
$\rho$	density ( $kg/m^3$ )
$\nu$	kinematic viscosity ( $m^2/s$ )

## Dimensionless Groups

$Bi = hL/k$	= Biot number
$Gr = g\beta\Delta TL^3/\nu^2$	= Grashof number
$Nu = hL/k$	= Nusselt number
$Ra = GrPr$	= Rayleigh number
$Pr = \nu/\alpha$	= Prandtl number
$Re = uL/\nu$	= Reynolds number
$Sc = \nu/D$	= Schmidt number
$Sh = h_d L/D$	= Sherwood number

## Nomenclature (continued)

### Subscripts

a	aluminum
amb	ambient
avg	average
C	constant concentration
cond	conduction
conv	convection
d	mass diffusion
f	film temperature $((T_x + T_{amb})/2)$
L	based on characteristic length
mass	due to mass transfer
p	specific aluminum plate
P	constant pressure
r	reference
rad	radiative
s	surface
T	constant temperature
w	wall

## **1. Introduction**

### **1.1 Motives for Investigation**

In order to more fully understand the mechanisms by which a refrigerator loses energy to the environment, it is important to know the energy loss during an open door condition. In order to determine the exact mechanisms by which the cabinet loses energy in this way, it is necessary to determine the heat transfer coefficients of the interior walls. It is also important to relate this information to the ambient conditions, as this correlation will aid in the modeling of a complete refrigerator system in a variety of operating environments. This information provides a means to determine design improvements that would reduce these energy losses in a refrigerator cabinet.

Although the current U.S. Department of Energy testing procedures currently do not include an open door test, a recent study by Alissi et al. (1988) has shown that adding a door opening schedule to the current DOE test procedure has a significant effect on the efficiency of a refrigerator, increasing energy use by as much as a 32%. In fact, Japanese testing procedures include a door opening schedule in the presence of high humidity in order to take this load into account. The ability to predict the magnitude of this loss would be helpful in the initial design process of a refrigerator as well as estimating the annual energy used by such appliances.

The energy loss due to door openings at first may not seem significant, but calculations show that this energy loss is of great

importance. Consider a single twenty second door opening in a room with 70 % humidity and a fresh food to ambient temperature difference of 20 K (36 °F). There are three major modes of energy gain. First, after the door is closed again, the air must be recooled. This energy load can be calculated to be 8.4 kJ (note: 1 Btu = 1.055 kJ, so dual units will not be further cited for these values). The water vapor also must be condensed out of the warm air in the compartment, and this gain can be calculated to be 11.8 kJ. Finally, the walls gain energy to the environment during the 20 s door opening. This gain, assuming an overall (latent and sensible) heat transfer coefficient of 15 W/m<sup>2</sup>-K determined from preliminary testing, is 18 kJ. The overall gain from the fresh food compartment for one door opening is 38.2 kJ.

Assuming 30 door openings per day, the overall energy lost by door openings per day is 1140 kJ. Normal energy use for a 19.9 cu. ft. refrigerator is 2.8 kwh/day, or 9936 kJ. It is assumed that the overall energy use is based on closed door testing, so fresh food door openings would constitute a 12 % increase in the amount of daily energy used by the refrigerator. Gains from the freezer are projected to be on the same order of magnitude (See section 4.3). If energy costs are assumed to be \$.10/kwh, the total open door load for the fresh food compartment is a yearly increase of \$12 to run the refrigerator. When this quantity is multiplied by some 50 million units, and it can be seen that approximately \$600 million is lost each year from the fresh food compartment. Imagine if a way could be found to reduce the open door loss by even only 25 %. One should note that the open door energy use calculations only include an

empty fresh food compartment, so actual field use could be even more significant.

A one dimensional heat transfer simulation has also shown that the temperature rise of the plastic liner of the refrigerator is only in the range of 2 K (4 °F) for a twenty second run. This small temperature rise shows that the driving potential for natural convection, the temperature difference that causes a buoyancy difference, does not disappear during the normal open door period.

## 1.2 Project Goals

This project follows the work of Dugenske (1990) on cabinet loads of a refrigerator. The objectives of the project are:

- (i) to determine the heat transfer coefficients of the inside surfaces of the the refrigerator. This will involve making a correlation between mass and heat transfer in order to account for both loads; hence, to properly interpret and correlate the results,
- (ii) to correlate the experimental Nusselt and Rayleigh numbers. This information will enable the prediction of the latent and sensible loads for any ambient condition and a variety of compartment sizes,
- (iii) to determine the effect of interior shelf geometry on these loads,
- (iv) to improve our understanding of the mechanisms which govern these loads.

## **2. Literature Review**

Because of new energy standards imposed by the DOE, there has been a significant amount of research done on refrigerator energy usage and alternative refrigerants. A study by Alissi et al. (1988) provided some information on open door energy loadings. Japanese testing procedures were used as a basis for their experiments, although the exact conditions were not the same. The Japanese test is run for two days, and door openings are performed for the first ten hours of each day. The fresh food compartment door is opened every 12 minutes during this time, and the freezer every 40 minutes. Two tests are required, one with the ambient temperature at 59 °F (288 K), and the other at 86 °F (303 K). The relative humidity is kept at 75 percent.

Alissi et al. used temperatures of 70 °F (284 K) and 85 °F (303 K), and varied the humidities at these temperatures; 12 % and 55 % for 85 °F, and 22 % and 91 % for 70 °F. A testing period of 16 hours a day was used, with the fresh food door being opened 40 times during this period, and the freezer door opened 16 times. Regular time intervals of 24 minutes for the fresh food door and 60 minutes for the freezer door were used for simplicity of testing and analysis. The temperature setting of the refrigerator was fixed at the medium settings during the entire 24 hour test.

Alissi et al. found that the presence of door openings caused increases in the daily energy use of the refrigerator unit by up to 32% over the energy used during a closed door test under the same ambient conditions. It was also discovered that an increase of 15 °F

(8 K) in the ambient temperature for an open door test caused an increase in energy consumption by 44%, and at 70 °F, an increase of the relative humidity from 22% to 91% caused an increase in the energy consumption by 13%. The effect of ambient humidity on energy consumption was never greater than 16%. The effect of the fresh food compartment door openings was determined to be much greater than that of the freezer compartment.

Clausing et al. (1987) conducted an investigation of natural convective heat transfer from isothermal cubical cavities with a variety of side-facing apertures, which has a relation to the fresh food compartment of a refrigerator. The goal of Clausing's investigation was to obtain heat transfer coefficient information from the cavity and use this information to more fully understand heat loss in large solar receivers. This investigation was done under cryogenic conditions, using the cryogenic wind tunnel facility at the University of Illinois at Urbana Champaign, which generates air temperatures in the range of 80 K to 310 K (-315 °F to 104 °F). This investigation placed an emphasis on large Rayleigh numbers, in the range of  $3 \times 10^7 < Ra < 3 \times 10^{10}$ . Clausing found that it was possible to make accurate correlations between Nusselt and Rayleigh numbers, and that one could accurately predict cavity connective losses with the resulting empirical correlation.

An investigation of convective heat transfer between building zones was performed by Clausing et al. (1991) using similar techniques, including liquid nitrogen cooled zones. The Rayleigh number range covered by the data is  $3 \times 10^8 < Ra < 10^{10}$ . The dimensionless interzonal heat transfer rate was correlated as a

function of the Rayleigh number, and an accurate correlation was obtained. The convective heat transfer coefficient, therefore, also was highly dependent on the Rayleigh number.

### **3. Experimental Apparatus and Procedure**

In order to determine heat transfer coefficients, a method to determine the rate of temperature increase of the walls of the refrigerator must be designed. It was determined that the method used by Clausing et al. (1991) was ideal for the experiment. This method involves the use of polished aluminum calorimeters to determine the rate of heating of a surface exposed to known ambient conditions. Aluminum was chosen because of its high heat capacity, high thermal conductivity, and low emissivity. Multiple thermocouples were used in each plate, both for averaging purposes and in case of thermocouple failure. The thermocouples were mounted in small holes drilled into the rear of the calorimeter, and were held in place by a thermally conductive epoxy. The thermocouple leads were run along the rear of the calorimeter to eliminate errors due to conduction along these leads.

#### **3.1 The Transient Calorimeter Method**

One great advantage of using aluminum is its high thermal conductivity. This high conductivity results in negligible temperature gradients through the thickness of the plate. This is the main requirement for the lumped capacitance model. This model assumes that the problem is no longer in the realm of the heat equation. Now the problem is dealt with as an energy balance, using the thermal capacitance of the material as an internal energy storage

and the convection as a loss of this energy. The equation can be formulated as:

$$m_a c_a \frac{dT}{dt} = -h A_s (T - T_{amb}) \quad (3.1.1)$$

where the left side is the rate of change of internal energy, and the right side is the rate of heat loss due to convection, mass transfer, and radiation. In order to determine the validity of this assumption for any problem, a dimensionless parameter called the Biot number (Bi) is introduced. The Biot Number is defined as:

$$Bi = \frac{R_{cond}}{R_{conv}} = \frac{hL}{k} \quad (3.1.2)$$

In order for the lumped capacitance method to have little error, it is assumed that the following condition must be satisfied:

$$Bi = \frac{hL}{k} \leq 0.1 \quad (3.1.3)$$

As the Biot number decreases in magnitude, the method becomes more accurate. Calculation of this number should be the first step in solving any transient conduction problem, as the lumped capacitance model is much simpler than other methods.

### 3.2 Calorimeter Installation and Testing

In order to gain initial estimates of heat transfer coefficients and to determine design parameters for the latter stages, initial testing was done using a single aluminum calorimeter that was moved around to various locations in the refrigerator. A 15" by 15" by 1/4 " plate of 6061-T6 aluminum, a very pure type of aluminum, was used. Five small holes were drilled in the plate at approximately a 45 degree angle, as shown in Figure 3.1, to allow insertion of type T thermocouples. The angle of the hole allows the thermocouple wire to be pressed against the plate without causing fatigue in the wire. A special accuracy, 24 guage thermocouple was used, as the temperature rises were not expected to exceed more than 2-4 degrees K (4-6 °F) over an entire test run; hence exceptional accuracy is needed. The thermally conductive epoxy prevents any unwanted temperature gradients around the thermocouple bead.

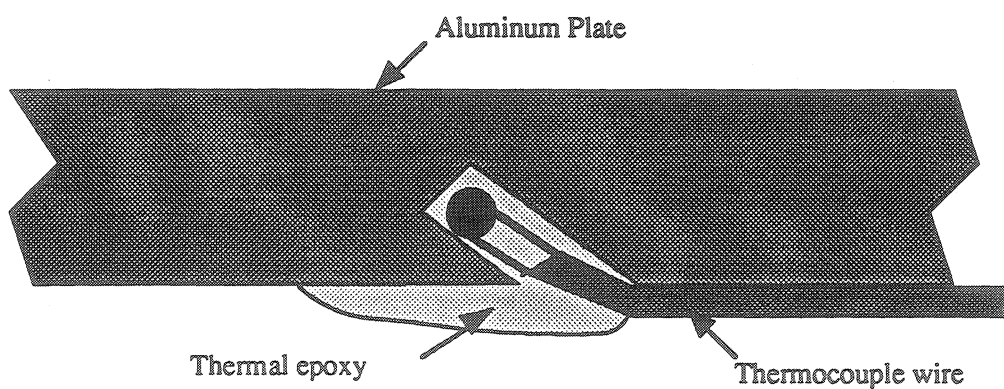


Figure 3.1 Placement of thermocouple bead into aluminum

In order to isolate the calorimeters from contact with any other heat transfer source, it was necessary to insulate the plates from the plastic refrigerator walls. Styrofoam beadboard was both inexpensive and readily available, so it was used to construct the insulating frame for the calorimeters. Styrofoam has a conductance of 0.036 W/m-K (0.0208 Btu/hr-ft-°F), so it is also a sufficient insulator. Thicknesses of 3/4" and 1" were used so that the plate would remain flush with the Styrofoam frame, giving a good simulation of a flat refrigerator wall. The plate is held in the frame using Duck tape, which is allowed to cover a 1/4" border around the entire plate. The thermocouple wires are run out the back of the insulation and to the data acquisition unit. A diagram of the calorimeter arrangement is given in Figure 3.2.

The refrigerator used in testing was a standard 20 cu. ft. refrigerator, with some modifications. The fan is operated by an on-off switch, so as to eliminate any uncertainties about when the fan will come on or turn off, and to allow testing under fan on or fan off conditions. The defrost system is also controlled by an on-off switch, also to eliminate any uncertainties about refrigerator conditions.

The same 24 gauge Type-T thermocouple wire was used for the cabinet and room ambient temperatures. Temperatures were measured at six different locations throughout the fresh food compartment during certain open door runs, in order to determine the air temperature variation in the cabinet volume. However, the majority of the testing was done with one ambient and one bulk thermocouple. A diagram of fresh food compartment dimensions and a typical test setup for the initial tests can be found in Figure 3.3.

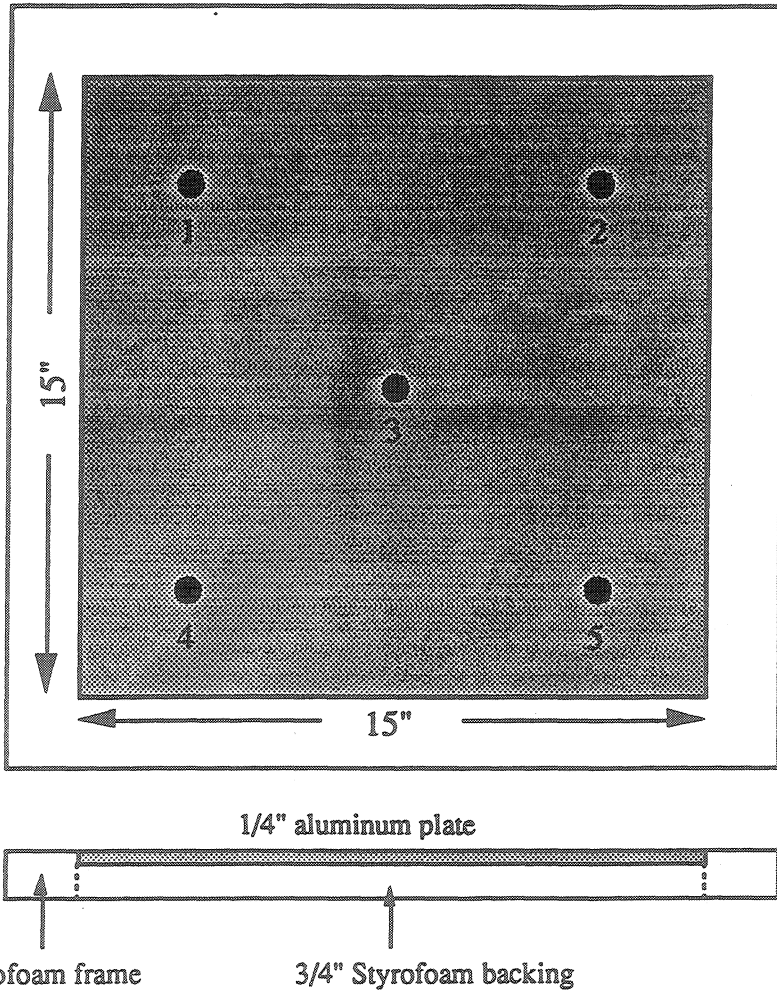


Figure 3.2. Thermocouple placements and arrangement of calorimeter in frame

From the information gained in the initial testing, it was determined that the aluminum calorimeter method was ideal for the full scale experimental procedure. It was decided to concentrate on the fresh food compartment, as previous studies (Alissi et al.) had shown that the fresh food door openings dominated the energy losses in field testing. For the full scale experiment, instrumented walls

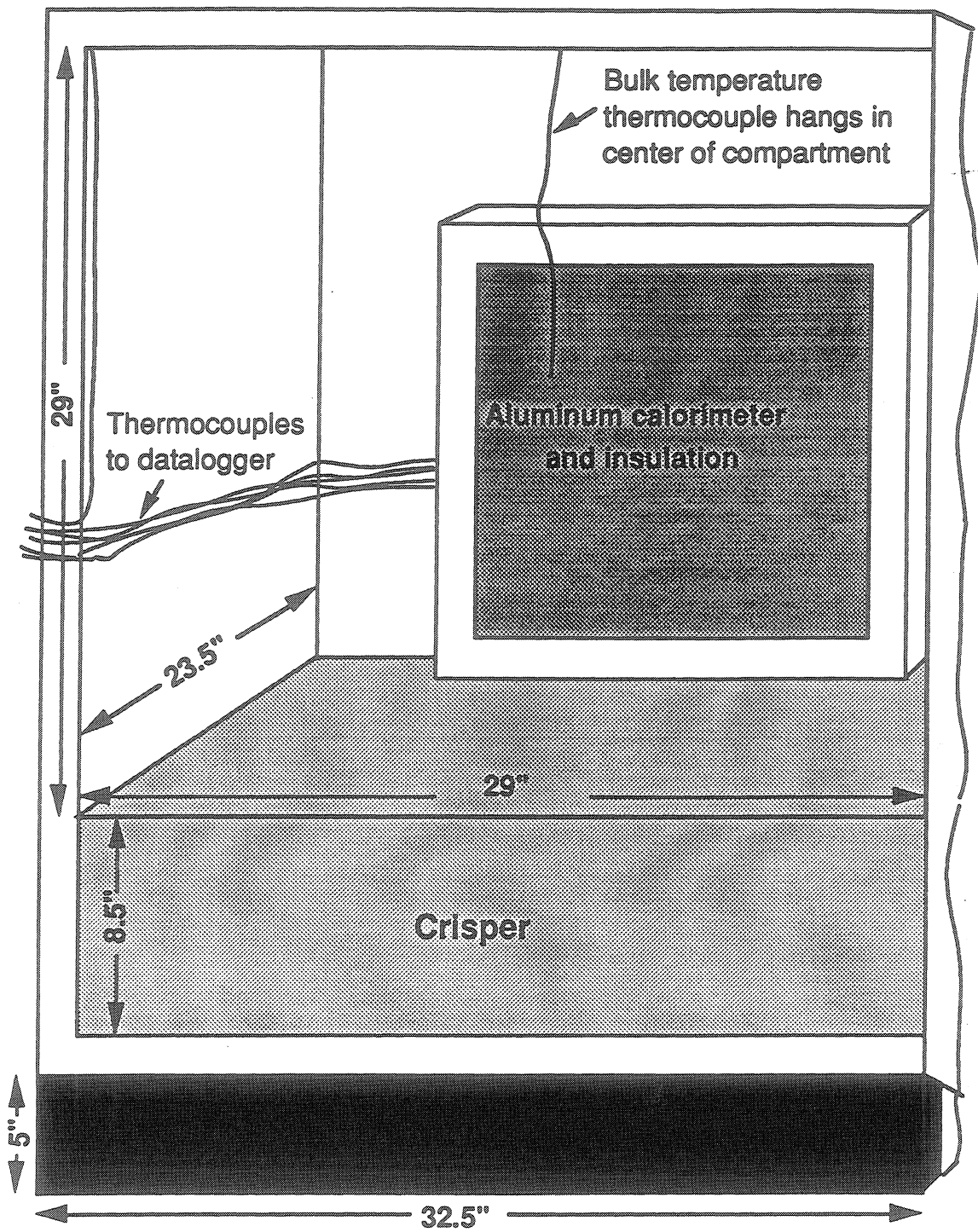


Figure 3.3. Fresh food dimensions and typical test setup

were designed and constructed. The shelves were removed from the fresh food compartment, and the crisper unit was left in.

Because it was desirable to determine the variations in heat transfer coefficients over the surface in the cabinet, the walls were made up of a series of calorimeters isolated from each other by insulating material. Each wall was divided into eight sections, the floor into two, as shown in Figure 3.4. This sectioning would allow determination of differences from top to bottom, as well as differences front to back. Because of symmetry, the floor was only divided into front and back sections. A decision was also made to not cover the ceiling of the fresh food compartment with calorimeters. This was done because the ceiling has many controls mounted on it, as well as a light bulb fixture and the fan vent. A false ceiling was rejected because it would not have been a good simulation of the actual ceiling.

The instrumented walls were designed to cover as much surface area of the actual walls as possible, without interfering with the door or the fan vent. The same 1" and 3/4" Styrofoam was used for the wall frames and calorimeter backings, and the same drilling and thermocouple cementing procedure was also used for calorimeter design. A total of twenty-six calorimeters were used in the full scale test. These calorimeters were also polished in order to reduce their emissivity. For good thermal isolation, it was desired to have about 1" of insulation between all of the plates. From the fresh food dimensions, it was determined that the sidewall calorimeters should be 5" by 8", the back wall calorimeters 5" by 12", and the floor calorimeters 8" by 25". These dimensions allowed for

maximum calorimeter area with adequate thermal isolation. A diagram of the instrumented walls and the calorimeter numbering is given in Figure 3.5.

Initially in this phase of the experiment, each calorimeter was instrumented with only one Type-T 24 guage thermocouple. This was done because of the sampling limits of the data acquisition system, which could sample this number of channels at about 2 Hz. A description of the data acquisition system can be found in Appendix A. The thermocouple was located in the center of gravity of each plate. A decision was made to insert another thermocouple into each plate, for a number of reasons. First, the data acquisition unit could sample all 64 channels at 1 Hz, which would be fast enough to observe the quasi-steady-state effects. If the transient effects were to be studied, a shorter test time with less channels and a higher sampling speed could be used. Results showed that the transient period is only about 5 seconds. Also, in case of failure of one thermocouple, there would be a back-up thermocouple in the plate. Additionally, it was found that a great deal of noise was encountered in this phase, so the two thermocouples could be averaged to get a smoother data set. The back-up thermocouples were inserted, spaced two inches to the right of the original wire, this time using a Type-T 30 guage special accuracy wire. The only difference noted between the 30 and 24 guage wire was that the 24 guage wire was a little more stable in certain noisy tests. Two Type-T 36 guage ambient thermocouples, which are much more responsive than the 24 guage thermocouples used in the

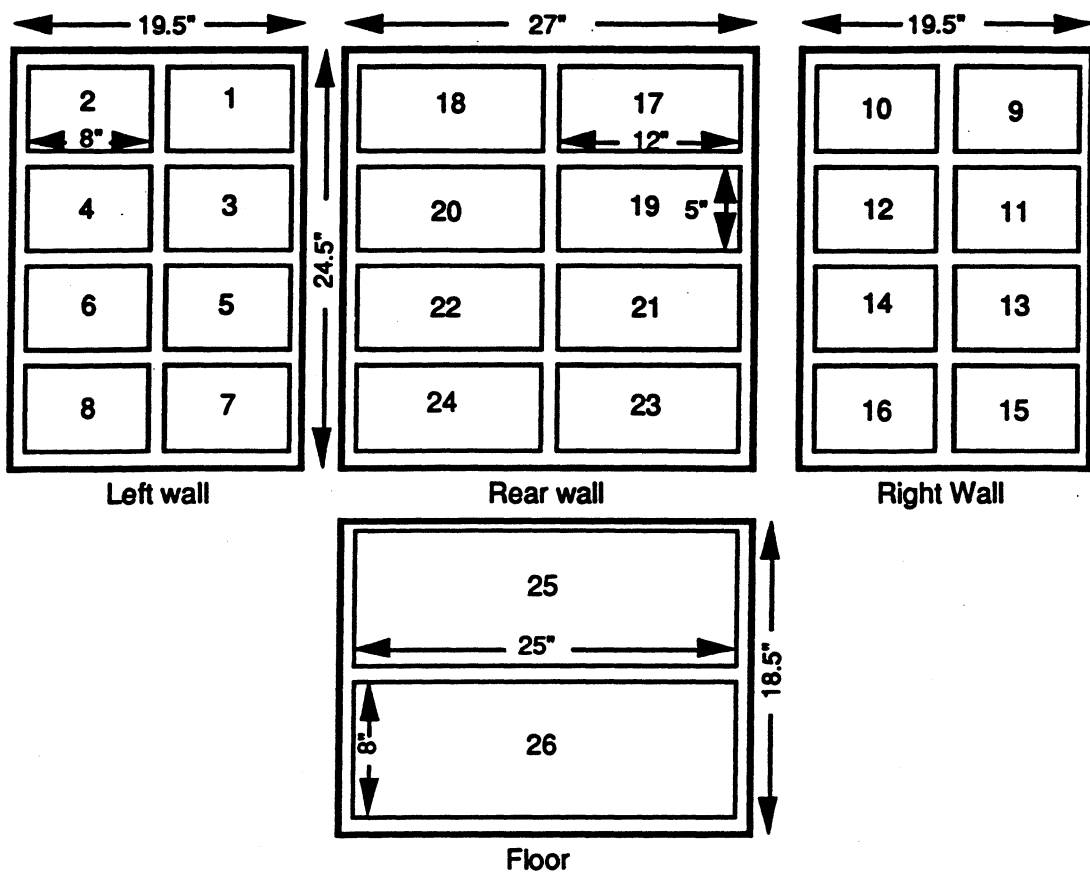


Figure 3.4. Wall arrangement and calorimeter numbering

initial test, were used, one in the fresh food compartment and one in the room ambient air.

After the walls were constructed and fixed with Duck tape as in the preliminary experiment, they were inserted into the fresh food compartment. The left wall was inserted first, then the right wall, and finally the rear wall and floor. All wires for the left wall run down its door facing edge and to the bottom of the refrigerator, and the wire from the other walls run underneath the instrumented floor and out the bottom of the door. Duck tape was used to make a ribbon cable out of the wires in order to minimize the effect of the

wires on the door seal. The wire ends were then soldered into female 15-pin connectors, as the data acquisition system use a junction box with male 15-pin connectors. The thermocouple junction box, described in Appendix B, is covered with insulation to isolate it from cold air flows out of the refrigerator.

In order to analyze the problem with no interference from unknown conditions, it was decided to run all tests with the fan off. The room air conditioning also proved to be a source of interference, so the tests were run with the air conditioning off. Movement about the room by researchers was also limited, so as not to cause a disturbance in the flow of air through the refrigerator. A test time of 180 s was used to get a good set of data over which to average heat transfer coefficients. It is doubtful that anyone would open their refrigerator door for this period of time, but the heat exchange reaches quasi-steady state conditions within 5 s, so the information gained throughout the test run is pertinent.

The test procedure for the full scale is similar to the preliminary testing. The refrigerator is cooled to the desired temperature, and then the compressor and fan are shut off. The refrigerator is allowed to sit for approximately five minutes to allow any longitudinal temperature gradients in the aluminum due to the cooling air circulation pattern to disappear. The data acquisition program is then started, and the door is opened over a period of about two seconds. After the 180 s test time, the data acquisition is terminated. The refrigerator is allowed to defrost before it is set up for the next run. A humidity reading is taken from the room using a

sling psychrometer, so that the mass transfer can be determined in the data reduction routine.

Another goal of this phase of the experiment was to determine the effect of the latent energy load (condensation of water vapor) on the observed heat transfer coefficient. As the relative humidity in the test environment was typically at approximately 75 %, there was condensation formation on the calorimeters, causing a latent load. The inverse test was run to provide a verification of the heat and mass transfer analogy described in Section 3.4. The refrigerator was heated to a temperature of 20 K (36 °F) above that of the ambient, and the same test procedure was run. This test eliminates the latent load, as the compartment temperatures are above the dew point temperature of the ambient air. The problem of separating out all of the loads will be dealt with in more detail in Section 4.

### 3.3 Governing Equations and Mass Transfer Analogy

The mass transfer in the experiment was in the form of condensation on the aluminum plates. The energy by this condensation can be determined by the relation:

$$q_{\text{mass}} = h_d A_a (C_w - C_{\text{amb}}) h_{fg} \quad (3.3.1)$$

where  $h_{fg}$  is the heat of vaporization of water, and  $h_d$  is the mass transfer coefficient. The lumped capacitance model becomes:

$$-m_a C_a \frac{dT_a}{dt} = (h_{conv} + h_{rad}) A_a (T_{amb} - T_a) \\ + h_d A_a (C_w - C_{amb}) h_{fg} \quad (3.3.2)$$

where  $h_{rad}$  is the radiative heat transfer coefficient. This model takes into account the mass transfer, the radiative transport and the convective heat transfer. The heat and mass transfer analogy is used to eliminate the mass transfer coefficient, which in Eq. (3.3.2) is an unknown. In order to do this, consider the laminar, incompressible boundary layer approximations of the momentum, energy, and continuity of mass concentration equations for a flat plate. All of these equations are normalized using the following relations:

$$x^* = \frac{x}{L}, \quad y^* = \frac{y}{L}, \quad u^* = \frac{u}{u_r}, \quad v^* = \frac{v}{u_r}, \quad T^* = \frac{T - T_w}{T_{amb} - T_w}, \quad C^* = \frac{C - C_w}{C_{amb} - C_w}$$

The equation from which the results are derived is the momentum equation. This equation in the unnormalized form is:

$$u \frac{\partial u}{\partial x} + v \frac{\partial u}{\partial y} = - \frac{1}{\rho} \frac{\partial p}{\partial x} - g + v \frac{\partial^2 u}{\partial y^2} \quad (3.3.3)$$

However, due to flat plate boundary conditions:

$$\frac{\partial p}{\partial x} = - \rho_{amb} g \quad (3.3.4)$$

Substituting this relation into equation (3) and rearranging

$$u \frac{\partial u}{\partial x} + v \frac{\partial u}{\partial y} = \frac{g}{\rho} (\rho_{amb} - \rho) + v \frac{\partial^2 u}{\partial y^2} \quad (3.3.5)$$

The density difference in this equation is the buoyancy force per unit mass. This can be expressed in terms of the volumetric coefficient of expansion,  $\beta$ . However, in this particular problem, there are two different sources driving the density difference, the air temperature difference and the water vapor concentration difference. Gebhart and Pera (1971) studied this problem, and formulated two different expansion coefficients, one for thermal expansion,  $\beta$ , and one for expansion with concentration,  $\beta^*$ . These are, for ideal gas behavior:

$$\beta = \frac{1}{\rho} \left( \frac{\partial \rho}{\partial T} \right)_{P,C} = \frac{1}{T_f} \quad (3.3.6)$$

$$\beta^* = \frac{1}{\rho} \left( \frac{\partial \rho}{\partial C} \right)_{P,T} = \left[ \frac{MW_{air}}{MW_C} - 1 \right] \frac{1}{\rho} \quad (3.3.7)$$

Where  $T_f$  is the film temperature,  $MW_{air}$  is the molecular weight of air, and  $MW_C$  is the molecular weight of the diffusing species.

Inserting these relations into Eq. (3.3.5):

$$u \frac{\partial u}{\partial x} + v \frac{\partial u}{\partial y} = v \frac{\partial^2 u}{\partial y^2} + g\beta(T-T_{amb}) + g\beta^*(C-C_{amb}) \quad (3.3.8)$$

If Eq. (3.3.8) is then normalized, it becomes:

$$u^* \frac{\partial u^*}{\partial x^*} + v^* \frac{\partial u^*}{\partial y^*} = \left( \frac{v}{u_r L} \right) \frac{\partial^2 u^*}{\partial y^{*2}} + \frac{g\beta(T_w - T_{amb})L}{u_r^2} T^* \\ + \frac{g\beta^*(C_w - C_{amb})L}{u_r^2} C^* \quad (3.3.9)$$

From this relation the inverse of the Reynolds number ( $Re^{-1}$ ) in parenthesis is recognizable. It is also possible to obtain another dimensionless group from this relation, the combined Grashof number  $Gr_L$ . However, in the above form the reference velocity  $u_r$  is unknown, so the parameter is multiplied by the Reynolds number squared to obtain the relation:

$$Gr_L = \left( \frac{g\beta(T_s - T_{amb})L}{u_r^2} + \frac{g\beta^*(C_w - C_{amb})L}{u_r^2} \right) \left( \frac{u_r^2 L^2}{v^2} \right) \\ = \frac{g\beta(T_s - T_{amb})L^3}{v^2} + \frac{g\beta^*(C_w - C_{amb})L^3}{v^2} \quad (3.3.10)$$

The Rayleigh number ( $Ra$ ) is obtained by multiplying this relation by the Prandtl number, and takes the form:

$$Ra_L = \frac{g\beta(T_w - T_{amb})L^3}{v\alpha} + \frac{g\beta^*(C_w - C_{amb})L^3}{v\alpha} \quad (3.3.10a)$$

The normalized energy equation takes the form

$$u^* \frac{\partial T^*}{\partial x^*} + v^* \frac{\partial T^*}{\partial y^*} = \frac{\alpha}{v} \left( \frac{v}{u_r L} \right) \frac{\partial^2 T^*}{\partial y^{*2}} \quad (3.3.11)$$

Now from this equation the inverse Prandtl number ( $\text{Pr} = \frac{\nu}{\alpha}$ ) arises.

Finally the normalized mass concentration equation takes the form:-

$$u^* \frac{\partial C^*}{\partial x^*} + v^* \frac{\partial C^*}{\partial y^*} = \frac{D}{\nu} \left( \frac{\nu}{u_r L} \right) \frac{\partial^2 C^*}{\partial y^{*2}} \quad (3.3.12)$$

This also has a recognizable relation, the inverse Schmidt number ( $\text{Sc} = \frac{\nu}{D}$ ). These relations in Eqs. 3.3.11 and 3.3.12 will be useful in making the mass transfer analogy.

The relations involving the mass and heat transfer coefficients can be found in the Nusselt number (Nu) and the Sherwood number (Sh). These relations are defined in Incropera and Dewitt (1985) as

$$\text{Nu} = \frac{hL}{k} = - \frac{\partial T^*}{\partial y^*} \quad \text{at } y^* = 0 \quad (3.3.13)$$

$$\text{Sh} = \frac{h_d L}{D} = - \frac{\partial C^*}{\partial y^*} \quad \text{at } y^* = 0 \quad (3.3.14)$$

These two relations have similar differential equations and similar function values. For a flat plate problem the energy equation is identical for Nu and Sh, with the only difference being that the heat relation contains Pr, and the mass relation Sc. Dividing the Nusselt number by the Sherwood number, the following relation is obtained:

$$\frac{\text{Nu}}{\text{Sh}} = \left\{ \frac{\text{Pr}_n}{\text{Sc}_n} \right\} \quad (3.3.15)$$

substituting in relations for all parameters and rearranging:

$$\frac{h}{h_d} = \frac{k}{D(1-n) \alpha^n} \quad (3.3.16)$$

This provides the needed relation between  $h$  and  $h_d$ . The most common value for  $n$  in a flat plate case is  $1/3$ . Solving for  $h_d$  and substituting into Eq. (3.3.2):

$$-m_a c_a \frac{dT_a}{dt} = (h_{conv} + h_{rad}) A_a (T_{amb} - T_a) \\ + \frac{h_{conv} D^{2/3} \alpha^{1/3} A_a}{k} (C_w - C_{amb}) h_{fg} \quad (3.3.17)$$

Equation 3.3.17 can now be solved for the heat transfer coefficient, as it now becomes the only unknown in the equation, as the temperatures and  $\frac{dT_a}{dt}$  are known from test data. This is easily formulated in a computer program, and is done so in the data reduction routine.

### 3.5 Data Reduction Procedure

In order to effectively reduce large quantities of data, a computer program is needed. Because the data reduction in this project was fairly repetitive in terms of analysis, one program could be written that, when given the test conditions, could reduce any set of data. In this project, the computer program also had additional subroutines written to obtain correlations as the project progressed .

True Basic was chosen as the language for the data reduction programs. This language is simple in structure, and can incorporate many matrix commands that facilitate programming. The following paragraphs describe the basic data reduction steps involved in the program. A fully documented program listing can be found in Appendix B.

The data acquisition unit uses an IBM compatible computer, but the best available software for data reduction was available on a Macintosh IIci. A program called Apple File Exchange was used to translate files between Apple and IBM formats. The data was in the form of a comma-delimited matrix, and was 181 rows by 57 columns in size in the no-shelf case. This allowed a single command to be used for matrix input, in the subroutine INPUT1. After the data matrix was entered, the two thermocouples in each plate were averaged together by the subroutine AVG, in order to smooth the data. Failures in some of the thermocouples necessitated adding the subroutine CORRE to make the necessary compensations.

A least squares curve fit of the temperature data was used to determine the temperature versus time derivative for the lumped capacitance model. Different sections of the data were curve fit, in order to determine if the slope had any significant change with time. The subroutine FEV sets up the matrices necessary for a least squares curve fit to be made, and the curve fit itself is made by the subroutine LS. A variable controls the number of time intervals used in the linear least squares curve. For most experiments, 6 time intervals were used, resulting in six data points for each plate.

After these curve fits are made and the slopes are stored in a matrix, the lumped capacitance model is used to determine the heat transfer coefficients, in the subroutine HTCOEFF. The lumped capacitance model derived from the mass transfer analogy is used, in the form of Eq. (3.3.17). For this analysis, the ambient temperature over that time period is averaged, as well as the plate temperature. It is also necessary to supply textbook parameters, such as pressures of saturated water vapor. The humidity level in the room exhibited only a few different values during the testing, so an interpolation routine was inserted into the program for water vapor partial pressure values.

In order to determine the effects of an open door experiment on the entire wall of the refrigerator and to determine the amount of energy lost from the aluminum plate to the refrigerator wall, a one-dimensional heat transfer simulation was performed. A computer program, HT10, written by Clusing, was used. Temperature changes, total energy losses, and heat transfer rates for a user defined RC network were calculated. Initial calculations were performed with just a simulation of the refrigerator wall to determine the significance of wall temperature changes during a door opening. The network in Figure 3.5 was added to the wall network, which can be found in Appendix C.2, to simulate the refrigerator with the calorimeters in place.

All of the resistances and capacitances can be calculated using the properties listed in Table 3.1. The Styrofoam used is an expanded polystyrene molded beadboard, and the aluminum properties are that of 6061-T aluminum. The aluminum properties

were calculated by a computer program written by Clausing, ALPT, which can be found in Appendix C.1. The resistance of aluminum was assumed to be zero, as the calculated value was several times lower in magnitude than the resistance of the Styrofoam and the refrigerator insulation.

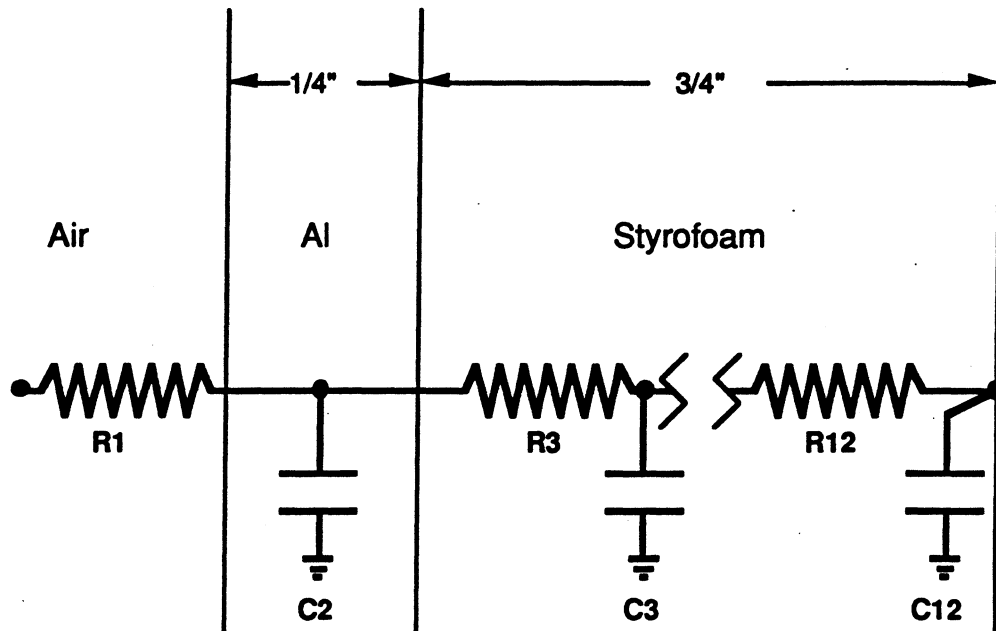


Figure 3.5. Network representation of calorimeter setup for one dimensional simulation

After the network values were calculated and nondimensionalized with respect to the values for the refrigerator wall insulation, a requirement for the HT10 program, the simulation was run for a 30 second door opening. The total simulation included a 3 hr cool down period to reach steady state, and then the 30 sec door opening. From this simulation, it was found that an average of 10% of the energy gain of the calorimeter was from refrigerator wall

itself; hence, a correction in the data reduction program to account for this gain was made.

Table 3.1. Material properties for calorimeter setup

Property: metric (english)	Aluminum	Styrofoam
$c_p$ : J/kg-K (Btu/lbm-°F)	876 (209)	1210 (290)
$\rho$ : kg/m <sup>3</sup> (lbm/ft <sup>3</sup> )	2707 (169)	16 (0.998)
d: m (in)	0.00635 (0.25)	0.01905 (0.75)
k: W/m-K (Btu/hr-ft-°F)	157.5 (91.0)	0.036 (0.0208)

The heat transfer must be corrected to account for the radiative heat gain or loss. This involves a full analysis of the radiative heat transfer, using view factors and radiosities. The fresh food compartment is considered to be an enclosure, with the open door treated as a black surface at the ambient temperature. The emissivity of the plates is assumed to be in the range of 0.03, the value for polished aluminum, and 0.13, the value for steel sheet metal. The radiative heat transfer coefficient for a wall was calculated for a range of these emissivities, and results are given in Figure 3.6. Assuming a worse case, the value for emissivity was set at 0.1. The emissivity of the uninstrumented ceiling of the fresh food compartment was assumed to be 0.9, which is a value for most common plastics.

The view factors were determined using the subroutine VIEWS and the functions OPPVIEW and ADJVIEW, which calculate view factors for opposing planes and adjacent planes, respectively. VIEWS calculates all view factors these functions, symmetry, and the

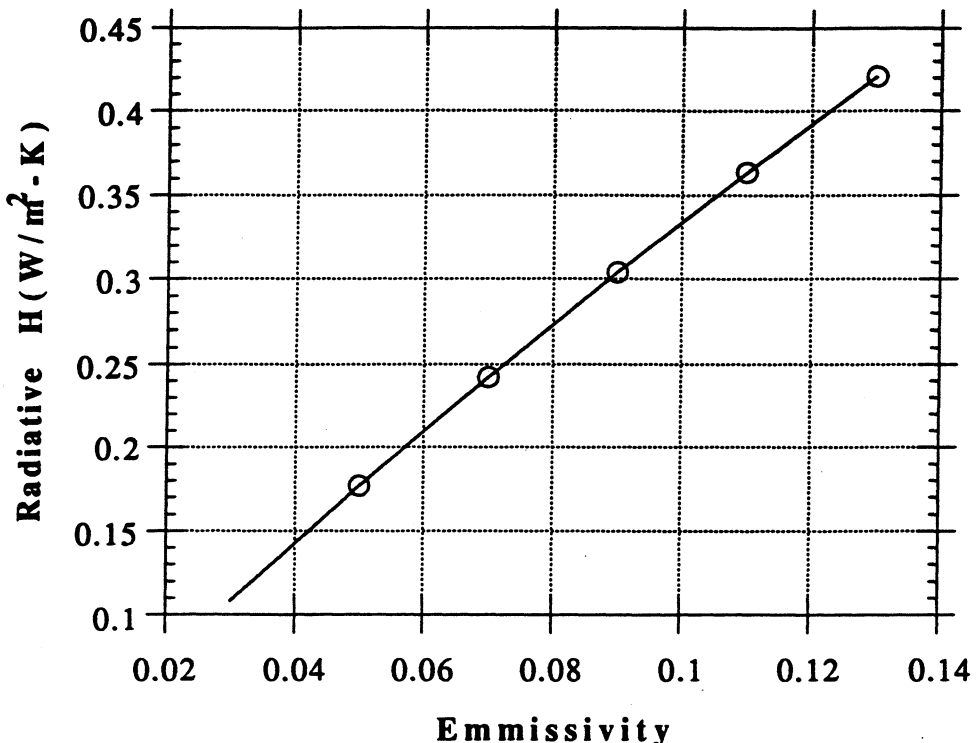


Figure 3.6. Radiative heat transfer coefficient versus aluminum emissivity

summation rule of view factors, which states that the sum of a surface's view factors must equal 1. The INFO subroutine deals with all of the necessary information to make the radiative calculation, including the presence of up to three shelves. Here the wall average temperatures are assigned; the ambient temperature is set; and the emissivities are assigned. The subroutine SCRIPTF does a gray body

radiative exchange using the wall areas, the view factors, and the emissivities. The relation matrices for radiosities are reduced to a single factor called the script F factor, SF, which is then used in the subroutine QRAD to calculate the radiative heat transfer from the surface. The formulation for this calculation is:

$$Q_{\text{rad}i} = \sum_{j=1}^n (SF_j) \sigma (T_i^4 - T_j^4) \quad (3.5.1)$$

where  $\sigma$  is Boltzman's constant and  $j$  is the number of surfaces in the enclosure. After the radiative heat transfer is calculated for each wall, the radiative heat transfer coefficient is determined in the subroutine COEFF, using the relation:

$$h_{\text{radi}} = \frac{Q_{\text{rad}i}}{T_{\text{amb}} - T_i} \quad (3.5.2)$$

The radiative heat transfer coefficient is then subtracted off in the subroutine CORR.

The Rayleigh and Nusselt numbers are calculated in the subroutine NURA. It contains the mass transfer correlations for the combined Rayleigh number described in Section 3.3. The subroutine uses information calculated in other parts of the program to determine the average Nusselt and Rayleigh numbers over the entire period of the test. Average values are calculated for each wall. The characteristic length used is the wall height, as the vertical wall surfaces are the driving force in the flow. This same length is also

used for floor calculations. The Nusselt number is calculated for the convective heat transfer coefficient only.

All information necessary for data analysis is output to a text file. The file "HTC" contains the entire heat transfer coefficient matrix determined by the data reduction program. The file "Averages" contains the average heat transfer coefficient for each plate over the entire test run. The file "Summary" contains the information found in Appendix D, which includes average wall heat transfer coefficients, average wall temperatures, Rayleigh and Nusselt numbers for each wall, and the relative humidity for each experiment.

## **4. Experimental Results and Analysis**

### **4.1 Temperature Data**

Temperature data were taken over a period of 180 s for each test run. This test time was considered to be acceptable for data collection purposes, as the refrigerator reaches quasi-steady state conditions in a period of about 5 s. After this time period, there is little change in the slope of the temperature versus time data over the duration of the test. This quasi-steady condition allows the test duration to be as long as desired. A typical temperature-time data set is given in Figure 4.1. The small perturbations are due to thermocouple accuracy limits and a small amount of noise.

Another problem addressed in the temperature data is that of temperature gradients within the aluminum plates. This was not expected to be a problem throughout the thickness of the aluminum, but was considered a possibility along the length, as in previous experiments with the larger single calorimeter, there was an indication of a small gradient, 0.1 to 0.3 K (0.2 to 0.6 °F) in the plate during some test runs. This led to the instrumentation of the plates with two different thermocouples placed 1/3 plate length apart.

Figure 4.2 presents data for one of the calorimeters during a test run. It can be seen that there is no temperature gradient between the two thermocouples. This is true for all calorimeters, and indicates testing procedures eliminate any unwanted gradients.

Although there were no temperature gradients within the plates themselves, there was a temperature gradient on all of the

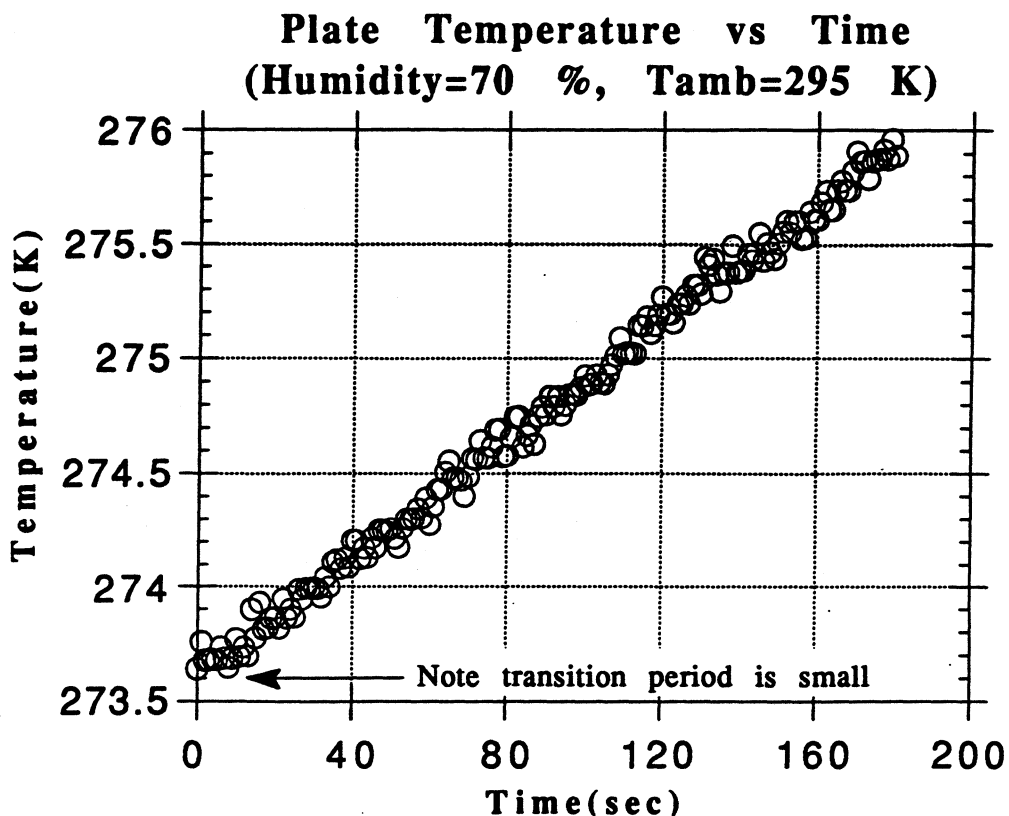
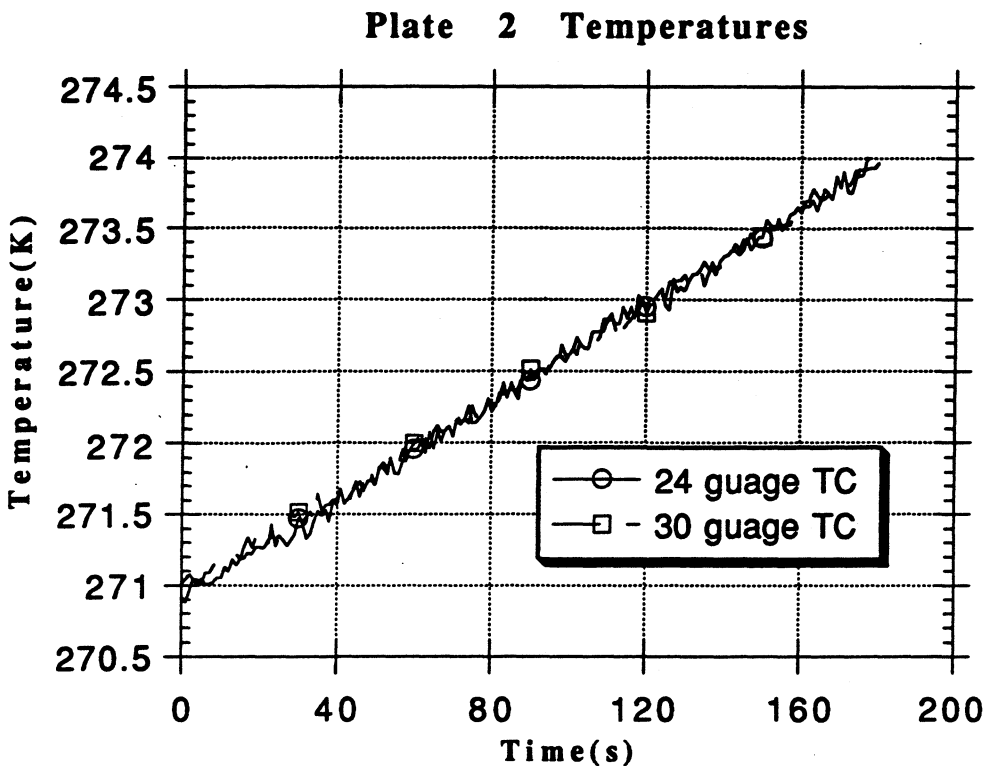


Figure 4.1. Typical temperature data for 180 s run

walls and the floor. This is due to the fact that the cold air supply is at the top of the fresh food compartment, causing more forced convection on the upper part of the compartment, and therefore lower temperatures. A typical temperature distribution for initial full scale testing can be found in Figure 4.3a. The wall temperature gradient was as much as 7 K (13 °F) under some test conditions. This was not viewed as a realistic situation, rather, a result of the fan operation used in this study. In order to correct this problem, the duct was instrumented with two rubber hoses, which were pointed at the door in order to reduce the wall gradients. This change did not



**Figure 4.2. Comparison of thermocouple readings for gradient information**

totally eliminate the wall gradients, but made them more realistic. A typical temperature distribution of the compartment after this modification can be found in Figure 4.3b.

From these distributions, it is also possible to determine some of the characteristics of airflow within this refrigerator unit. The left wall had the most level temperature distribution, and had a fairly uniform top to bottom gradient. In the unmodified case, it seemed as if the top left corner of the refrigerator was receiving far less airflow than the front corner, resulting in a 2.5 K (4.5 °F) temperature

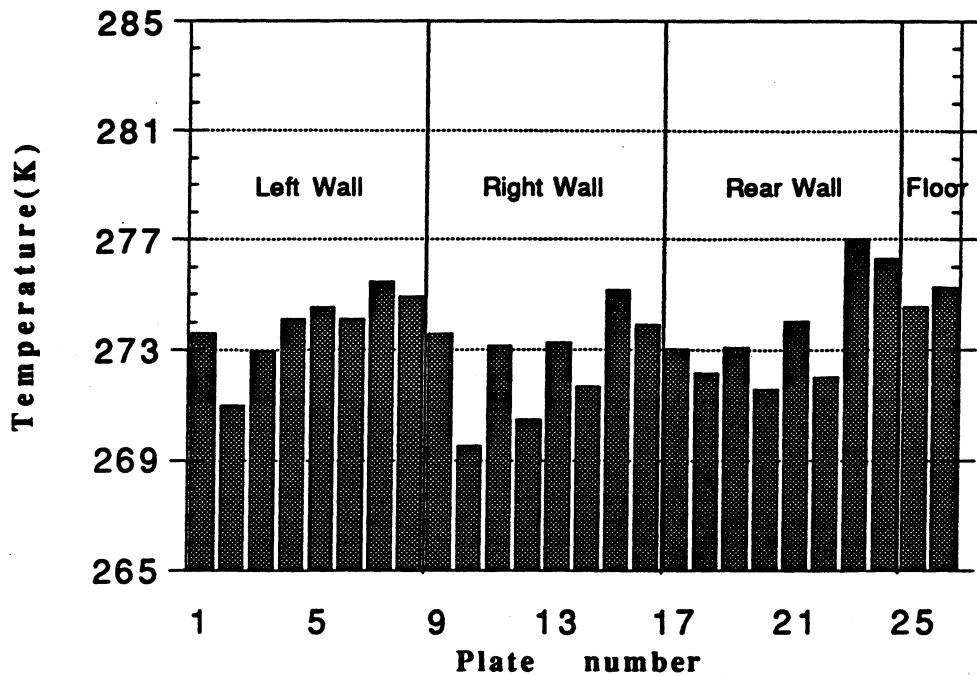


Figure 4.3a. Typical temperature distribution for fresh food compartment (without hose modification)

difference. This was reduced by the addition of the rubber hoses. The right wall had a much larger front to back gradient in both cases. The front plates of the wall seemed to be at least 2 K (3.6 °F) warmer than the rear plates in all cases, and the wall only weakly exhibited a top to bottom gradient. This indicates that airflow in the refrigerator is not symmetric. The rear wall shows a top to bottom gradient in both cases, and a left to right gradient in the unmodified case. Although the right wall on average is colder, the right side of the rear wall is warmer than the left in the unmodified case. This indicates uneven airflow throughout the compartment. In the

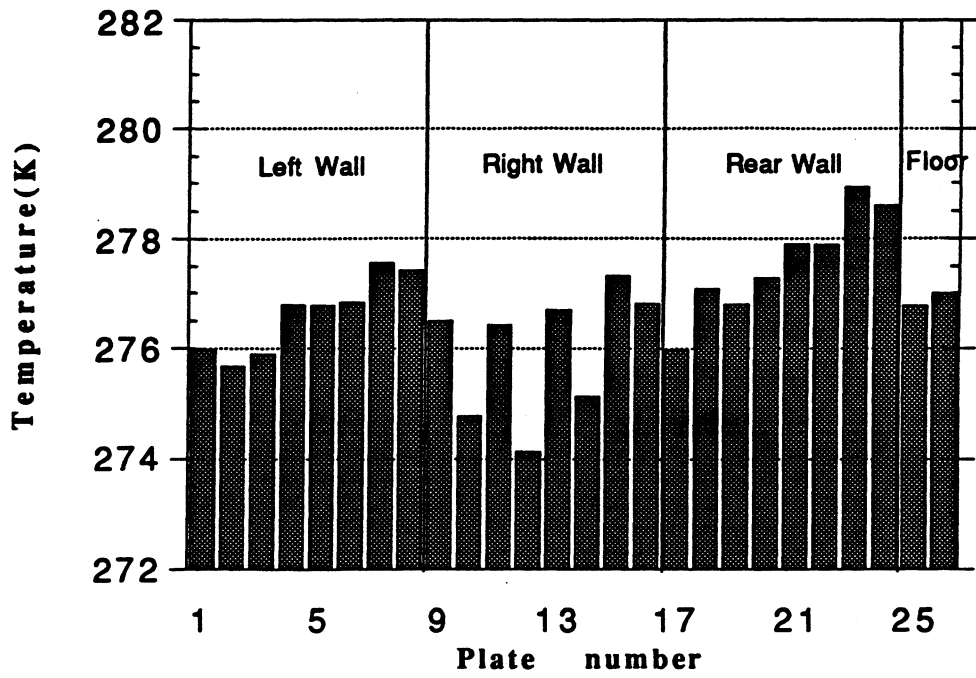


Figure 4.3b. Typical temperature distribution for fresh food compartment (with hose modification)

modified case, the rear wall left to right trend was reversed, and the gradient is considerably smaller. This is expected, however, as the hoses in this test are blowing the cold air onto the door of the refrigerator.

## **4.2 Heat Transfer Coefficients**

### **4.2.1 Empty Compartment Coefficients**

The convective coefficients obtained in this study are in the expected range. The latent energy load was anywhere from .5 to 1.2 times the convective value. Figure 4.4 presents the fraction of the total (latent + sensible) load that the latent load represents versus the humidity level, for the given conditions. These values were taken from tests with the same compartment to ambient temperature difference, as the convective value is dependent on this condition. It can be seen that the relation is not linear for the tested humidity range, and that the latent fraction is at zero at approximately 34 % relative humidity. This is due to the way in which energy is exchanged at the wall. Saturated conditions at the wall, which are assumed in the correlations made in this study, are higher in concentration than the ambient air when the humidity is this low. This results in stagnated vapor condensation, and the latent load contribution is negligible.

The convective heat transfer coefficients were determined for all tests. The results for one test run are displayed in Figures 4.5a-e. These graphs present the heat transfer coefficients versus test time for each calorimeter in the experiment. Test conditions are a  $\Delta T$  of 22 K (40 °F), and a relative humidity of 70 %.

The left wall heat transfer coefficients are displayed in Figure 4.5a. It can be seen that the wall displays a coefficient gradient from top to bottom. Values of the upper two plates are in the range of 6

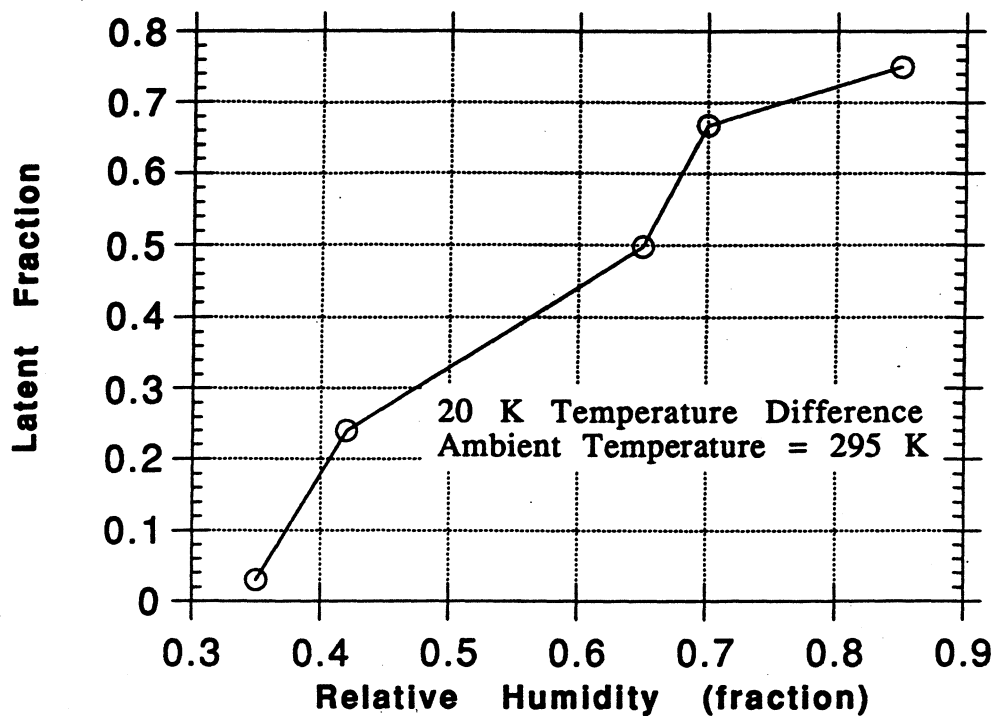


Figure 4.4. Latent fraction of total energy gain versus relative humidity

to 7.5 W/m<sup>2</sup>-K (1.1 to 1.3 Btu/hr-ft<sup>2</sup>-°F), and the lower two plates have a range of 4 to 6 W/m<sup>2</sup>-K (0.7 to 1.1 Btu/hr-ft<sup>2</sup>-°F). This is not only due to the temperature gradient in the wall, but also due to the fact that the warm air is entering at the top of the fresh food compartment, and is cooled as it travels through the compartment. Thus, the lower plates are exposed to a smaller temperature difference and have a relatively lower heat transfer coefficient. This is proven by plates 7 and 8. These plates are usually at the same temperature, yet plate 8, which is the last plate that the flow passes

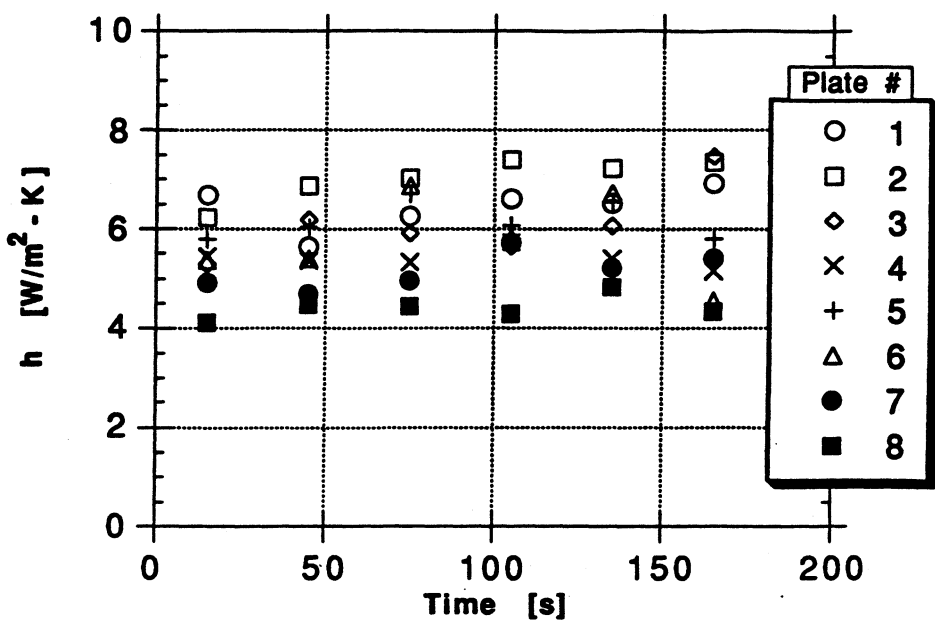


Figure 4.5a. Left wall heat transfer coefficients

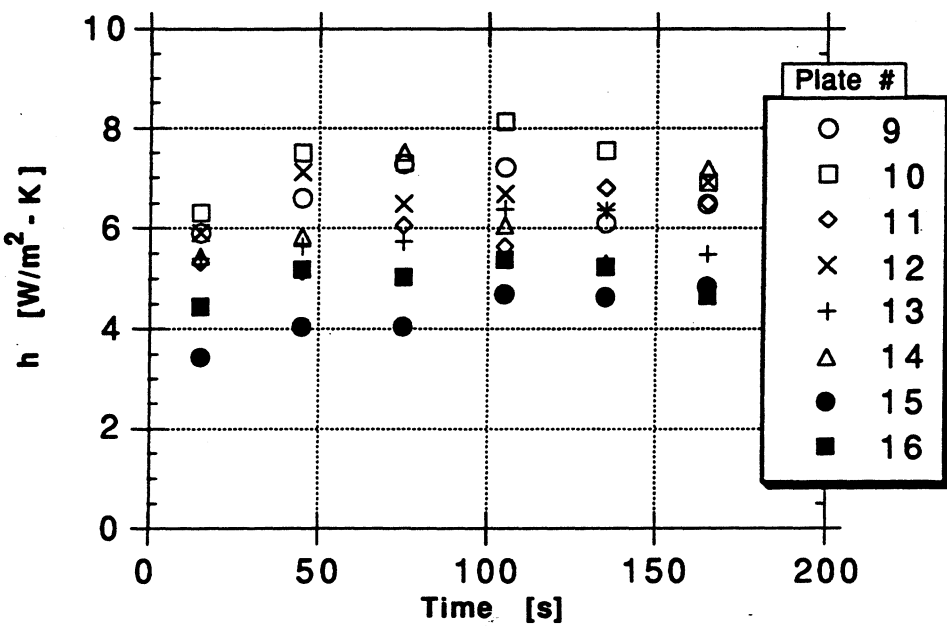


Figure 4.5b. Right wall heat transfer coefficients

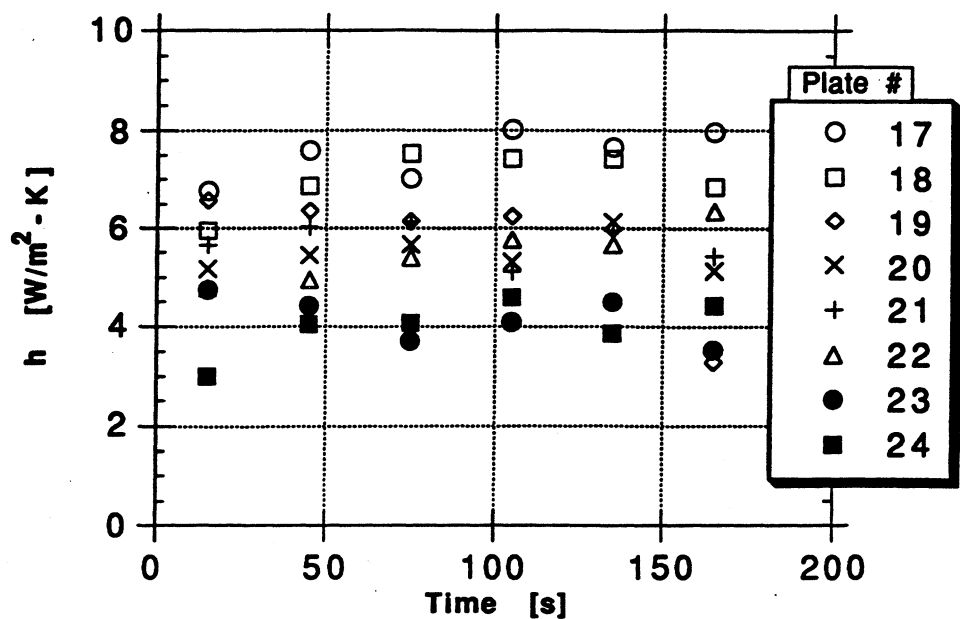


Figure 4.5c. Rear wall heat transfer coefficients

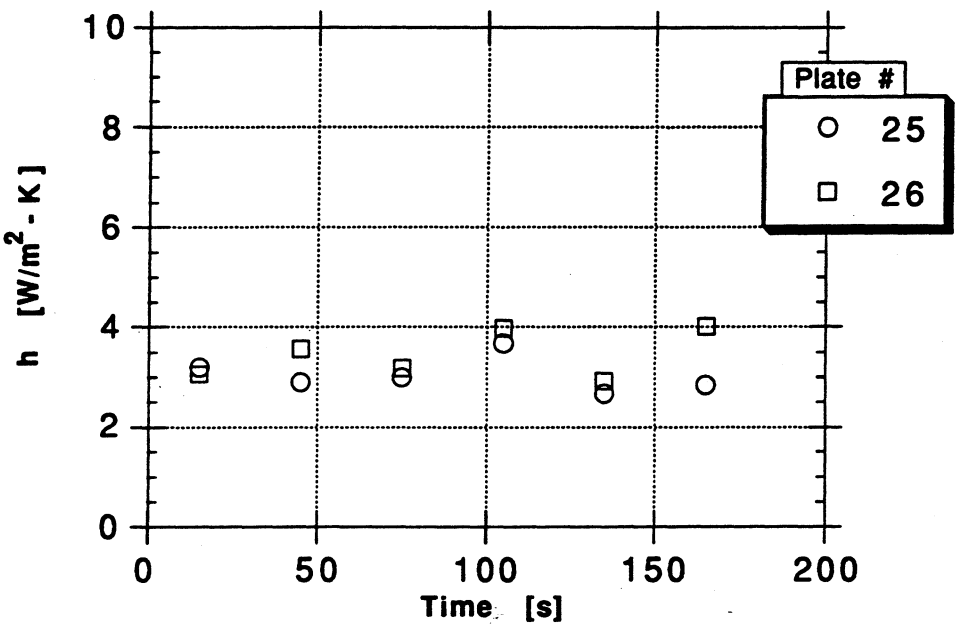


Figure 4.5d. Floor heat transfer coefficients

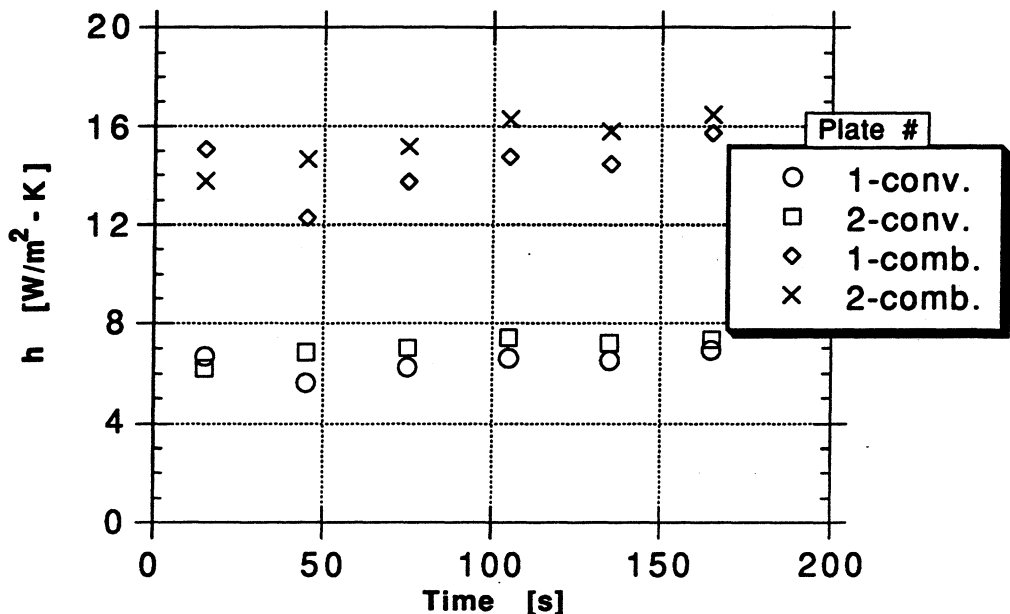


Figure 4.5e. Comparison of combined and convective heat transfer coefficients

on its way out of the refrigerator, has a lower heat transfer coefficient than plate 7.

Figure 4.5b displays the right wall coefficients. One difference from the left wall is the spread in the data. The upper two plates have coefficients in the range of 6-8 W/m<sup>2</sup>-K (1.1-1.4 Btu/hr-ft<sup>2</sup>-°F), and the lower two plates are in the range of 3.5 to 5.5 W/m<sup>2</sup>-K (0.6-1.0 Btu/hr-ft<sup>2</sup>-°F). This is not necessarily due only to a difference in the flow, but also to the fact that the right wall becomes quite stratified in terms of temperature level, as previously shown in Figure 4.3b. However, there is evidence of a weaker flow on this wall, as the lower plates on this wall, 15 and 16, have a lower coefficient than plates 7 and 8 on the left wall, even though they are

at about the same temperature level, if not a little colder in some tests. This is probably due to the fact that the door is attached on this side of the refrigerator, and its extended shelves and contours could interfere with the flow on this side of the compartment. Plates 15 and 16 also exhibit the trends of 7 and 8. Plate 15 has the lower coefficient.

The coefficients for the rear wall are shown in Figure 4.5c. The range is the same as the right wall. This indicates a stronger flow on the rear wall, as on average this wall is warmer than the right wall. Vertical flow on vertical plates is much more strongly driven than horizontal flow, due to the mechanisms which drive natural convection. The only differences right to left in transfer coefficients on this wall seem to be due to the temperature gradients, as two plates at the same height on this wall with equal temperatures have the same overall average heat transfer coefficient.

The floor coefficients, shown in Figure 4.5d, are in the range of 2.5 to 4.0 W/m<sup>2</sup>-K (0.4 to 0.7 Btu/hr-ft<sup>2</sup>-°F). These values are slightly lower than the coefficients of the lower wall plates, again indicating the weaker horizontal flow on the surfaces. However, even though the plate nearer the door, plate 26, is on average warmer than the rear plate, it has a higher average heat transfer coefficient. This would indicate that in the rear bottom of the refrigerator the flow is relatively stagnated.

Figure 4.5e gives a comparison of combined and convective heat transfer coefficients for plates 1 and 2. In this case, the latent load adds about 8 W/m<sup>2</sup>-K (1.4 Btu/hr-ft<sup>2</sup>-°F) to the total heat transfer coefficient. The same trends are followed by both

coefficients, as would be expected, as the latent load adds a certain percentage for each case, as shown previously in Figure 4.4. Figure 4.6 presents overall average coefficients for another test run, with conditions of  $\Delta T = 17$  K ( $30$  °F) and a relative humidity of  $70\%$ . The values of convective, latent, and radiative heat transfer coefficients are shown for each plate. In most plates, the latent load is greater than the convective load. The plates which have higher convective coefficients are the colder plates in the compartment. The greater temperature difference causes these plates to have a greater percentage convective load. Radiative coefficients are also shown, and are approximately  $0.3$  W/m<sup>2</sup>-K ( $0.05$  Btu/hr-ft<sup>2</sup>-°F). There is little variance from this value due to the fact that all of the walls have similar average temperatures, and all have similar views of the aperture. It is important to note that the radiative coefficient is quite low in this case due to the fact that aluminum has a low emissivity. Plastic refrigerator walls, with an emissivity of  $0.9$ , generate a radiative heat transfer coefficient in the range of  $2$  to  $3$  W/m<sup>2</sup>-K ( $0.35$  to  $0.5$  Btu/hr-ft<sup>2</sup>-°F). The same trends in convective coefficient values described in Figures 4.5a-e also are present in the case in Figure 4.6.

The inverse test was run to determine if the mass transfer analogy was valid. The inverse case involves the heating of the refrigerator compartment, to a level about  $20$  K ( $36$  °F) above the ambient conditions. This keeps the wall temperatures above the dew point level of the ambient conditions and eliminates any mass transfer. Figure 4.7 shows the data for the left wall from a hot test with a temperature difference of  $21$  K ( $38$  °F). The coefficients are in

Values given: Convective, Latent, Radiative (W/m<sup>2</sup>-K)

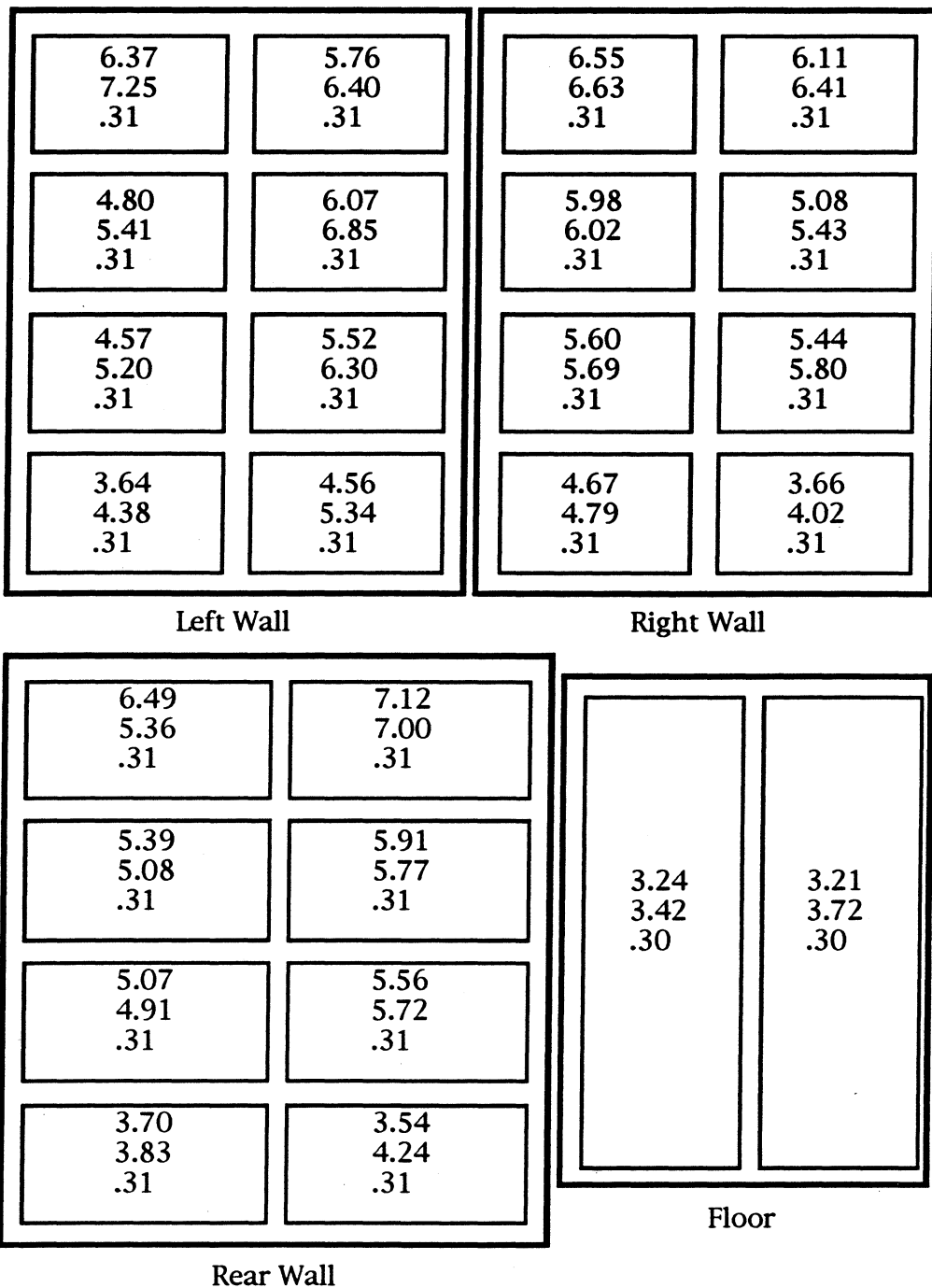


Figure 4.6. Average plate heat transfer coefficient values for different transfer modes

the same range as those shown in Figure 4.5a, indicating that the mass transfer analogy is accurate. However, the upper plate coefficients are not as stable, indicating that possibly the inverse case is not as stable as the cold test case. Plates 7 and 8, the flow entrance plates for the hot case, are stable.

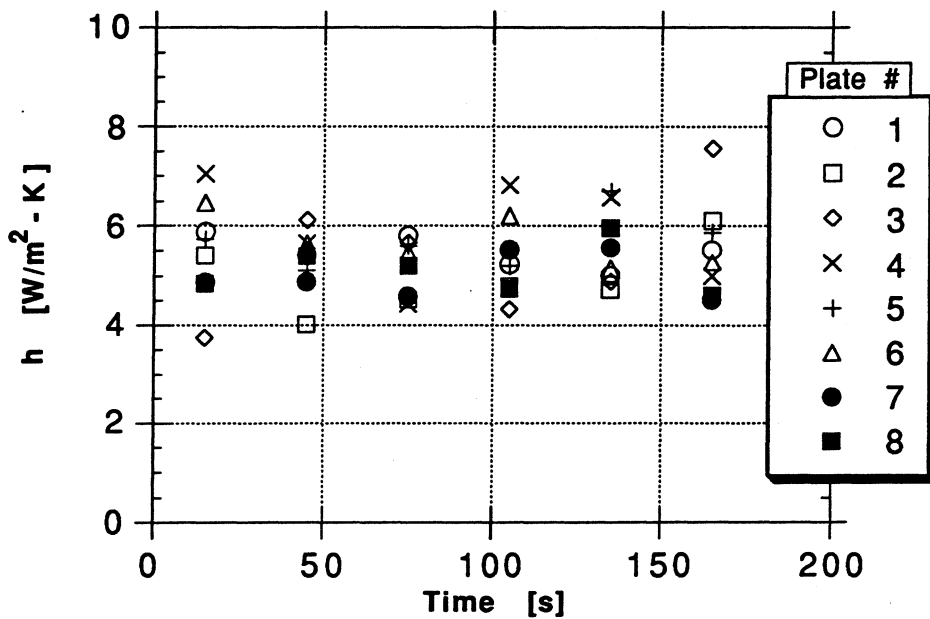


Figure 4.7. Left wall heat transfer coefficients for hot run

#### 4.2.2 Compartment with One Shelf

Testing was also done with one shelf inserted into the fresh food compartment. The shelf was inserted at a point which divided the instrumented wall surfaces into two equal halves, although because of the ceiling geometry and placement of the instrumented walls, the upper compartment is slightly greater in volume. Support

for the shelf, which is quite heavy due to the aluminum plates, is provided by four 1/2" PVC pipe "legs". The shelf is composed of four aluminum calorimeters, two on each side of the shelf, constructed in the same manner as previous calorimeters. Due to channel limitations of the data acquisition unit, there is only one 30 gauge Type-T thermocouple in each plate. The calorimeters and the Styrofoam frame are the same width and depth as the instrumented floor, and the shelf is double-sided. A sheet of Thermax insulation is placed between back to back calorimeters, in order to prevent conduction from plate to plate. Figure 4.8 shows the calorimeter numbering convention of the shelf unit.

Testing procedures were similar to the empty cabinet tests, however the airflow had to be further altered. The lower compartment did not receive proper air flow for cooling even with vents cut in the shelves, as the shelf is not only heavily insulated but also does not allow radiative exchange between upper and lower

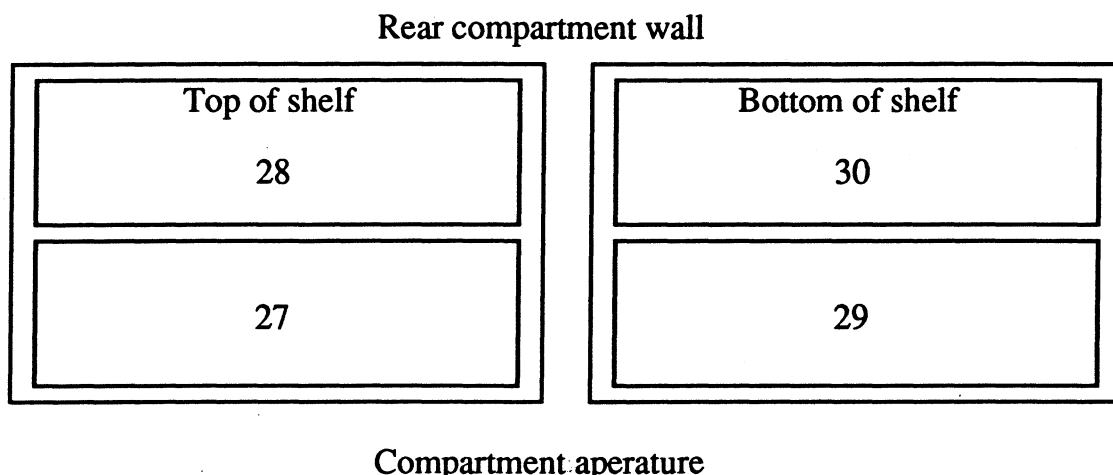


Figure 4.8. Shelf calorimeter arrangement and numbering

compartment surfaces. To remedy this situation, one of the two air flow hoses was extended to the lower compartment.

Smoke tests were performed during an open door test with the shelf in place to determine flow characteristics. The results of these tests can be found in the flow diagrams in Figure 4.9. Smooth flow

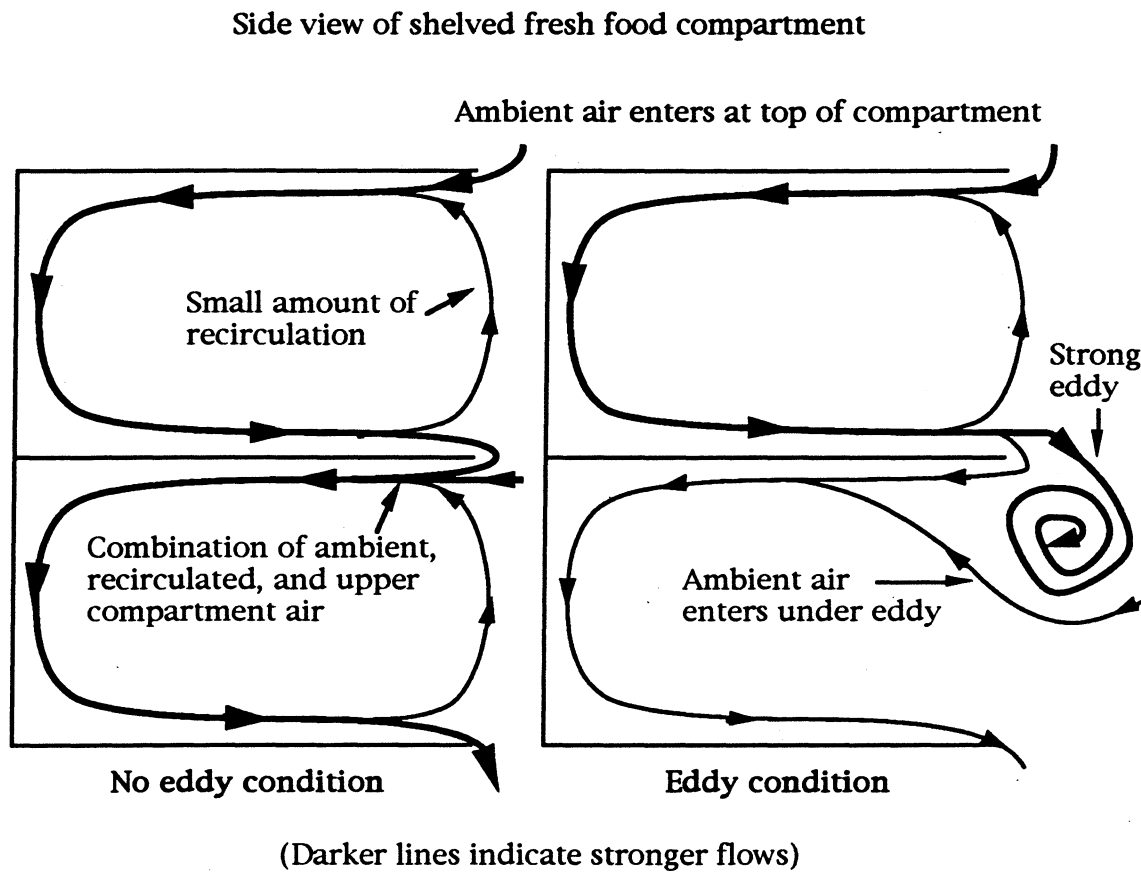


Figure 4.9. Results of air flow smoke test for one-shelf tests

entrance could be observed at the top of the upper division of the fresh food compartment, however the areas around the shelf experienced very unsteady flow conditions. At some points in the test, the air flowing out of the upper division would pour down off

the shelf an would form eddies which did not enter the lower compartment division. A small amount of air from the upper compartment division would enter the lower compartment behind the eddies. This eddy condition would last from 5 to 20 s, during which time the lower division flow seemed to be more stagnant than the upper division. Ambient air entered the lower compartment division under these relatively strong eddies, and would circulate through the lower compartment. The flow exit area of the upper division exhibited high flow rate conditions during this eddy period.

At other points in the experiment, the eddy condition would cease and the flow was observed to flow immediately into the lower division, directly up against the bottom of the shelf. This no-eddy condition would also last about 5 to 20 s, and alternated with the eddy condition. During this condition, the lower division seemed to exhibit a steady flow. Both compartment divisions experienced recirculation of a small amount of the air flow. The results of these flow conditions can be seen in the scatter of the shelf data.

The results of a typical test run are shown in Figures 4.10a-f. The test condition for this test run include  $\Delta T = 17$  K ( $31$  °F) and a relative humidity of 30 %. Figure 4.10a displays the left wall convective coefficients for the upper compartment division. The front to back and top to bottom trends described in Section 4.2.1 are valid in this situation. However, the flow exit plates, 3 and 4, exhibit more perturbations than in previous tests. These fluctuations are due to the type of flow which exists in the shelved refrigerator.

Figure 4.10b displays the coefficients for the left wall in the lower compartment division. On average, the coefficient values for



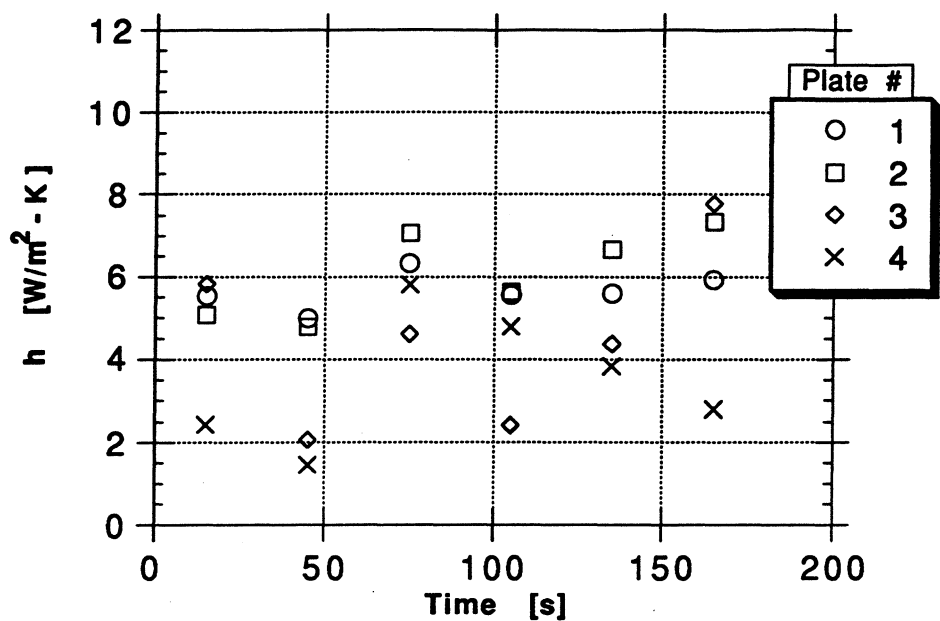


Figure 4.10a. Left wall coefficients, upper division

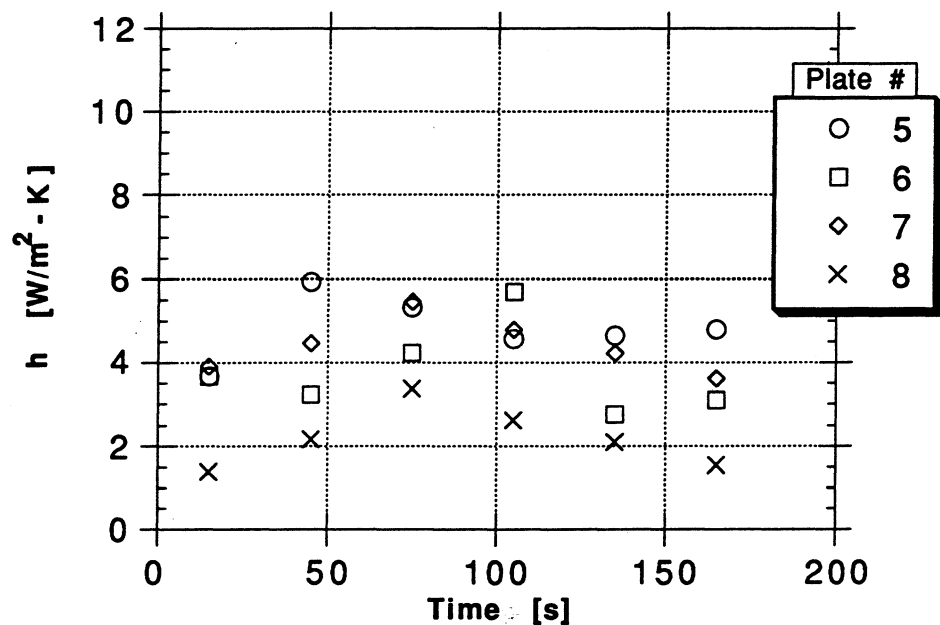


Figure 4.10b. Left wall coefficients, lower division

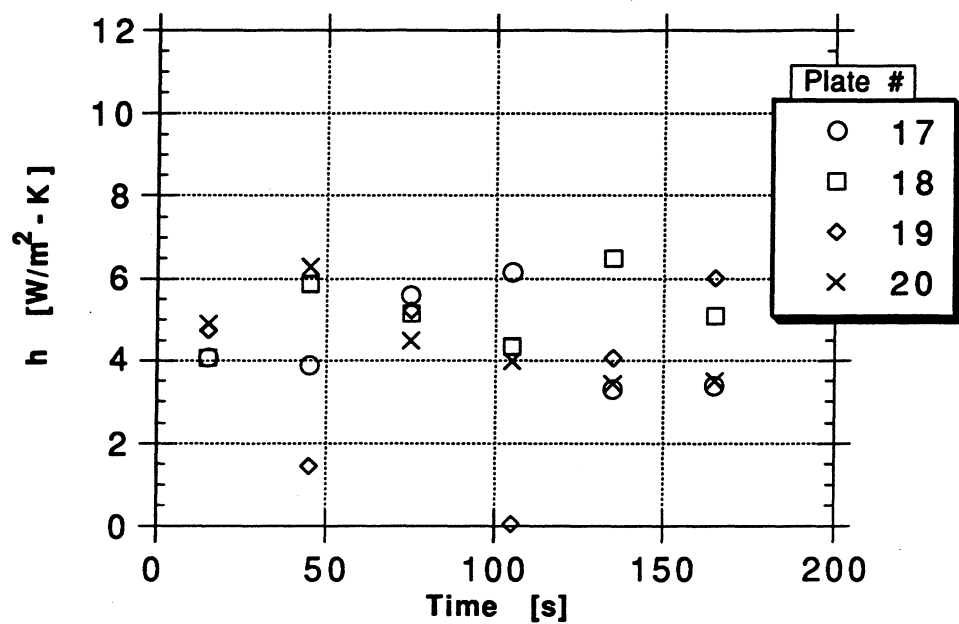


Figure 4.10c. Rear wall coefficients, upper division

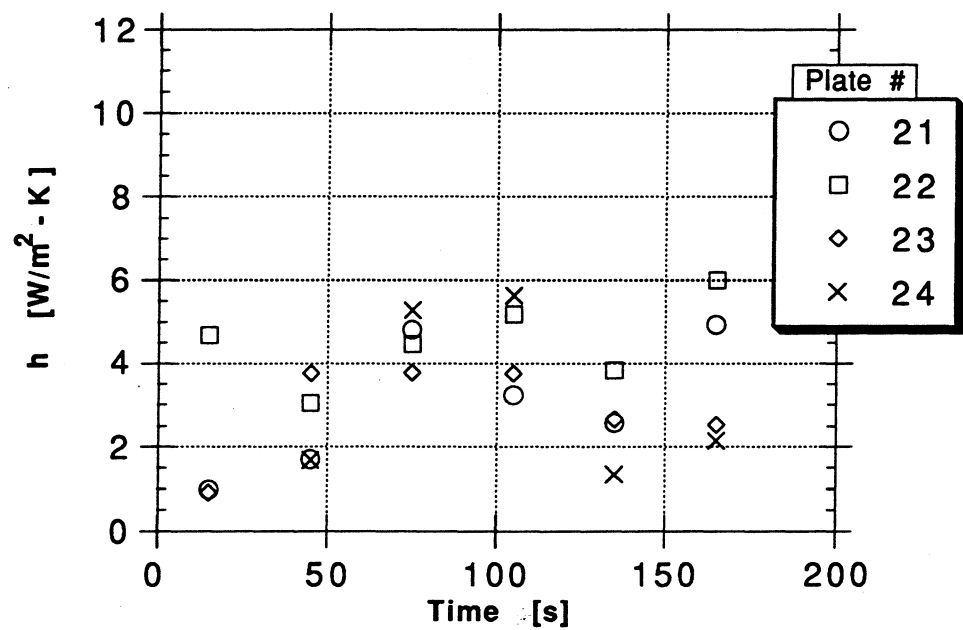


Figure 4.10d. Rear wall coefficients, lower division

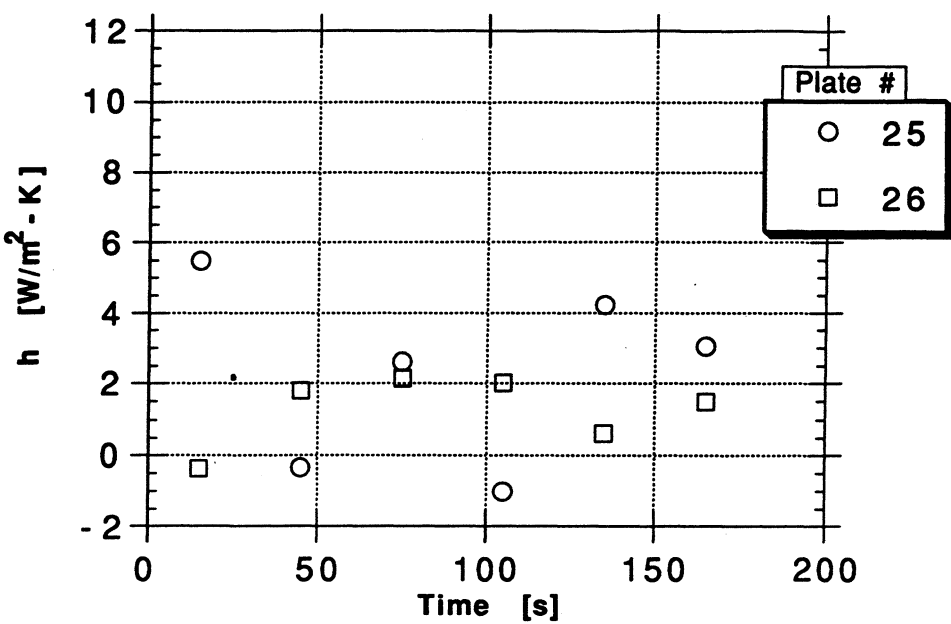


Figure 4.10e. Floor heat transfer coefficients

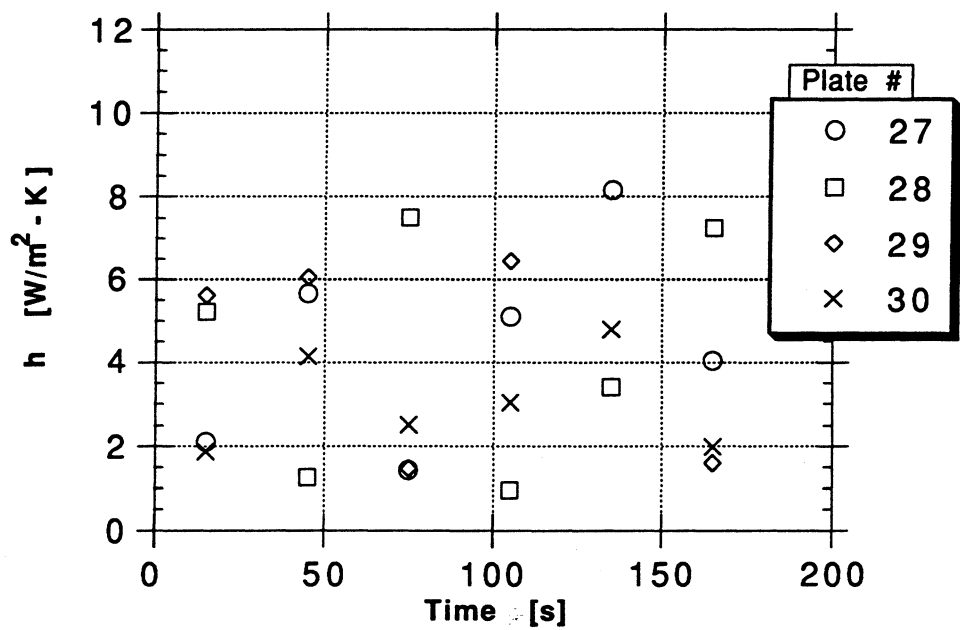


Figure 4.10f. Shelf heat transfer coefficients

the lower compartment division are less than the upper division by about 10 %. This is due to the more restricted flow. Once again, the top to bottom and front to back trends of Section 4.2.1 can be seen, but are not as strong because of the more restricted flow of the lower compartment division. The coefficients for both compartments are also less than that of the no shelf case. This is also expected, as there is less potential driving the flow (a lower wall height), and also, because the extra hoses added to the air flow system reduce cooling capacity, the temperature difference is not as high as in no shelf cases. The data for the right wall are similar to the left wall data.

Figures 4.10c and 4.10d show the data for the upper and lower divisions of the rear wall, respectively. These plots both indicate that the rear wall receives a more unstable flow than the right or left walls. This instability is also present but not as pronounced in the no-shelf test runs. The upper compartment division also seems to be more stable than the lower division on the rear wall due to the previously described flow conditions. The large perturbations are only present in one upper rear wall plate, 19, and are present in two lower rear wall plates, 21 and 24. This does not indicate that only these plates receive the unstable flow, just that it may be more unstable in these areas.

The data for the floor section can be found in Figure 4.10e. The floor coefficients display an unstable condition, even negative heat transfer coefficients. This again is caused by the type of flow entering the lower compartment. Plate 25 has the most unstable data set, with two points below zero. One should note that these points are near zero, and likely represent a stagnation condition

during eddy flow, as there is no source of cold air to force a negative heat transfer coefficient. Plate 26, the front plate on the floor, has a more stable coefficient. The front plate receives both kinds of flow, eddy and no-eddy, so its coefficients are less affected.

Figure 4.10f show the heat transfer coefficients for the shelf calorimeters. Plate 27, the front plate on the top of the shelf, and plate 28, the rear plate on the top of the shelf, show an alternation of heat transfer coefficient magnitude. This alternation is likely due to the alternation of eddy and no-eddy flow. Plate 29, the front plate on the underside of the shelf, also shows large fluctuations. During eddy flow, plate 29 receives warm air flowing into the compartment below these eddies. However, during no-eddy conditions, plate 29 is receiving air already cooled by the top compartment division, resulting in a lower coefficient. Plate 30, the rear underside plate, has the greatest stability, as it only receives minimal flow.

### 4.3 Energy Calculations

It is possible to calculate some energy loads on the refrigerator using known test conditions and the heat transfer coefficients. There are three main loads imposed on the refrigerator during a typical door opening. The first is that the warm air in the compartment must be recooled after the door is closed. The second load is the latent load contained in that air volume. The third load is the wall energy gains during the open door period. The third load has sensible, latent, and radiative components.

In order to calculate a total energy load, the ambient conditions must be specified, as well as the door opening schedule. For these calculations, it was assumed that a fresh food door opening averages 20 s, and that a freezer door opening averages 15 s. It was also assumed that there are 30 fresh food door openings and 20 freezer openings per day. The refrigerator used in the experiment has a yearly energy rating of \$64. This value is for an energy cost of \$.0675/kW-hr, so an average daily energy usage can be calculated to be 9640 kJ/day. A temperature difference of 20 K (36 °F) was assumed for the fresh food compartment, and 40 K (72 °F) for the freezer. A coefficient of performance of 1.1 was assumed for this refrigerator unit. The value of the fresh food wall heat transfer coefficient was changed to accommodate the humidity level, and freezer coefficients were assumed to be the half the value of the fresh food walls, from information gained in preliminary testing and trends shown by the shelf experiments. These assumptions were used for the values displayed in Table 4.1.

Three different humidity levels were chosen, to represent winter conditions (40 %), average conditions (70 %), and humid summer conditions (85 %). The percentage of the rated usage that this load represents increases significantly with an increase in humidity. Even though the freezer is smaller in volume and experiences less door openings than the fresh food compartment, the percentage loss is on the same order of magnitude of the fresh food compartment due to the much larger temperature difference. Alissi et al. gives larger figures for these conditions, about 32 % for a 91 % humidity case, but indicates that the fresh food compartment

**Table 4.1 Energy load calculations for daily door opening schedule and various humidity levels**

Mode of Energy Loss	Humidity Level		
	40 %	70 %	85 %
<b>Fresh Food Air Replacement:</b> kJ (Btu)	7.89 (7.48)	7.89 (7.48)	7.89 (7.48)
<b>Water Vapor Removal:</b> kJ (Btu)	6.28 (5.95)	11.0 (10.4)	13.3 (12.6)
<b>Wall Energy Gain:</b> kJ (Btu)	12.0 (11.4)	18.0 (17.1)	21.6 (20.5)
<b>Total Fresh Food Gain:</b> kJ (Btu)	26.2 (24.8)	36.9 (35.0)	42.8 (40.6)
<b>% of Rated energy usage</b>	7.9	11.1	12.9
<b>Freezer Air Replacement:</b> kJ (Btu)	7.69 (7.29)	7.69 (7.29)	7.69 (7.29)
<b>Water Vapor Removal:</b> kJ (Btu)	3.06 (2.90)	5.36 (5.08)	6.51 (6.17)
<b>Wall Energy Gain:</b> kJ (Btu)	5.86 (5.55)	10.3 (9.76)	14.6 (13.8)
<b>Total Freezer Gain:</b> kJ (Btu)	16.6 (15.7)	23.3 (22.1)	28.8 (27.3)
<b>% of rated energy usage</b>	5.01	7.03	8.71
<b>Total Refrigerator Gain:</b> kJ (Btu)	42.8 (40.6)	60.2 (57.1)	71.7 (68.0)
<b>% of Rated Energy Usage</b>	12.9	18.2	21.6

dominates the load. However, Alissi uses a freezer opening schedule of 16 times per 24 hr and a freezer open time of 15 s. The larger percent increase in energy usage would also include such factors as increased defrost time, some transient heat transfer after the door is closed, and the way in which the refrigerator disposes of these gains. Assuming current energy rates of \$.10/kW-hr, this refrigerator uses \$95 in energy a year. So the average load causes an increase in this value of 21 %, or \$20 a year.

#### 4.3 Nusselt and Rayleigh Numbers

Nusselt and Rayleigh numbers, as defined in Section 3.3, were calculated for all test runs, and the results are displayed in the summary tables found in Appendix D. All values were calculated based on air properties at the film temperature. The range of the Rayleigh numbers is about  $2 \times 10^8$  to  $1 \times 10^9$ . This range is very small in comparison to most published data, and in effect represents only one data point on the large scale. This range is also very close to the transition regime from laminar to turbulent, so the data is scattered. However, it is still possible to check correlations for the Rayleigh and Nusselt number correlations described in the literature. Figure 4.11 presents data from the right wall of the refrigerator compartment. The log of the Rayleigh number ranges from 8.36 to about 8.8, and the Nusselt number from about 1.98 to 2.16. If this is compared to the curve fit found in Incropera and DeWitt, pg. 392, the numbers are all in the approximate range of the

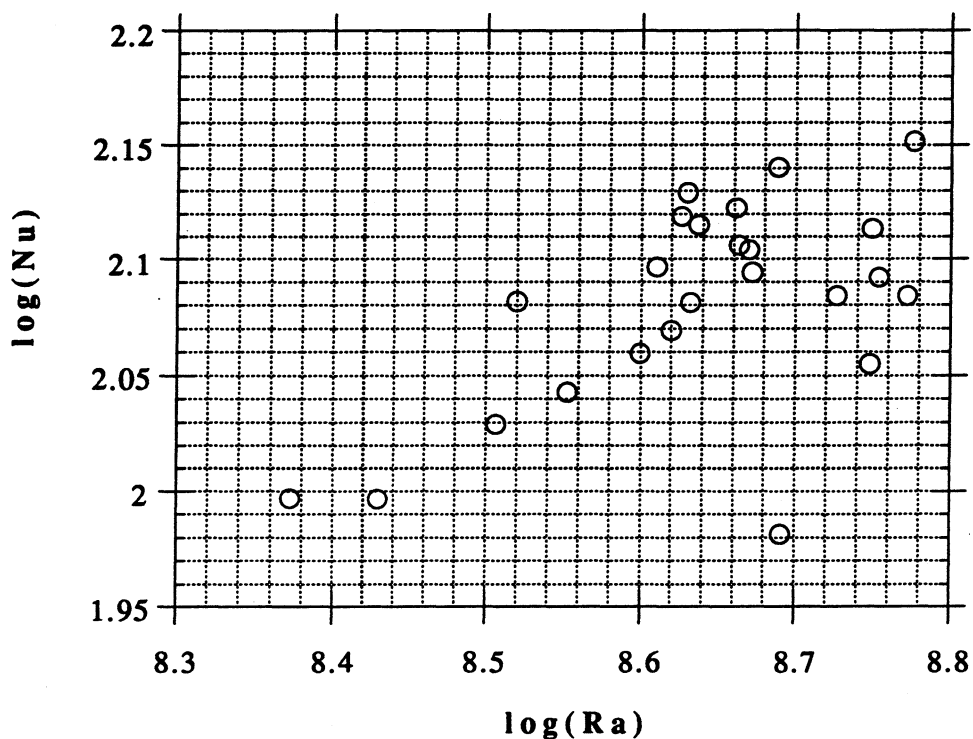


Figure 4.11. Nusselt and Rayleigh number comparison for right wall

curve fit on this graph, which has a value of 1.95 for  $\log(Nu)$  at a value of 8.5 for  $\log(Ra)$ , and an overall range of -1 to 14 for  $\log(Ra)$ .

The Rayleigh number in this experiment is a combination of the effects of temperature difference and mass concentration difference. The correlation presented in Eq. 3.3.10a has two terms, one for the temperature effect and one for the mass concentration. In this experiment, the mass concentration effect ranged from 0 to 11 % of the temperature effect, with an average of about 5 %. The main driving force for natural convection in this experiment is therefore the temperature difference. At  $T_{amb} = 295$  K (72 °F), a change from

a  $\Delta T = 10$  K ( $18$  °F) to  $\Delta T = 20$  K ( $36$  °F) more than doubles the Rayleigh number, increasing it by a factor of 2.17.

For the correlations made for the compartment data, the Nusselt number,  $Nu_L$ , is based on the characteristic length,  $L$ . The length used is the vertical height of the right, rear, and left walls, which is 0.61 m (2 ft). The same  $L$  is used for the Rayleigh number,  $Ra_L$ . A typical function which correlates the Nusselt and Rayleigh numbers is:

$$Nu_L = C Ra_L^{1/3} \quad (4.4.1)$$

This correlation assumes that the flow is in the turbulent region, an assumption that is also made for the compartment flow in this study. The constant  $C$  can be determined from a curve fit of the data, and for comparison, Incropera and Dewitt list this constant as 0.10.

Figures 4.12a-d show the  $Nu_L$  versus  $Ra_L$  correlations for all no-shelf tests. The data in all of these plots were also curve fit using Eq. 4.4.1, and the constant  $C$  is derived. Figure 4.12a shows the left wall data, and the corresponding curve fit. The derived constant is higher than the textbook value of 0.10, but the data is in the transition regime and has quite a bit of scatter. The  $Ra_L$  range of the data is also quite small.

These results compare extremely well with the right wall data, which are displayed in Figure 4.12b. The derived constant  $C$ , equal to 0.159, is essentially the same as that of the left wall. This would be expected as both have similar Nusselt numbers for any test.

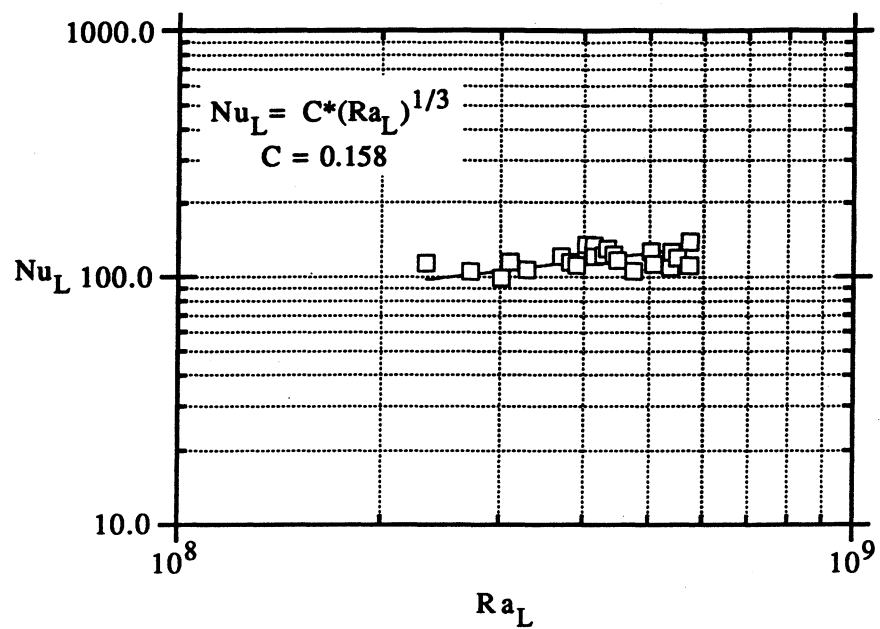


Figure 4.12a. Left wall:  $Nu_L$  versus  $Ra_L$  and curve fit

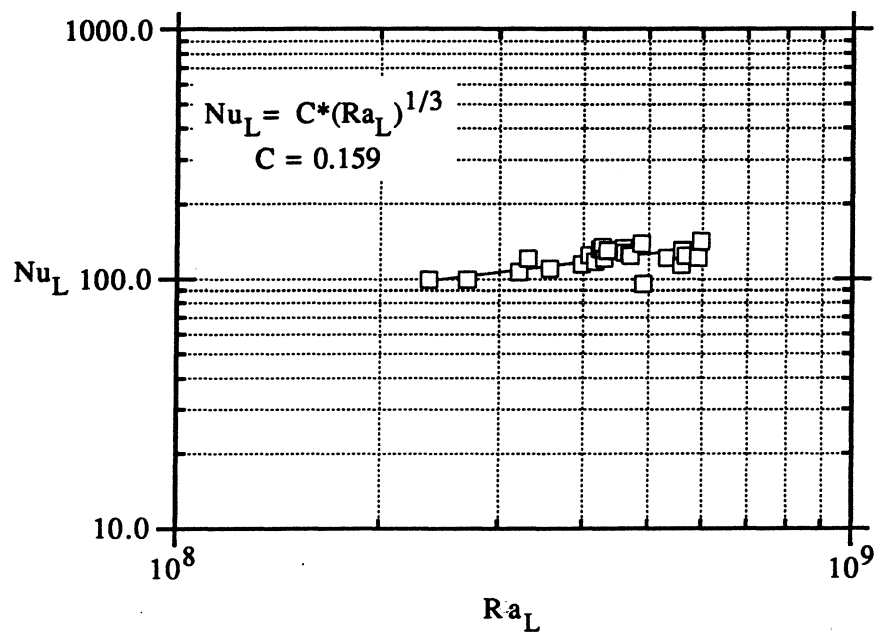


Figure 4.12b. Right wall:  $Nu_L$  versus  $Ra_L$  and curve fit

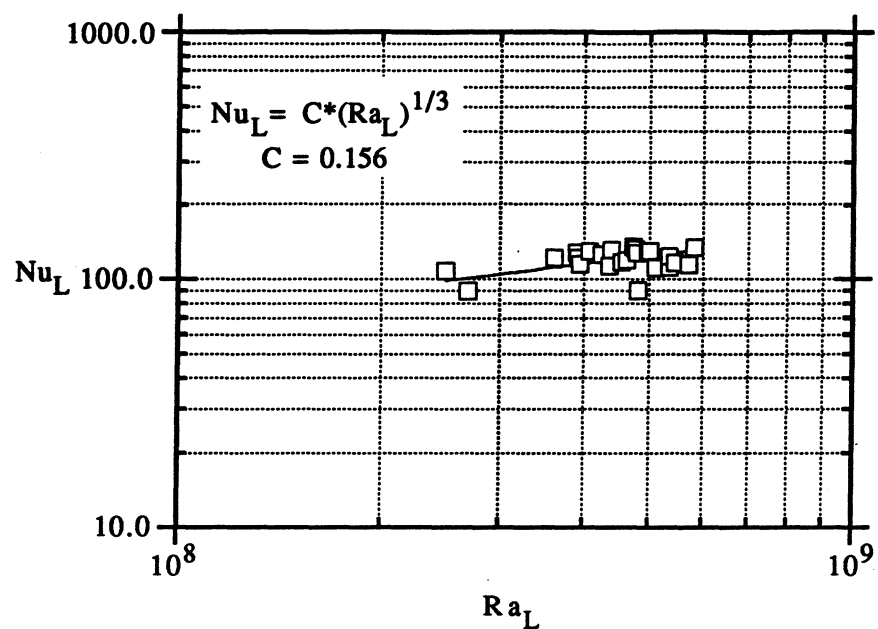


Figure 4.12c. Rear wall:  $Nu_L$  versus  $Ra_L$  and curve fit

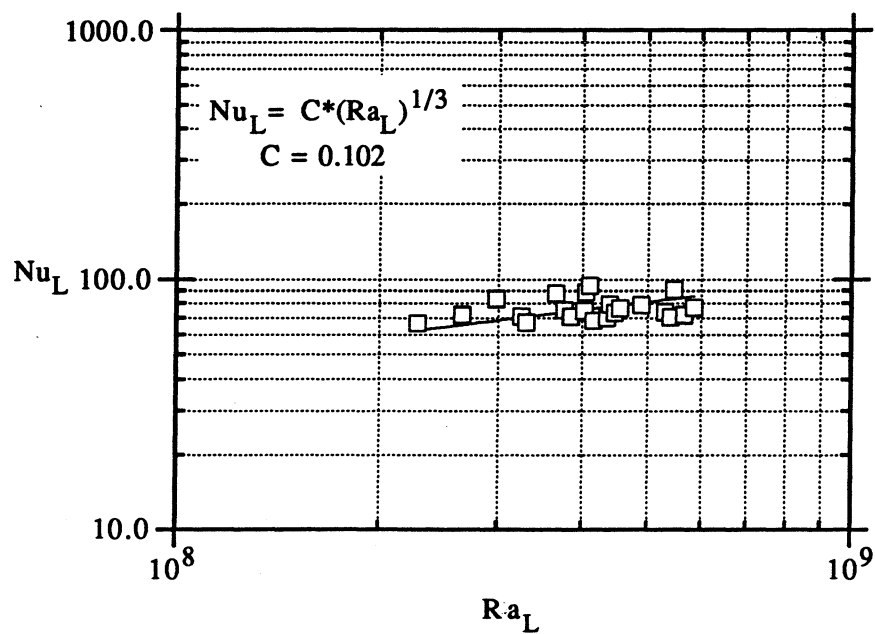


Figure 4.12d. Floor:  $Nu_L$  versus  $Ra_L$  and curve fit

One difference between the two is data scatter, which is not as prevalent on the right wall as the left. The rear wall also compares extremely well with the right and left walls, with the coefficient  $C = 0.156$ , as shown in Figure 4.12c. Again, the rear wall has the same vertical height as the right and left walls. This vertical height is the major driving force in free convection flows. The floor data, shown in Figure 4.12d, has different characteristics. The derived coefficient  $C = 0.102$  is 35 % lower than any of the vertical surfaces. Because the floor is a horizontal surface, the major flow driving force in this case are the surrounding vertical walls. The flow slows down as it passes over the horizontal surface, resulting in lower heat transfer coefficients, and therefore a lower  $Nu_L$  for the same  $Ra_L$ .

It is also possible to make a relation of the dimensionless heat transfer out of the compartment. The dimensionless heat transfer is defined as:

$$q^* = \frac{q}{L(T_{amb} - T_p)k_{amb}} \quad (4.4.2)$$

which, in this experiment, can be reduced to:

$$q^* = \frac{hA_s}{Lk_{amb}} \quad (4.4.3)$$

The  $q^*$  for each wall is calculated, and all values for each test run are added to obtain the total  $q^*$  for the entire compartment. The data for the no-shelf test runs and the corresponding curve fit can be found in Figure 4.13.

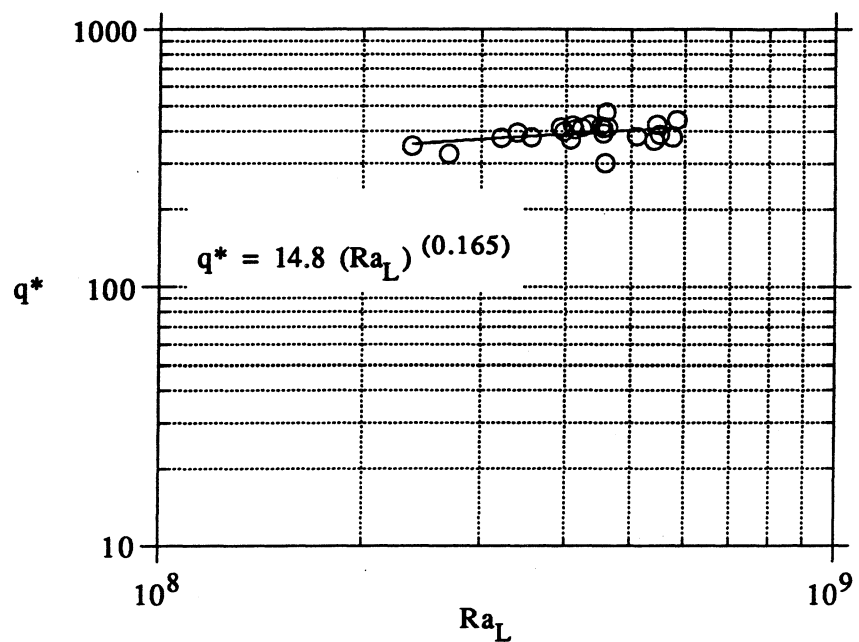


Figure 4.13. Dimensionless heat transfer versus  $Ra_L$ : no-shelf

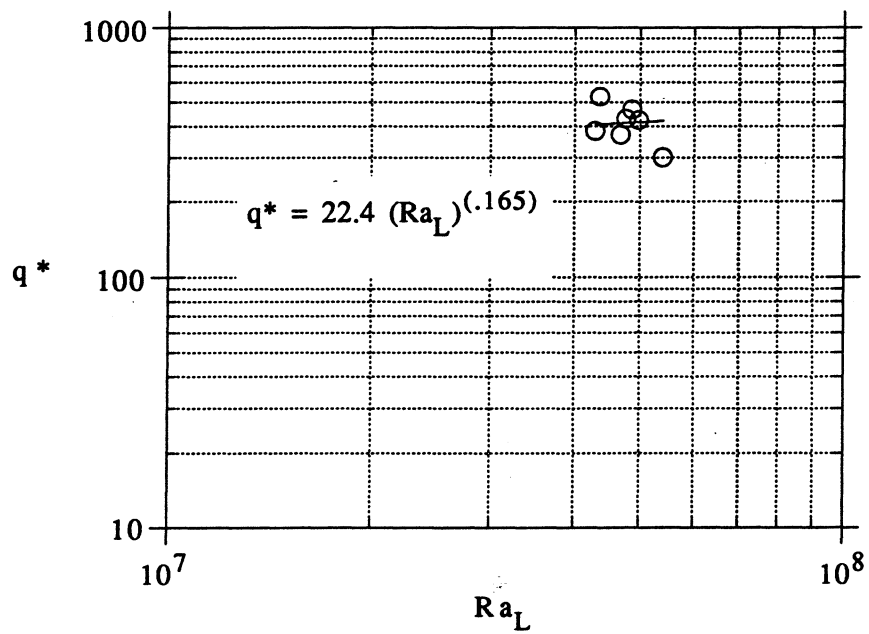


Figure 4.14. Dimensionless heat transfer versus  $Ra_L$ : 1-shelf

This heat transfer data can be compared to the tests with the shelf inserted. Figure 4.14 displays  $q^*$  for the seven shelf runs. The  $Ra_L$  range is on the order of  $5 \times 10^7$ , due to the fact that when the compartment is halved by the shelf, the characteristic length is also halved. There are only seven data points for the shelf tests, and they lie in close proximity, so the function and derived from Figure 4.12, with the same power value of 0.165, was forced through these points and a new coefficient obtained. The obtained coefficient, 22.4, is 50 % higher than that of the no shelf case, indicating that shelf addition causes a higher overall energy loss, due to the fact that heat transfer coefficients are not proportionally reduced with respect to the increase in instrumented surface area with shelf addition.

## 5. Conclusions

The following conclusions are drawn from the results of this investigation.

(1) The convective heat transfer coefficients for the walls and floor of the fresh food compartment are within a range of values from 2-8 W/m<sup>2</sup>-K (0.4-3.5 Btu/hr-ft<sup>2</sup>-°F) for typical operating conditions, with an average value of about 5 W/m<sup>2</sup>-K (0.9 Btu/hr-ft<sup>2</sup>-°F) being typical for the walls, and 3.5 W/m<sup>2</sup>-K (0.6 Btu/hr-ft<sup>2</sup>-°F) for the floor.

(2) The heat transfer coefficient values along the walls changes relative to the flow received. The top sections of the wall, which receive the warmest flow, have larger values than the lower plates on the wall, which receive the exit flow.

(3) The latent load is a significant contribution in a humid environment. At about 60 % relative humidity, the latent load equals the convective load.

(4) For typical plastic refrigerator linings, the radiative heat transfer coefficient is in the range of 2-3 W/m<sup>2</sup>-K (0.35-.5 Btu/hr-ft<sup>2</sup>-°F); thus, the radiative load represents about 50 % of the convective load. In the case of aluminum calorimeters does not pose a significant energy load, and can be easily separated from the convective load.

(5) The buoyancy term of the Rayleigh number is more greatly affected by temperature difference changes than by mass concentration differences, as the density difference caused by mass

concentration is only 5 % the value of the density difference caused by temperature differences under typical operating conditions.

(6) Shelf addition causes a reduction in the values of average convective heat transfer coefficients by about 20 %, however the overall energy loss is greater, due to the increased surface area.

(7) Alissi et al. (1987) found that for a typical door opening schedule, the load for conditions of 91 % relative humidity and a 20 K (36°F) temperature difference accounted for a 32 % increase in energy usage, as compared to a 22 % increase for similar conditions in this study. However, Alissi et al. used a "power plug" study, taking measurements of energy usage with a power meter, which would account for transient effects, increased defrost time, etc.

## References

- Alissi, M.S., Ramadhyabi, S., and Schoenals, R.J., 1988, "Effects of Ambient Temperature, Ambient Humidity, and Door Openings on Energy Consumption of a Household Refrigerator-Freezer", *ASHRAE Transactions*, Vol. 94, Pt. 2.
- Angirasa, D., Srinivasan, J., 1989, "Natural Convection Flows Due to the Combined Buoyancy of Heat and Mass Diffusion in a Thermally Stratified Medium", *ASME Journal of Heat Transfer*, Vol. 111, pp. 657-663.
- Clausing, A.M., 1982, "Simple Functional Representations for Thermophysical Properties of Gases at Standard Pressure", *ASHRAE Transactions*, Vol. 88, Pt. 2.
- Clausing, A.M., Lister, L.D., and Waldvogel, J.M., 1987, "Natural Convection from Isothermal Cubical Cavities with a Variety of Side-Facing Aperatures", *ASME Journal of Heat Transfer*, Vol. 109, pp. 407-412.
- Clausing, A.M., Debaillie, L.P., and Lister, L.D., 1991, "Interzonal Natural Convective Heat Transfer Between Isothermal Cubic Zones Using a Cryogenic Facility", *Proceedings of the 1992 ASME/JSME/KSES International Solar Energy Conference*, April 1992, pp. 425-431.
- Debaillie, L. P., "An Experimental Investigation of Interzone Natural Convective Heat Transfer Using the Cryogenic Method", Master's Thesis, University of Illinois, 1991.
- Dugenske, J.D., "An Investigation of Cabinet Loading on a Household Refrigerator", Master's Thesis, University of Illinois, 1990.
- Gebhart, B., and Pera, L., 1971, "The Nature of Vertical Natural Convection Flows Resulting from the Combined Buoyancy Effects of Thermal and Mass Diffusion", *International Journal of Heat and Mass Transfer*, Vol. 14, pp. 2025-2050.
- Howell, J.R., and Buckius, R.O., *Fundamentals of Engineering Thermodynamics*, McGraw-Hill, Inc., New York, 1987.

Incropera, F.P. and DeWitt, D.P., *Fundamentals of Heat and Mass Transfer*, 2nd ed., John Wiley & Sons, New York, 1985.

Meier, A.K., Heinemeier, K.E., 1988, "Energy Use of Residential Refrigerators: A Comparison of Laboratory and Field Use", *ASHRAE Transactions*, Vol. 94, Pt. 2.

Turiel, I., Heydari, A., 1988, "Analysis of Design Options to Improve the Efficiency of Refrigerator-Freezers and Freezers", *ASHRAE Transactions*, Vol. 94, Pt. 2.

## Appendix A: Data Reduction Routine

The code presented in this section was written by Mark Laleman throughout the course of the project. All borrowed subroutines give credit to other when credit is due. Further discussion of subroutines and fuctions can be found in Section 3.6.

!Program to evaluate heat transfer coefficients from raw data  
!Written by Mark Laleman, May 1991

```
OPTION NOLET
SET MARGIN 300
RUN$= "9"
RH=.70          !relative humidity
ZZ=6           !number of data points for output
YY=180/ZZ      !time step
NGAS=1          !NGAS=1 is air
DIM TEMPS(181,29),TEMPSA(181,57),H(10,26),f(60,2),y(60)
DIM AVH(26),AVGT(4),HA(4),HR(5),HRM(5),HRB(5),Q(6),EM(6)
DIM FF(6,6),SF(6,6),SFM(6,6),SINFO(3),A(6),T(6),TM(6),TB(6),E(6)
DIM SLOPE(10,26),NU(4),RA(4)
```

!TEMPSA is the original temperature matrix from the data acquisition  
!TEMPS is the temperature matrix after plate TC's are averaged.

!H is the matrix of heat transfer coefficients(HTC's)

!f and y are function matrices for the least squares operation

!SLOPE is the matrix of temperature slopes for each plate, gained  
!from the least squares routine

!AVH is the matrix of average plate HTC's

!AVGT is the matrix of average wall temperatures

!HA is the matrix of average wall HTC's

!HR,HRM, and HRB are matrices of radiative HTC's for no shelf and  
!one or two shelf conditions

!Q is the matrix of radiative heat transfer rate

!EM and E are emissivity matrices for the walls

!FF is the matrix of view factors for the compartment

!SF and SFM are the scriptF matrices for no-shelf and shelf conditions

!SINFO contains compartment measurements

!A is the wall area matrix

!T, TM, and TB are the average temperatures of individual

!compartments for shelving conditions

!NU and RA are matrices of wall Nusselt and Rayleigh numbers

```

MAT H=zer(ZZ,26)
MAT SLOPE=zer(ZZ,26)
DECLARE DEF OPPVIEW,ADJVIEW

CALL INPUT1(TEMPSA,RUN$)
CALL AVG(TEMPSA,TEMPS)
CALL CORRE(TEMPSA,TEMPS,AVGT)
CALL GASPT(NGAS,TEMPS(1,28),RHO,XMU,XK,CP,GRB,PR,IER)
FOR I=2 TO 27
  FOR J=1 TO ZZ
    CALL FEV(f,y,TEMPS,I,J,ZZ,YY)
    CALL ls(f,y,SLOPE(J,I-1))
  NEXT J
NEXT I
CALL HTCOEFF(TEMPS,H,SLOPE,ZZ,YY,cw,camb,AVGT,XK,RHO,CP,RH)
CALL INFO(SINFO,A,T,E,EM,SHELVES,TEMPS)
CALL VIEWS(FF,SINFO,A)
CALL SCRIPTF(A,FF,E,SF)
CALL COMP(SHELVES,TB,TM,T)
CALL QRAD(SF,T,Q,A)
CALL COEFF(Q,T,HR)
IF SHELVES>0 THEN
  CALL SCRIPTF(A,F,EM,SFM)
  CALL QRAD(SFM,TB,Q,A)
  CALL COEFF(Q,TB,HRB)
END IF
IF SHELVES>1 THEN
  CALL QRAD(SFM,TM,Q,A)
  CALL COEFF(Q,TM,HRM)
END IF
CALL CORR(H,AVH,ZZ)
CALL AVERG(H,AVH,ZZ,HA,RUN$)
CALL NURA(XK,RHO,XMU,GRB,CP,cw,camb,HA,AVGT,TEMPS,NU,RA)
CALL OUTPUT2(H,TEMPS,HR,ZZ,YY,RUN$,NU,RA,AVGT,HA,RH)
END

SUB INPUT1(TEMPSA(,),RUN$)
  !Input temperature matrix from converted IBM file
  F$="TEMP" & RUN$
  OPEN #1:name F$, create old, org text
  MAT INPUT #1:TEMPSA
  CLOSE #1

```

END SUB

SUB AVG(TEMPSA(,),TEMPS(,))

!Average both thermocouples in each plate together for data  
!smoothing

FOR I=1 TO 181

  TEMPS(I,1)=TEMPSA(I,1)

  TEMPS(I,28)=TEMPSA(I,54)

  TEMPS(I,29)=TEMPSA(I,55)

  FOR J=2 TO 52 STEP 2

    TEMPS(I,J/2+1)=(TEMPSA(I,J)+TEMPSA(I,J+1))/2

  NEXT J

NEXT I

END SUB

SUB CORRE(TEMPSA(,),TEMPS(,),AVGT())

!Correct TEMPS matrix for plates with one bad thermocouple

FOR I=1 TO 181

  TEMPS(I,4)=TEMPSA(I,6)

  TEMPS(I,12)=TEMPSA(I,22)

  TEMPS(I,20)=TEMPSA(I,38)

  TEMPS(I,23)=TEMPSA(I,45)

  TEMPS(I,7)=TEMPSA(I,12)

  TEMPS(I,26)=TEMPSA(I,51)

NEXT I

!calculate average wall temperature over test run

FOR I=1 TO 180

  FOR J=2 TO 9

    AVGT(1)=AVGT(1)+TEMPS(I,J)/1440

    AVGT(2)=AVGT(2)+TEMPS(I,J+8)/1440

    AVGT(3)=AVGT(3)+TEMPS(I,J+16)/1440

  NEXT J

    AVGT(4)=AVGT(4)+(TEMPS(I,26)+TEMPS(I,27))/360

NEXT I

END SUB

SUB

HTCOEFF(TEMPS(,),H(,),SLOPE(,),ZZ,YY,cw,camb,AVGT(),XK,RHO,CP,RH)

!calculate mass transfer information

MW=18    !molecular weight of water

```

R=8315           !universal gas constant
hfg=2.456E6     !latent heat of water
pamb=2340 + ((TEMPS(1,28)-293.15)*166)
IF AVGT(1) > 278.15 THEN
    pw=870 + ((AVGT(1)-278.15)*72)      !partial pressures of water
ELSE IF AVGT(1)> 273.15 THEN
    pw=610 + ((AVGT(1)-273.15)*52)
ELSE
    pw=450 + ((AVGT(1)-268.15)*32)
END IF
alpha=XK/(RHO*CP)          !air properties
d=25E-6
camb=pamb*MW/(R*TEMPS(1,28))*RH
cw=pw*MW/(R*AVGT(1))       !species concentrations
IF AVGT(1)>290 THEN
    massfactor=0             !no mass transfer in hot runs
ELSE
    massfactor=hfg*(D)^(2/3)*(alpha)^(1/3)/XK*(camb-cw)
END IF
FOR I=2 TO 27
    IF I>25 THEN
        mc=1947.3            !plate properties
        A=.119
    ELSE IF I>7 AND I<17 THEN
        mc=584.2
        A=.0334
    ELSE
        mc=389.5
        A=.0218
    END IF
    FOR J=1 TO ZZ
        Tavg=0
        Tamb=0
        FOR X=(1+YY*(J-1)) TO (YY+YY*(J-1))
            Tavg=Tavg+TEMPS(X,I)
            Tamb=Tamb+TEMPS(X,29) !average temperatures over
                                !time interval
        NEXT X
        Tdel=(Tamb-Tavg)/YY
        H(J,I-1)=.9*mc*SLOPE(J,I-1)/(A*(Tdel+massfactor))
    NEXT J           !calculate H with correction factor=.9
NEXT I
MAT PRINT AVGT

```

END SUB

\*\*\*\*\*  
! RAYLEIGH AND NUSSELT NUMBER ROUTINE  
\*\*\*\*\*

SUB

NURA(XK,RHO,XMU,GRB,CP,cw,camb,HA(),AVGT(),TEMPS(),NU(),RA())

!calculate nusselt and Rayleigh numbers

v=XMU/RHO !kinematic viscosity

alpha=XK/(RHO\*CP)

MWA=28.97

MWW=18 !molecular weights of air and water

L=.61 !characteristic length

P=RHO !air density

G=9.81 !gravity

BS=(MWA/MWW-1)/P !beta star(mass transfer)

B=GRB\*v^2/G !beta(temperature difference)

print camb,cw

BFACTOR=BS\*(camb-cw)/(B\*(TEMPS(1,28)-AVGT(1))) !check

correlation

PRINT "Bfactor=",BFACTOR

FOR I=1 TO 4

NU(I)=HA(I)\*L/XK !calculate Ra and Nu

RA(I)=(GRB\*(TEMPS(1,28)-AVGT(I))\*v/alpha+BS\*G\*(camb-cw)/(v\*alpha))\*L^3

PRINT "NU",I,"=",NU(I)

PRINT "RA",I,"=",RA(I)

NEXT I

END SUB

SUB FEV(f(),y(),TEMPS(),I,J,ZZ,YY)

!subroutine to set up function matrix for linear least squares fit

MAT f=con(YY,2)

MAT Y=zer(YY)

FOR K=1 TO YY

f(K,2)=TEMPS(K+(YY\*(J-1)),1)

y(K)=TEMPS(K+(YY\*(J-1)),I)

NEXT K

END SUB

```

SUB ls(f(),y(),Slope)
! title: LS-Least Squares Routine
! subroutine to do least squares fit using normal equations
! c o pedersen
! univ of ill
!
! inputs
!   f(nobs,ncoef) = array of function values evaluated
!                     at the observation points
!   y(nobs) = array of dependent variable values
!
!   nobs= number of observations
!   ncoef= number of coefficients in fit
!
! output
!   coef(ncoef) = array of coefficients
!   yc(nobs) = calculated values of fit corresponding to y
!   detr = the value of the determinant of ftf (indicates
!         condition and possible bad fit)
DIM ft(10,50)
DIM ftf(10,10),fty(10),ftfinv(10,10),coef(2)
LET ncoef=2           ! number of coefficients in model
LET nobs=size(y)      ! number of observations (data points).
!   resize and initialize
!MAT yc=zer(nobs)
MAT ft=zer(ncoef,nobs)
MAT ftf=zer(ncoef,ncoef)
MAT fty=zer(ncoef)
MAT coef=zer(ncoef)
MAT ftfinv=zer(ncoef,ncoef)
!
!   set up normal equation system
!
MAT ft=trn(f)
MAT ftf=ft*f
MAT fty=ft*y
!
!   solve the linear system
!
MAT ftfinv=inv(ftf)
MAT coef=ftfinv*fty
!
!   calculate the fit at obs points

```

```

!
!MAT yc=f*coef
!LET detr=det(ftf)
SLOPE=coef(2)
END SUB

SUB AVERG(H(),AVH(),ZZ,HA(),RUN$)
  !calculate average H for each plate and each wall
  FOR I= 1 TO 26
    FOR J=1 TO ZZ
      AVH(I)=AVH(I)+H(J,I)
    NEXT J
    AVH(I)=AVH(I)/ZZ          !for each plate
  NEXT I
  F$="Plate Averages" & RUN$
  OPEN #1: name F$, create newold
  ERASE #1
  FOR I=1 TO 26
    PRINT #1: I;CHR$(009);AVH(I)
  NEXT I
  CLOSE #1
  FOR I=1 TO 8
    FOR J=1 TO ZZ
      HA(1)=HA(1)+H(J,I)/(8*ZZ)      !for each wall
      HA(2)=HA(2)+H(J,8+I)/(8*ZZ)
      HA(3)=HA(3)+H(J,16+I)/(8*ZZ)
    NEXT J
  NEXT I
  FOR I=1 TO ZZ
    HA(4)=HA(4)+(H(I,25)+H(I,26))/(2*ZZ)
  NEXT I
  MAT PRINT HA

END SUB

SUB
OUTPUT2(H(),TEMPS(),HR(),ZZ,YY,RUN$,NU(),RA(),AVGT(),HA(),RH)
!Subroutine to output results to individual wall files
F$= "HTC" & RUN$
OPEN #2: name F$, create newold
ERASE #2
SET #2: margin 450
PRINT #2: "Heat Transfer Coefficients"

```

```

FOR I=1 TO ZZ
    PRINT #2: YY*(I-1)+YY/2;chr$(009);
    FOR J=2 TO 27
        PRINT #2: H(I,J-1);chr$(009);
    NEXT J
    PRINT #2
NEXT I
PRINT #2:

FOR I=1 TO ZZ
    PRINT YY*(I-1)+YY/2;chr$(009);
    FOR J=2 TO 27
        PRINT H(I,J-1);chr$(009);
    NEXT J
    PRINT
NEXT I
CLOSE #2
F2$= "SUMMARY" & RUN$
OPEN #3: name F2$, create newold
ERASE #3
SET #3: margin 300
SET #3: zonewidth 15
PRINT #3:"Test #",RUN$
PRINT #3:
PRINT #3:"", "Left Wall", "Right Wall", "Rear Wall", "Floor"
PRINT
#3: _____
"_____
PRINT #3:"Avg. HTC's", HA(1), HA(2), HA(3), HA(4)
PRINT #3:"(W/m^2-K)"
PRINT #3:"Avg. Temps(K)", AVGT(1), AVGT(2), AVGT(3), AVGT(4)
PRINT #3:
PRINT #3:"Rayleigh #", RA(1), RA(2), RA(3), RA(4)
PRINT #3:
PRINT #3:"Nusselt #", NU(1), NU(2), NU(3), NU(4)
PRINT #3:
PRINT #3:"Relative Hum.=", RH
CLOSE #3
END SUB
*****!
!      SUBROUTINE TO DETERMINE COMPARTMENT
!          CHARACTERISTICS
!
```

```

!*****
SUB INFO(SINFO(),A(),T(),E(),EM(),SHELVES,TEMPS())
!subroutine returns sinfo and a
  SHELVES=0          !number of shelves
  SINFO(1)=.635/(SHELVES+1)  !divide compartment height by no.
                           !of shelves
  SINFO(2)=.6604
  SINFO(3)=.4318
  A(1)=SINFO(2)*SINFO(3)      !Calculate areas
  A(2)=A(1)
  A(3)=SINFO(1)*SINFO(3)
  A(4)=A(3)
  A(5)=SINFO(1)*SINFO(2)
  A(6)=A(5)
FOR I=2 TO 9
  TL=TEMPS(1,I)+TL
  TR=TEMPS(1,I+8)+TR
  TB=TEMPS(1,I)+TB
NEXT I
  !Input initial temperatures
  T(2)=(TEMPS(1,26)+TEMPS(1,27))/2
  T(3)=TL/8
  T(4)=TR/8
  T(5)=TB/8
  T(6)=TEMPS(1,28)
  T(1)=T(5)
FOR I= 2 TO 5           !Input emmissivities
  E(I)=.1
NEXT I
  E(1)=.9
  E(6)=.9999
MAT EM=E
IF SHELVES>0 THEN
  EM(1)=EM(2)
END IF
END SUB
!*****
!      DEFINITIONS FOR VIEW FACTORS OF OPPOSING AND
!          ADJACENT RECTANGLES
!*****
```

DEF OPPVIEW(L,W,H)  
 X=W/L

```

Y=H/L
A=LOG(((1+X^2)*(1+Y^2)/(1+X^2+Y^2))^.5)
B=Y*SQR(1+X^2)*ATN(Y/SQR(1+X^2))
C=X*SQR(1+Y^2)*ATN(X/SQR(1+Y^2))
D=X*ATN(X)+Y*ATN(Y)
OPPVIEW=2/(PI*X*Y)*(A+B+C-D)
END DEF

```

```

DEF ADJVIEW(L1,L2,W)
H=L2/W
W=L1/W
A=W*ATN(1/W)+H*ATN(1/H)
B=SQR(H^2+W^2)*ATN(1/SQR(H^2+W^2))
C=((1+W^2)*(1+H^2))/(1+W^2+H^2)
D=((W^2*(1+W^2+H^2))/((1+W^2)*(W^2+H^2)))^(W^2)
E=((H^2*(1+W^2+H^2))/((1+H^2)*(W^2+H^2)))^(H^2)
ADJVIEW=1/(W*PI)*(A-B+.25*LOG(C*D*E))
END DEF

```

```

!*****SUBROUTINE TO CALCULATE THE VIEW FACTORS*****
!*****SUBROUTINE TO CALCULATE THE VIEW FACTORS*****
SUB VIEWS(F(),SINFO(),A())
!subroutine inputs sinfo and a and outputs f
DECLARE DEF OPPVIEW,ADJVIEW           !Self view factors
FOR I=1 TO 6
  F(I,I)=0
NEXT I
F(1,2)=OPPVIEW(SINFO(1),SINFO(2),SINFO(3))      !surface 1 and 2's
                                                   !views
F(2,1)=F(1,2)
F(1,3)=ADJVIEW(SINFO(2),SINFO(1),SINFO(3))
F(1,4)=F(1,3)
F(1,5)=ADJVIEW(SINFO(3),SINFO(1),SINFO(2))
F(1,6)=F(1,5)
FOR I=3 TO 6          !reciprocity
  F(2,I)=F(1,I)
  F(I,1)=A(1)/A(I)*F(1,I)
  F(I,2)=A(1)/A(I)*F(1,I)
NEXT I
F(3,4)=OPPVIEW(SINFO(2),SINFO(3),SINFO(1))      !surface 3 and 4's
                                                   !views
F(4,3)=F(3,4)
F(4,5)=ADJVIEW(SINFO(3),SINFO(2),SINFO(1))

```

```

F(4,6)=F(4,5)
F(3,5)=F(4,5)
F(3,6)=F(4,5)
FOR I=5 TO 6           !reciprocity
    F(I,3)=A(3)/A(I)*F(3,I)
    F(I,4)=A(4)/A(I)*F(4,I)
NEXT I
F(5,6)=OPPVIEW(SINFO(3),SINFO(1),SINFO(2))      !remaining view
                                                    !factors
F(6,5)=F(5,6)
END SUB

```

```

!*****
SUB scriptf(a(),f(),emiss(),sf())
    !      script f calculation subroutine
    !      c o pedersen, mech and ind eng, university of illinois
    !      input:
    !          a=area vector- assumed to be n elements long
    !          f= direct view factor matrix (n x n)
    !          emiss = vector of surface emissivities (n)
    !          where: n = number of surfaces
    !      output: sf = matrix of script f factors (n x n)
    !      local variables:
    !          af= (area * direct view factor) matrix
    !          cmtrx = (af- emiss/reflectance) matrix
    !          excit = excitation vector = a*emiss/reflectance
    !          jmtrx = matrix of partial radiosities
    DIM jmtrx(10,10),excit(10,10),cmtrx(10,10)
    DIM af(10,10),cinv(10,10)
    ! zero and resize arrays
LET n=size(a)
MAT af=zer(n,n)
MAT cmtrx=zer(n,n)
MAT cinv=zer(n,n)
MAT excit=zer(n,n)
MAT jmtrx=zer(n,n)
MAT sf=zer(n,n)
FOR i=1 to n
    FOR j = 1 to n
        LET af(i,j)=f(i,j)*a(i)
        LET cmtrx(i,j)=af(i,j)
    NEXT j
NEXT i

```

```

!
FOR i=1 to n
    LET excit(i,i)=-a(i)*emiss(i)/(1.-emiss(i))
    LET cmtrx(i,i)=af(i,i)-a(i)/(1.-emiss(i))
NEXT i
    ! solve the linear system
    MAT cinv=inv(cmtrx)
    MAT jmtrx=cinv*excit
FOR i=1 to n
    FOR j=1 to n
        IF i = j then
            LET delta=1.
        ELSE
            LET delta = 0.
        END IF
        LET sf(i,j)=emiss(i)/(1.-emiss(i))*(jmtrx(i,j)-delta*emiss(i))
    NEXT j
NEXT i
END SUB
*****
!
!      SUBROUTINE TO CALCULATE COMPARTMENTS AND
!      TEMPERATURES
!
SUB COMP(SHELVES,TB(),TM(),T())
!subroutine inputs no. of shelves and T and outputs revised T, TM, TB
    MAT TB=T
    MAT TM=T
    IF SHELVES>0 THEN
        T(2)=T(3)          !For one shelf
        TB(1)=T(3)
    END IF
    IF SHELVES>1 THEN
        TM(1)=T(3)          !for more than one shelf
        TM(2)=T(3)
    END IF
END SUB
*****
!
!      SUBROUTINE TO MAKE RADIATIVE CORRECTION
!
SUB CORR(HR(),H(),ZZ)
    FOR J=1 TO ZZ
        FOR I=1 TO 8
            H(J,I)=H(J,I)-HR(3)

```

```

        H(J,I+8)=H(J,I+8)-HR(4)
        H(J,I+16)=H(J,I+16)-HR(5)
NEXT I
        H(J,25)=H(J,25)-HR(2)
        H(J,26)=H(J,26)-HR(2)
NEXT J
END SUB
!*****
!      SUBROUTINE TO CALCULATE RADIATIVE HEAT
!      TRANSFER
!*****
SUB QRAD(SF(),T(),Q(),A())
!subroutine inputs SF, T, and A and outputs Q
    MAT Q=zer(6)
    FOR JJ=1 TO 6
    FOR II=1 TO 6
        RADD=SF(JJ,II)*(5.67E-8)*((T(II))4-(T(JJ))4)
        Q(JJ)=Q(JJ)+RADD
    NEXT II
    NEXT JJ
END SUB

!*****
!      SUBROUTINE TO CALCULATE TRANSFER COEFFICIENTS
!*****
SUB COEFF(Q(),T(),HR())
!Subroutine inputs Q and T and outputs HR
    FOR I=1 TO 5
        HR(I)=(Q(I)/(T(6)-T(I)))      !Hr=Q/(T-Tamb)
    NEXT I
END SUB

!*****
!      GAS PROPERTIES SUBROUTINE
!*****
SUB GASPT(NGAS,T,RHO,XMU,XK,CP,GRB,PR,IER)

!PROPERTIES OF GASES IN SI UNITS(T.GT.0) OR ENGLISH(T.LT.0)
!FUNCTIONAL REPRESENTATIONS IN THE FORM OF Y=A*T**B
!ARRAYS A AND B CONTAIN THE RESPECTIVE CONSTANTS
!INPUT
!NGAS- NGAS=1 IS AIR, NGAS=2 IS NITROGEN
!T-- ABSOLUTE TEMP.(K) OR NEGATIVE OF ABS TEMP(R)

```

!OUTPUT  
 !RHO--DENSITY  
 !XMU--VISCOSITY  
 !XK--TNERMAL CONDUCTIVITY  
 !CP-- SPECIFIC HEAT  
 !GRB--G\*BETA/XNU\*\*2  
 !PR--PRANDTL NUMBER  
 !IER--ERROR PARAMETER  
 !IER=1--GAS NUMBER DOES NOT EXIST. ASSUMED AIR  
 !IER=2-- TEMPERATURE IS OUT OF RANGE

```

DIM A(2,15),B(2,15),R(2,3)
MAT READ A
DATA 364.1,.1764E-6,.1423E-3,990.8,.4178E20,1.23
DATA 350.6,.4914E-6,.2494E-3,299.4,.4985E19,.59,.0,.0,.0
DATA 432.4,9.1E-8,1.239E-4,1553.,4.379E20,1.137
DATA 351.6,.18E-6,.221E-3,1031.,.408E20,.841,.0,.0,.0
MAT READ B
DATA -1.005,.814,.9138,.00316,-4.639,-.09685
DATA -.999,.6429,.8152,.1962,-4.284,.0239,.0,.0,.0
DATA -1.046,.938,.9466,-.079,-5.102,-.0872
DATA -1.005,.8058,.8345,.00239,-4.636,-.02652,.0,.0,.0
MAT READ R
DATA 150.,400.,2100.,83.,160.,450.
  
```

```

IER=0
IF NGAS<0 AND NGAS >3 THEN
  IER=1
  NGAS=1
END IF
I=1
TP=T
IF T<0 THEN TP=-T/1.8
IF (TP<R(NGAS,1) OR TP>R(NGAS,3)) THEN IER=2
IF TP>R(NGAS,2) THEN I=7
RHO=A(NGAS,I)*TP^B(NGAS,I)
  XMU=A(NGAS,I+1)*TP^B(NGAS,I+1)
  XK=A(NGAS,I+2)*TP^B(NGAS,I+2)
  CP=A(NGAS,I+3)*TP^B(NGAS,I+3)
  GRB=A(NGAS,I+4)*TP^B(NGAS,I+4)
  PR=A(NGAS,I+5)*TP^B(NGAS,I+5)
  IF T<0 THEN
    RHO=RHO/16.02
  
```

**XMU=XMU/1.488  
XK=XK/1.731  
CP=CP/4187.  
GRB=GRB/63.57  
END IF  
END SUB**

## Appendix B: Data Acquisition and Control System

Corresponding with the construction of the experimental apparatus was the purchase and assembly of a data acquisition and control system. The system itself was designed to meet the needs of a variety of experiments and is therefore a very flexible system.

The system consists of six DC power supplies, a data acquisition chassis, a computer, a rack of digital relays, and a variety of analog and digital inputs and outputs. A data acquisition and control software package orchestrates the interactions between these components and regulates outgoing signals as well as providing data storage.

External signals enter the system through a Keithley 500P data acquisition chassis. These signals consist of voltage and current measurements from the power supplies as well as thermocouple voltages. At present, a total of ninety-six thermocouple inputs are available with an optimal resolution of + 0.012 degrees C. The addition of more thermocouple input boards could expand the capability to 128 inputs. Also, special boards can be installed to allow strain gauge, thermistor, digital, or other standard data acquisition functions. The Keithley chassis can contain a total of nine interface boards, and its 16-bit A/D conversion allows for very high resolution.

The six DC power supplies consist of two Hewlett Packard and four Sorensens with a combined power of 7560 watts. The Sorensens are rated at 0-150 volts at a maximum of 12 amps, while the Hewlett Packards produce 0-60 volts at a maximum of 3 amps. All of the power supplies are computer-controlled, however the Sorensens may be operated manually if desired. Voltage measurements from the power supplies are fed into the Keithley acquisition chassis and are then routed to the computer. A voltage from the computer is buffered and fed into the control circuits of the power supplies. This voltage completes the loop and controls the output voltage of the power supplies. The software is responsible for reading the output voltage of the power supplies, comparing it with the intended setpoint, and adjusting the control voltage as needed. This arrangement allows the user to vary the output voltage of the power supplies from within a program. Computer-controlled safety relays are in place to disconnect the power supplies should they stray too far from the intended voltage setpoint. Fig. B.1 displays the system.

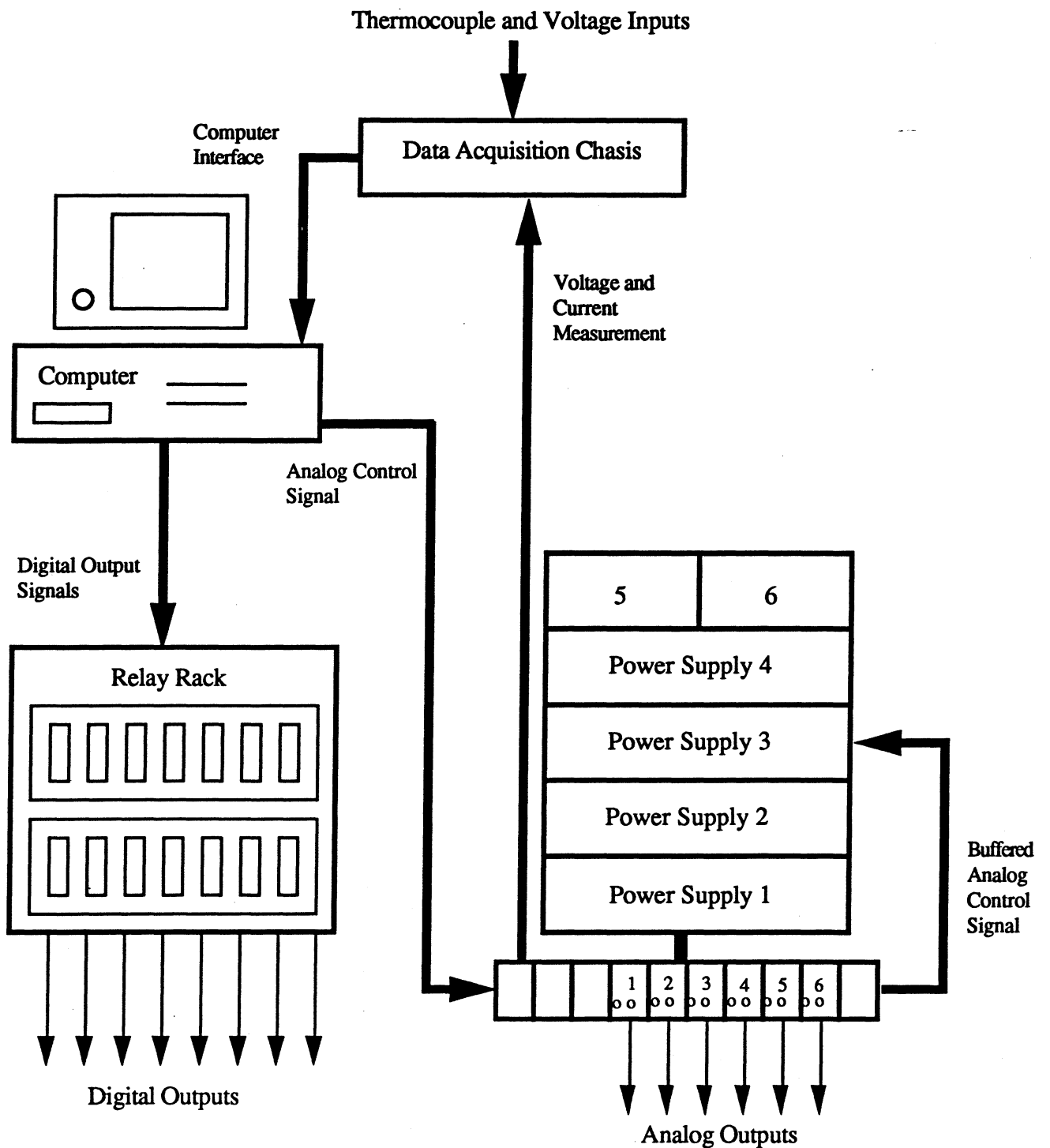


Fig. B.1. Data Acquisition and Control System

## Appendix C: Utility Programs

### C.1 ALPT(Aluminum properties subroutine)

```
SUB ALPT(T,CP,E,XK,RHO,IER)
!TRUE BASIC VERSION
!ORIGINAL SUBROUTINE BY A.M. CLAUSING
!GIVEN THE ABSOLUTE TEMPERATURE (K), THIS SUBROUTINE
!DETERMINES THE THERMAL PROPS. OF ALUMINUM ALLOY 6061-T6
!CP--SPECIFIC HEAT (J/KG-K); 70<T<500K
!RHO--DENSITY (KG/M3); 273,7,483
!E--HEMISPERICAL TOTAL EMISSIVITY; 0<T<850K
!XK--THERMAL CONDUCTIVITY (W/M-K); 100<T<400K
!IER--ERROR PARAMETER: IER=1--TEMPERATURE IS OUT OF RANGE
OPTION NOLET
RHOZ=2704.
RZ=1.505E-2
R1=3.79E-5
R2=4.59E-8
EZ=.04
E1=6.E-5
XKZ=86.6
XK1=.261
CPZ=689.6
CP1=.6741
AZ=-473.
A1=14.03
A2=-.05920033
A3=.11568388E-3
A4=-.82212796E-7
A5=0.
!CHECK IF TEMPERATURE IS IN PROPER RANGE--70<T<500K
IF T<70 OR T>500 THEN
    IER=1
    EXIT SUB
END IF
IER=0
!CALCULATE PROPERTIES FOR GIVEN TEMPERATURE
RHO=RHOZ*EXP(-RZ-R1*T-R2*T^2)
E=EZ+E1*T
XK=XKZ+XK1*T
IF T>273 THEN
    CP=CPZ+CP1*T
```

```

ELSE
  CP=AZ+T*(A1+T*(A2+T*(A3+T*(A4+T*A5))))
ENDIF
ENDSUB

```

## C.2 Refrigerator Wall Representation

The following describes the resistor network used to represent the refrigerator wall for heat transfer simulation purposes. Figure C.1 shows the resistor-capacitor set-up which describes the wall cross section itself.

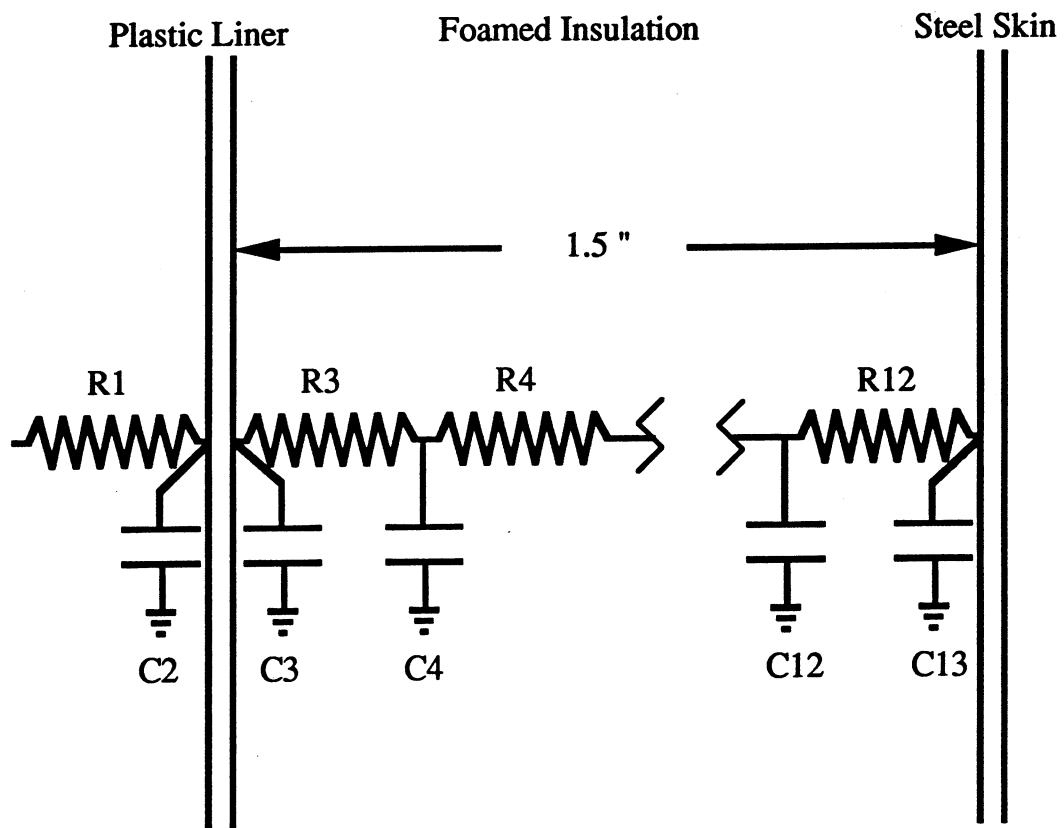


Figure C.1. Resistor network for refrigerator wall

Definitions for R and C

$$C_0 = \rho_0 c_{po} A_0 D_0 ; C = \rho_x c_{px} A_x D_x / C_0$$

$$R_o = \frac{D_o}{A_o k_o} ; R = \frac{D_x}{A_x k_x} / R_o$$

Values for  $C_0$  and  $R_0$  are reference values, and the properties of the foamed insulation are used.

$\rho_0$  = density = 16.0 kg/m<sup>3</sup> (0.998 lbm/ft<sup>3</sup>)

$c_{po}$  = specific heat = 1100 J/kg-K (263 Btu/lbm-°F)

$A_0$  = wall area = 3.44 m<sup>2</sup> (37 ft<sup>2</sup>)

$D_0$  = thickness = .038 m (1.5 in)

$k_0$  = thermal conductivity = .02 W/m-K (0.0116 Btu/hr-ft-°F)

$C_0$  = 2300 J/K (1211 Btu/°F)

$R_0$  = 0.552 K/W (1.05 hr-°F/BTU)

All values, once normalized, are in dimensionless form. Thick material is divided into a series of resistors, such as the insulation in this case, as is the capacitance. However, if the node is at an interface of two different materials, the capacitance at the interface is an average of the two values.

Values for this case:

$R1 = .105$

$C1 = 0.0$  (Air assumed 0.0 capacitance)

$R2 = .00667$

$C2 = 1.80556$

$R3-12 = .1$

$C3 = 1.8556$ ,  $C4-12 = .1$

$R13 = .0526$

$C13 = 8.2$

### C.3 HT10 Code(one dimensional heat transfer; Fortran)

The following code is used for all one dimensional heat transfer calculations done for this experiment. The program draws all of the necessary information from a data file, and outputs all information into a separate data file.

#### PROGRAM HT10A

C\*\*ONE-DIMENSIONAL TRANSIENT HEAT CONDUCTION PROGRAM

C\*\*Copyright 1988 by A.M.CLAUSING; All Rights Reserved

C\*\*THIS PROGRAM IS A GENERAL PROGRAM FOR THE SOLUTION OF

C\*\*ONE-DIMENSIONAL RC NETWORKS, VERSION = 21 OCTOBER 1989

LOGICAL SI,SECOND,RESET

CHARACTER UTIME,UNITQ\*7,UNITQT\*9,NTP(16)\*2

PARAMETER (NN=60,IUIN=5)

DIMENSION TT(NN),DE(NN),GE(NN),FE(NN)

```

C**INCLUDE definition of named common: BLK1, BLK2, and BLK4
$INCLUDE:HT10A$
    FUN2(TIME)=.0*TIME
        FUN1(TIME)=6.*SIN((TIME/2.880E3-1.)*2.*3.142/3)
C**DETERMINE DIRECTION OF OUTPUT AND READ FIRST CASE
    NCASE=1
    WRITE(0,118)
118   FORMAT(T10,'DIRECT OUTPUT TO://T20,'SCREEN:',T32,'Type 1'
    $ //T20,'PRINTER:',T32,'Type 2'//T20,'FILE ANS:',T32,
    $ 'Type 3'//'?')
    READ(*,*) IUOUTP
    IUOUT = IUOUTP - 1
1   CALL DATAIN(NCASE,IUOUT)
    NCASE=NCASE+1
C**Determine CHARACTER variables to specify units of output
    TSEC = DZ**2*RHOZ*CPZ/XKZ
    IF(SI) THEN
        TABS=273.15
        UNITQ='[W]'
        UNITQT='[W-h]'
        IF(SECOND)UNITQT='[J]'
    ELSE
        TABS=459.67
        TSEC=TSEC*3600.
        UNITQ='[BTU/h]'
        UNITQT='[BTU]'
        IF(SECOND)UNITQT='[BTU-s/h]'
    ENDIF
    IF(SECOND) THEN
        UTIME='s'
        TCONV=TSEC
    ELSE
        UTIME='h'
        TCONV=TSEC/3600.
    ENDIF
C**CALCULATE OR INITIALIZE VARIOUS QUANTITIES
    DAK=DZ/AZ/XKZ
    DAKT = DAK/TDENOM
    HPD = HZ*PZ*DZ
    QCONV=DTIMEX*TCONV
    IBETAS=IQ(5)
    IBETAF=IQ(6)
    IIM1 = II - 1

```

```

IIM2 = II - 2
DDDTX=DDTX
N=0
IANS=1
TAUT = .0
TAU(1) = .0
IF(ANS(1).GT..0) GO TO 43
DO 41 I=1,30
41   ANS(I) = ANS(I)/TCONV
      ANS(1) = -ANS(1)
43   XXM=1./(DTIMEX*(FLOAT(II-3))**2)
C**Zero q's and Q's; Note: These quantities are stored in array T
      DO 45 I=1,8
45   T(II+I)=0
C**Store Initial Dt*; Store Initial Condition in Array TT; Calculate S*
and H*
      ATIME = DTIMEX
      DO 47 I=1,II
      SX(I)=S(I)*QGENZ*DZ**2/XKZ
      HX(I)=H(I)*XMXSQ
47   TT(I)=T(I)
      T(1)=TT(1)+FUN1(.0)*BCC
      T(II)=TT(II)+FUN2(.0)*BCC
C**DETERMINE NUMBER OF NODES TO BE SUMMARIZED, NPLT, AND
STORE INITIAL
C**CONDITION FOR THIS PURPOSE IN ARRAY YY(500,16)
      NC = 1
      NPLT = 0
      DO 49 I=1,16
      IF(NPLOT(I).GT.0) NPLT = I
      IF(NPLOT(I).LE.0) GO TO 51
49   CONTINUE
51   NPLTS=1
      NPLTF=NPLT
      IF(NPLTF.GT.8)NPLTF=8
      IF(NPLT.EQ.0) GO TO 24
C**Determine if tabulate columns are T's, q's, or Q's and node
numbers
      DO 17 J=1,NPLT
      K = NPLOT(J)
      IF(K.LE.II)THEN
          NTP(J)=-T
          NODET(J)=K

```

```

ELSE
  IF(K.GT.II+4)THEN
    NTP(J)='-'Q'
    NODET(J)=IQ(K-II-4)
  ELSE
    NTP(J)='-'q'
    NODET(J)=IQ(K-II)
  ENDIF
ENDIF
17  YY(1,J) = T(K)
C**START OF SOLUTION OF PROBLEM
C**POINT OF MAJOR LOOP ENTRY -- SN25(N0 NEW DTIMEX),
SN24(NEW DTIMEX)
24  DO 3 I=1,IIM1
    HCX(I)=1./R(I)
3   CX(I)=C(I)/DTIMEX
25  TIME=(TAUT+DTIMEX)*TCONV
    T(1)=TT(1)+FUN1(TIME)*BCC
    T(II)=TT(II)+FUN2(TIME) *BCC
    IF(BETA.EQ..0)GO TO 66
    DO 5 I=IBETAS,IBETAF
5   HCX(I)=(1.+BETA*(T(I+1)+T(I))/2.)/R(I)
C**START OF ELIMINATION
66  GE(2)=-CX(2)-HCX(2)-HCX(1)-HX(2)
    FE(2)=(-CX(2)*T(2)-HX(2)*TA(2) - HCX(1)*T(1) -SX(2))/GE(2)
    DO 7 I=3,IIM1
      DE(I)= HCX(I-1)/GE(I-1)
      GE(I)=(-CX(I)-HCX(I)-HCX(I-1)-HX(I)) -HCX(I-1)*DE(I)
7   FE(I)=(-HX(I)*TA(I)-CX(I)*T(I) -SX(I)-HCX(I-1)*FE(I-1))/GE(I)
    FE(IIM1)=FE(IIM1)-HCX(IIM1)*T(II)/GE(IIM1)
C**BACK SUBSTITUTION
    T(IIM1)=FE(IIM1)
    DO 9 I=IIM2,2,-1
9   T(I)=FE(I) -DE(I+1)*T(I+1)
    TAUT = TAUT +DTIMEX
    N=N+1
C**CALCULATE AND STORE IN T ARRAYS FLOW RATES AND NET
TRANSFERS
    DO 19 I=1,4
      K=II+I
      T(K)=HCX(IQ(I))*(T(IQ(I))-T(IQ(I)+1))/DAK
19  T(K+4)=T(K+4)+T(K)*QCONV

```

```

C**IF N/IX IS AN INTEGER CALCULATE VARIOUS QUANTITIES AND
STORE ITEMS
C**UNLESS NO SUMMARY INFORMATION IS DESIRED, NPLT.EQ.0
    IF((MOD(N,IT).NE.0).OR.(NPLT.EQ.0)) GO TO 13
    NC = NC + 1
    DO 11 J=1,NPLT
    K = NPLOT(J)
11    YY(NC,J) = T(K)
    TAU(NC) = TAUT
C**END OF TIME STEP
C**IF TIMEX=DDDTX DOUBLE TIME INCREMENT
13    IF(TAUT.GE.DDDTX) THEN
        IRET = 1
        DTIMEX = DTIMEX*2.
        DDDTX = 2.*DDDTX
        XXM=XXM/2.
        WRITE(IUOUT,109) TAUT,DTIMEX
109   FORMAT(/' Time increment doubled at t* =',F7.3,'; dt* is now '
&,F7.4)
        GO TO 33
    ELSE
        IRET = 2
    ENDIF
C**IF TAUT.GT.ANS(IANS) PRINT TEMPERATURE DISTRIBUTIONS ETC.
33    IF(TAUT.LT.ANS(IANS)) THEN
        GO TO (24,25),IRET
    ENDIF
    IANS = IANS + 1
    CALL RESULT(TAUT,TIME,XXM,NTP,UTIME,UNITQ,UNITQT,IUOUT)
    IF(ANS(IANS).NE.0) THEN
        GO TO (24,25),IRET
    ENDIF
C**RESET INITIAL CONDITION AND TIME INCREMENT -- READ NEXT
CASE -- SN1
35    DTIMEX = ATIME
    IF(RESET) THEN
        DO 37 I=1,II
37    T(I) = TT(I)
    ENDIF
C**PRINT SUMMARY OF RESULTS
36    IF(NPLT.LE.0) GO TO 1

```

48

WRITE(IUOUT,95)UNITQ,UNITQT,UTIME,(NODET(I),NTP(I),I=NPLTS,NP  
LTF)

95 FORMAT(///4X,'t\*',4X,'t',6X,'Temperature, T, q',A,' or Q',A,'for'  
&,' indicated node or resistor'9X,['',A,''],0X,I4,A2,8(I8,A2))

DO 27 I=1,NC

TIME = TAU(I) \* TCONV

27 WRITE(IUOUT,111) TAU(I),TIME, (YY(I,J),J=NPLTS,NPLTF)

111 FORMAT(F6.3,F7.1,8G10.4)

IF((NPLT.LT.9).OR.(NPLTS.GT.1))GO TO 1

NPLTS=9

NPLTF=NPLT

GO TO 48

END

C

SUBROUTINE DATAIN(NCASE,IUOUT)

LOGICAL SI,SECOND,RESET

CHARACTER\*64 FNAME

PARAMETER (NN=60,IUIN=5)

\$INCLUDE:HT10A\$

C\*\*IF First Case, Files; Write Program Description and Date

IF(NCASE.EQ.1) THEN

WRITE(0,100)

100 FORMAT("// TYPE NAME OF INPUT DATA FILE'//?)

READ(\*,'(A)') FNAME

C Open input file

OPEN(5,FILE=FNAME)

REWIND 5

IF(IUOUT.EQ.2) OPEN(2,FILE='ANS')

CALL WINDTB(20,IDATE,IMONTH,IYEAR,IDAY)

CALL WINDTB(21,IHOUR,IMIN,ISECS)

C\*\*WRITE PROGRAM DESCRIPTION AND DATE

WRITE(IUOUT,102) IMONTH,IDATE,IYEAR,IHOUR,IMIN,ISECS

102 FORMAT('1Heat Transfer Program HT10A',T69,'Date:

',I2,'.',I2,'.',

&I4/' Version: 21 OCTOBER 1989',T69,'Time: ',I2,'.',I2,'.',I2/

&' Standard Implicit Algorithm'/' Programmed by A.M.Clausing'/)

ENDIF

C\*\*Read and Write Input Data

READ(IUIN,\*,END=999) RESET,SECOND,SI

READ(IUIN,\*)CPZ,RHOZ,XKZ,BETA

READ(IUIN,\*)AZ,DZ,PZ

READ(IUIN,\*)QGENZ,HZ,BCC

```

READ(IUIN,*)II,IT,IX,DTIMEX,DDTX,TNUM,TDENOM
READ(IUIN,*)ANS,IQ,NPLOT
    READ(IUIN,*) (T(I),I=1,II),(S(I),I=1,II)
    READ(IUIN,*) (C(I),I=1,II),(R(I),I=1,II)
    READ(IUIN,*) (H(I),I=1,II),(TA(I),I=1,II)
DDTX2=DDTX*2
XMXSQ =HZ*PZ*DZ**2/(XKZ*AZ)
XMX=XMXSQ**.5
    IF(NCASE.GT.1) WRITE(IUOUT,'(1H1)')
    WRITE(IUOUT,104)NCASE,II,DTIMEX,DDTX,DDTX2
104  FORMAT(' CASE NUMBER',I2,T28,'INPUT DATA -- ',I2,
NODES'//
    &' Dimensionless time increment,',F7.4,', is doubled at t*'s of:'
    &,F6.3,',',F6.3,' ...')
    IF(HZ.NE..0) WRITE(IUOUT,106) XMX
106  FORMAT(' Fin Parameter: SQRT(HZ*PZ*DZ**2/(XKZ*AZ)) =',F6.3)
    IF(SI) THEN
    WRITE(IUOUT,108)DZ,QGENZ,AZ,RHOZ,PZ,CPZ,HZ,XKZ,BETA
108  FORMAT(' REFERENCE VALUES:/'
    &' Length, DZ [m]:',G11.3,T44,'Source, QGENZ [W/m3]:',G15.3/
    &' Area, AZ [m2]:',G12.3,T44,'Density, RHOZ [kg/m3]:',G14.3/
    &' Perimeter, PZ[m]:',G9.3,T44,'Specific Heat, CPZ[J/kg-K]:',G9.3/
    &/' Heat Transfer Coefficient, HZ [W/m2-K]:',F6.1/
    &' Thermal Conductivity [W/m-K]: k =',F8.3,'(1 + ',G9.3,'T)')
    ELSE
    WRITE(IUOUT,101)DZ,QGENZ,AZ,RHOZ,PZ,CPZ,HZ,XKZ,BETA
101  FORMAT(' REFERENCE VALUES:/'
    &' Length, DZ [ft]:',G12.3,T44,'Source, QGENZ [BTU/ft3]:',G15.3/
    &' Area, AZ [ft2]:',G13.3,T44,'Density, RHOZ [lbm/ft3]:',G14.3/
    &' Perimeter, PZ [ft]:',G9.3,T44,'Specific Heat, CPZ[BTU/lbm-F]:',
    &G9.3/ /' Heat Transfer Coefficient, HZ [BTU/h-ft2-F]:',F6.1/
    &' Thermal Conductivity [BTU/ft-F]: k=',F7.3,'(1 + ',G9.3,'T)')
    ENDIF
    IF(BETA.NE..0)WRITE(IUOUT,103) IQ(5),IQ(6)
103  FORMAT(' Variable conductivity starts with R(',I2,') and ends '
    &'with R(',I2,')')
    WRITE(IUOUT,105)
105  FORMAT(// THE NETWORK RESISTORS, CAPACITORS,
CONDUCTANCES,'
    &'POTENTIALS, AND SOURCES ARE://3X,T,8X,'R(I)',10X,
    &'C(I)',10X,'H(I)',9X,'TA(I)',10X,'T(I)',10X,'S(I)')
    WRITE(IUOUT,107)(I,R(I),C(I),H(I),TA(I),T(I),S(I), I=1,II,IX)
107  FORMAT(I4,1P6E14.3)

```

```

      RETURN
999  WRITE(IUOUT,199)
199  FORMAT(// ALL INPUT DATA HAS BEEN PROCESSED'//)
      STOP
      END
C
      SUBROUTINE
RESULT(TAUT,TIME,XXM,NTP,UTIME,UNITQ,UNITQT,IUOUT)
      LOGICAL SI,SECOND,RESET
      CHARACTER UTIME,UNITQ*7,UNITQT*9,NTP(16)*2
      PARAMETER (NN=60,IUIN=5)
      DIMENSION TX(NN),Q(NN),QX(NN),QC(NN),QCX(NN),QS(NN),QSX(NN)
$INCLUDE:HT10A$
      WRITE(IUOUT,101)
TAUT,UNITQ,UTIME,TIME,UNITQT,DTIMEX,XXM
101  FORMAT (// RESULTS AT:',T50,'UNITS OF RESULTS:'/T10,
      &'Dimensionless Time, t* =',F9.3,T55,'q, qc, and qs -- ',A/T14,
      &'Real Time, t [',A,'] =',F9.3,T55,' Q -- ',A/T2,
      &'CURRENT VALUES OF:'/T13,'Time Increment, dt* =',F9.4/T30,
      &'M =',F9.3)
      WRITE(IUOUT,103) (IQ(I),I=1,4)
103  FORMAT(/32X,4I12)
      WRITE(IUOUT,105) UNITQT, (T(II+I),I=5,8)
105  FORMAT(' THE TOTAL HEAT FLOWS, Q, IN ',A,T39,1P4G12.4)
C**Determine if two tables are to be printed including Indices
      ISTART=1
      IEND=II
      IF((II-1)/IX+1.GT.9) IEND=9*IX
1     WRITE(IUOUT,107) (I,I=ISTART,IEND,IX)
107  FORMAT(' NODE:',(I6,10I9))
      WRITE(IUOUT,109) (T(I),I=ISTART,IEND,IX)
109  FORMAT(' T :',(11F9.1))
C**Calculate and print the dimensionless temperatures if T*.NE.T
      IF((TNUM.EQ..0).AND.(TDENOM.EQ.1.)) GO TO 11
      DO 3 I=1,II
3     TX(I) = (T(I) - TNUM)/TDENOM
      WRITE(IUOUT,111) (TX(I),I=ISTART,IEND,IX)
111  FORMAT(' T*:',(11F9.3))
C**CALCULATE AND PRINT HEAT FLOW RATES -- q AND q*
11    DO 5 I=1,IIM1
      Q(I) = HCX(I)/DAK*(T(I) - T(I+1))
5     QX(I) = Q(I)*DAKT
      Q(II) = .0

```

```

QX(II) = .0
WRITE(IUOUT,113) (Q(I),I=ISTART,IEND,IX)
113  FORMAT(' q :(,1P11E9.2))
      WRITE(IUOUT,115) (QX(I),I=ISTART,IEND,IX)
115  FORMAT(' q*:(,11F9.3))
C**If HZ is not Zero, Calculate and Print qc and qc*
      IF(HZ.NE..0) THEN
          QC(II) = .0
          QCX(II) = .0
          QC(1) = .0
          DO 7 I=2,IIM1
              QC(I) = H(I)*HPD*(T(I) - TA(I))
              QC(1) = QC(1) + QC(I)
7           QCX(I) = QC(I)*DAKT
              QCX(1) = QC(1)*DAKT
              WRITE(IUOUT,117) (QC(I),I=ISTART,IEND,IX)
117     FORMAT(' qc :(,1P11E9.2))
              WRITE(IUOUT,119) (QCX(I),I=ISTART,IEND,IX)
119     FORMAT(' qc*:(,11F9.3))
      ENDIF
C**If QGENZ is not Zero, Calculate and Print qs and qs*
      IF(QGENZ.NE..0) THEN
          QS(II) = .0
          QSX(II) = .0
          QS(1) = .0
          DO 9 I=2,IIM1
              QS(I) = SX(I)/DAK
              QS(1) = QS(1) + QS(I)
9           QSX(I) = QS(I)*DAKT
              QSX(1) = QS(1)*DAKT
              WRITE(IUOUT,121) (QS(I),I=ISTART,IEND,IX)
121     FORMAT(' qs :(,1P11E9.2))
              WRITE(IUOUT,123) (QSX(I),I=ISTART,IEND,IX)
123     FORMAT(' qs*:(,11F9.3))
      ENDIF
      IF(((II-1)/IX+1.LE.9).OR.(IEND.EQ.II)) RETURN
      ISTART=9*IX+1
      IEND=II
      GOTO 1
      END
C
      BLOCK DATA
C**INITIALIZATION OF LABELED COMMON TO DEFAULT VALUES

```

**LOGICAL SI,SECOND,RESET**  
**PARAMETER (NN=60,IUIN=5)**  
**\$INCLUDE:HT10A\$**  
**DATA R,C,H,T,S,TA/NN\*.1,NN\*.1,NN\*.0,NN\*.0,NN\*.0/II,DZ,**  
**&AZ,PZ,HZ,QGENZ,RHOZ,XKZ,BETA,CPZ,DTIMEX,DDTX/10,3\*1.,.0,0,**  
**&2700.,200.,.0,890.,.005,.25/IQ,IX,IT,TDENOM,TNUM,ANS,NPLOT,BCC/**  
**&1,2,3,4,1,2,1,3,1.,.0,.2,.4,1.,2.,26\*.0,16\*0,.0/SI,SECOND,**  
**&RESET/.TRUE.,.TRUE.,.TRUE./**  
**END**

## Appendix D: Reduced Data Summary Tables

The following tables summarize all reduced test runs used in this thesis. A subroutine was written to output this information to a text file, and the results are presented in Tables D.1-33. Values are presented for convective heat transfer coefficients (HTC's), average wall temperatures, Rayleigh and Nusselt numbers, and relative humidity of the test conditions. Both cold and hot runs are presented.

### No-shelf data:

Table D.1. Reduced Data from Run 2-No Shelf

Test #	2			
	Left Wall	Right Wall	Rear Wall	Floor
Avg. HTC's (W/m <sup>2</sup> -K)	5.36742	5.52036	5.24007	3.86824
Avg. Temps (K)	275.318	274.336	275.51	274.954
Ra	5.39444e+8	5.61453e+8	5.35144e+8	5.47619e+8
Nu	126.236	129.833	123.241	90.9767
Relative Hum.=	.7			

Table D.2. Reduced Data from Run 3-No Shelf

Test #	3			
	Left Wall	Right Wall	Rear Wall	Floor
Avg. HTC's (W/m <sup>2</sup> -K)	4.58268	4.7575	4.68901	3.08719
Avg. Temps (K)	272.218	271.272	272.303	272.449
Ra	5.37248e+8	5.60012e+8	5.35201e+8	5.31704e+8
Nu	109.262	113.431	111.798	73.6064
Relative Hum.=	.7			

**Table D.3. Reduced Data from Run 4-No Shelf**

<b>Test #</b>	<b>4</b>	<b>Left Wall</b>	<b>Right Wall</b>	<b>Rear Wall</b>	<b>Floor</b>
Avg. HTC's (W/m <sup>2</sup> -K)	4.79905	4.18444	4.54423	2.81056	
Avg. Temps (K)	285.413	285.29	284.726	285.643	
Ra	2.33363e+8	2.36244e+8	2.49486e+8	2.27961e+8	
Nu	113.889	99.3038	107.842	66.6993	
Relative Hum.=	.7				

**Table D.4. Reduced Data from Run 5-No Shelf**

<b>Test #</b>	<b>5</b>	<b>Left Wall</b>	<b>Right Wall</b>	<b>Rear Wall</b>	<b>Floor</b>
Avg. HTC's (W/m <sup>2</sup> -K)	4.49438	4.09267	3.83803	1.98999	
Avg. Temps (K)	279.164	278.39	278.868	279.972	
Ra	4.74489e+8	4.91442e+8	4.80964e+8	4.56822e+8	
Nu	105.214	95.81	89.8489	46.586	
Relative Hum.=	.7				

**Table D.5. Reduced Data from Run 6-No Shelf**

<b>Test #</b>	<b>6</b>	<b>Left Wall</b>	<b>Right Wall</b>	<b>Rear Wall</b>	<b>Floor</b>
Avg. HTC's (W/m <sup>2</sup> -K)	4.70183	5.12786	4.83976	3.03487	
Avg. Temps (K)	272.461	271.649	272.557	272.761	
Ra	5.73318e+8	5.92133e+8	5.71099e+8	5.66392e+8	
Nu	111.283	121.367	114.548	71.8296	

Relative Hum.= .7

Table D.6. Reduced Data from Run 7-No Shelf

Test #	7	Left Wall	Right Wall	Rear Wall	Floor
Avg. HTC's (W/m <sup>2</sup> -K)		5.02518	5.21222	4.90093	2.97807
Avg. Temps (K)		272.972	272.262	273.142	273.401
Ra		5.50563e+8	5.67155e+8	5.46582e+8	5.40522e+8
Nu		119.159	123.594	116.212	70.617

Relative Hum.= .7

Table D.7. Reduced Data from Run 8-No Shelf

Test #	8	Left Wall	Right Wall	Rear Wall	Floor
Avg. HTC's (W/m <sup>2</sup> -K)		4.76966	5.12445	4.69292	3.3323
Avg. Temps (K)		274.846	273.726	274.684	275.646
Ra		5.07259e+8	5.333e+8	5.11036e+8	4.88653e+8
Nu		112.974	121.378	111.156	78.9289

Relative Hum.= .65

Table D.8. Reduced Data from Run 9-No Shelf

Test #	9	Left Wall	Right Wall	Rear Wall	Floor
Avg. HTC's (W/m <sup>2</sup> -K)		4.96048	5.36988	4.95106	3.10952
Avg. Temps (K)		277.545	276.7	277.322	277.631
Ra		4.48975e+8	4.68542e+8	4.54153e+8	4.46999e+8
Nu		117.406	127.096	117.183	73.5971

Relative Hum.= .7

Table D.9. Reduced Data from Run 17-No Shelf-Hot

Test #	17			
	Left Wall	Right Wall	Rear Wall	Floor
Avg. HTC's (W/m <sup>2</sup> -K)	5.40492	5.86001	5.50052	5.50724
Avg. Temps (K)	319.211	318.567	319.156	312.354
Ra	5.02546e+8	4.87951e+8	5.01309e+8	3.46996e+8
Nu	127.418	138.147	129.672	129.831

Relative Hum.= 0

Table D.10. Reduced Data from Run 18-No Shelf-Hot

Test #	18			
	Left Wall	Right Wall	Rear Wall	Floor
Avg. HTC's (W/m <sup>2</sup> -K)	4.95681	5.12153	5.07562	5.39267
Avg. Temps (K)	316.722	316.769	317.086	313.776
Ra	5.93754e+7	5.86375e+7	5.3613e+7	1.06041e+8
Nu	109.028	112.651	111.641	118.615

Relative Hum.= 0

Table D.11. Reduced Data from Run 19-No Shelf

Test #	19			
	Left Wall	Right Wall	Rear Wall	Floor
Avg. HTC's (W/m <sup>2</sup> -K)	5.16154	5.38607	5.34829	3.23035
Avg. Temps (K)	278.079	276.643	275.863	276.951
Ra	4.27418e+8	4.60917e+8	4.79112e+8	4.53736e+8
Nu	122.331	127.652	126.757	76.5608

Relative Hum.= .7

Table D.12. Reduced Data from Run 20-No Shelf

Test #	20			
	Left Wall	Right Wall	Rear Wall	Floor
Avg. HTC's (W/m <sup>2</sup> -K)	4.17677	4.48936	5.11627	3.49888
Avg. Temps (K)	281.849	281.039	279.285	281.962
Ra	3.01199e+8	3.20526e+8	3.62408e+8	2.98496e+8
Nu	99.4401	106.882	121.808	83.3008

Relative Hum.= .7

Table D.13. Reduced Data from Run 21-No Shelf

Test #	21			
	Left Wall	Right Wall	Rear Wall	Floor
Avg. HTC's (W/m <sup>2</sup> -K)	4.83698	5.08368	5.3825	2.98819
Avg. Temps (K)	282.265	281.357	278.887	281.663
Ra	3.10341e+8	3.31721e+8	3.89828e+8	3.24502e+8
Nu	114.834	120.691	127.785	70.942

Relative Hum.= .7

Table D.14. Reduced Data from Run 22-No Shelf

Test #	22			
	Left Wall	Right Wall	Rear Wall	Floor
Avg. HTC's (W/m <sup>2</sup> -K)	4.4849	4.63535	5.42058	2.82578
Avg. Temps (K)	280.741	279.563	277.453	280.68
Ra	3.28704e+8	3.56844e+8	4.07273e+8	3.30169e+8
Nu	106.792	110.374	129.071	67.2856

Relative Hum.= .7

Table D.15. Reduced Data from Run 23-No Shelf

Test #	23			
	Left Wall	Right Wall	Rear Wall	Floor
Avg. HTC's (W/m <sup>2</sup> -K)	5.8105	5.96258	5.64283	3.24988
Avg. Temps (K)	271.398	270.395	270.996	270.875
Ra	5.73893e+8	5.97686e+8	5.83421e+8	5.86289e+8
Nu	138.146	141.762	134.16	77.2669

Relative Hum.= .7

Table D.16. Reduced Data from Run 24-No Shelf

Test #	24			
	Left Wall	Right Wall	Rear Wall	Floor
Avg. HTC's (W/m <sup>2</sup> -K)	5.48496	5.5825	5.54486	2.96356
Avg. Temps (K)	277.352	276.273	275.474	277.265
Ra	4.33318e+8	4.58742e+8	4.77559e+8	4.35379e+8
Nu	130.246	132.562	131.668	70.3727

Relative Hum.= .7

Table D.17. Reduced Data from Run 25-No Shelf

Test #	25			
	Left Wall	Right Wall	Rear Wall	Floor
Avg. HTC's (W/m <sup>2</sup> -K)	4.68061	4.90872	4.72901	2.97641
Avg. Temps (K)	277.511	276.412	275.645	277.742
Ra	3.90227e+8	4.16938e+8	4.35556e+8	3.84624e+8
Nu	111.812	117.261	112.968	71.1016

Relative Hum.= .7

Table D.18. Reduced Data from Run 26-No Shelf

Test #	26			
	Left Wall	Right Wall	Rear Wall	Floor
Avg. HTC's (W/m <sup>2</sup> -K)	4.81384	5.23762	5.25683	3.14771
Avg. Temps (K)	278.238	277.121	276.416	278.424
Ra	3.80896e+8	4.07835e+8	4.24833e+8	3.76408e+8
Nu	114.836	124.946	125.404	75.0899

Relative Hum.= .7

Table D.19. Reduced Data from Run 27-No Shelf

Test #	27			
	Left Wall	Right Wall	Rear Wall	Floor
Avg. HTC's (W/m <sup>2</sup> -K)	5.20968	5.2492	5.45622	3.35349
Avg. Temps (K)	276.946	275.809	274.581	277.123
Ra	4.43507e+8	4.6983e+8	4.98274e+8	4.3941e+8
Nu	123.308	124.244	129.144	79.3742

Relative Hum.= .42

Table D.20. Reduced Data from Run 30-No Shelf

Test #	30			
	Left Wall	Right Wall	Rear Wall	Floor
Avg. HTC's (W/m <sup>2</sup> -K)	4.43235	4.19054	3.77561	3.03733
Avg. Temps (K)	284.069	284.126	284.13	284.314
Ra	2.70661e+8	2.69324e+8	2.69248e+8	2.64965e+8
Nu	104.959	99.233	89.4073	71.9247

Relative Hum.= .53

Table D.21. Reduced Data from New Run 1-No Shelf

Test #	1	Left Wall	Right Wall	Rear Wall	Floor
Avg. HTC's (W/m <sup>2</sup> -K)	5.10816	4.83389	5.52277	3.69549	
Avg. Temps (K)	279.414	278.182	276.447	279.619	
Ra	3.69667e+8	3.9846e+8	4.39051e+8	3.64875e+8	
Nu	121.129	114.625	130.961	87.6305	

Relative Hum.= .4

Table D.22. Reduced Data from New Run 2-No Shelf

Test #	2	Left Wall	Right Wall	Rear Wall	Floor
Avg. HTC's (W/m <sup>2</sup> -K)	5.65495	5.49211	5.69696	2.88054	
Avg. Temps (K)	277.221	276.402	274.682	277.181	
Ra	4.14719e+8	4.33915e+8	4.74243e+8	4.15641e+8	
Nu	134.163	130.3	135.16	68.3405	

Relative Hum.= .3

Table D.23. Reduced Data from New Run 3-No Shelf

Test #	3	Left Wall	Right Wall	Rear Wall	Floor
Avg. HTC's (W/m <sup>2</sup> -K)	5.71743	5.54262	5.00626	3.15936	
Avg. Temps (K)	277.887	277.022	275.312	277.878	
Ra	4.02738e+8	4.23002e+8	4.6305e+8	4.02955e+8	
Nu	135.62	131.474	118.751	74.9415	

Relative Hum.= .35

Table D.24. Reduced Data from New Run 4-No Shelf

Test #	4	Left Wall	Right Wall	Rear Wall	Floor
Avg. HTC's (W/m <sup>2</sup> -K)	5.16881	5.66293	5.13493	3.74031	
Avg. Temps (K)	276.777	276.227	277.684	277.124	
Ra	4.13685e+8	4.26735e+8	3.92156e+8	4.0544e+8	
Nu	122.911	134.661	122.106	88.9423	
Relative Hum.=	.32				

Table D.25. Reduced Data from New Run 5-No Shelf

Test #	5	Left Wall	Right Wall	Rear Wall	Floor
Avg. HTC's (W/m <sup>2</sup> -K)	5.09591	5.07782	4.83955	3.97116	
Avg. Temps (K)	277.111	276.502	277.996	277.307	
Ra	4.15056e+8	4.29397e+8	3.94191e+8	4.10441e+8	
Nu	121.02	120.59	114.931	94.3084	
Relative Hum.=	.35				

**1-shelf data:**

Table D.26. Reduced Data from Shelf Run 1

Test #	1	Left Wall	Right Wall	Rear Wall	Floor
Avg. HTC's (W/m <sup>2</sup> -K)	3.77408	3.49867	3.20795	2.03073	
Avg. Temps (K)	280.677	280.221	281.709	280.319	
Ra	4.22525e+7	4.35008e+7	3.94212e+7	4.32334e+7	
Nu	43.8907	40.6879	37.3069	23.6164	

Relative Hum.= .4

Table D.27. Reduced Data from Shelf Run 2

Test #

2

	Left Wall	Right Wall	Rear Wall	Floor
Avg. HTC's (W/m <sup>2</sup> -K)	2.92732	3.11573	2.56833	.967393
Avg. Temps (K)	277.182	276.632	277.942	276.55
Ra	5.27877e+7	5.42953e+7	5.07091e+7	5.45193e+7
Nu	34.0311	36.2215	29.8578	11.2463

Relative Hum.= .4

Table D.28. Reduced Data from Shelf Run 3

Test #

3

	Left Wall	Right Wall	Rear Wall	Floor
Avg. HTC's (W/m <sup>2</sup> -K)	4.19028	4.53284	3.89363	1.67343
Avg. Temps (K)	278.422	278.072	279.168	277.549
Ra	4.54687e+7	4.64485e+7	4.33848e+7	4.79105e+7
Nu	48.9129	52.9115	45.4501	19.5338

Relative Hum.= .3

Table D.29. Reduced Data from Shelf Run 4

Test #

4

	Left Wall	Right Wall	Rear Wall	Floor
Avg. HTC's (W/m <sup>2</sup> -K)	5.01696	4.82408	4.6071	2.43734
Avg. Temps (K)	279.362	279.03	280.004	278.251
Ra	4.20564e+7	4.29879e+7	4.02549e+7	4.51743e+7
Nu	58.6087	56.3555	53.8208	28.4733

Relative Hum.= .3

Table D.30. Reduced Data from Shelf Run 5

Test #	5	Left Wall	Right Wall	Rear Wall	Floor
Avg. HTC's (W/m <sup>2</sup> -K)	4.37493	4.78953	3.8312	1.81613	
Avg. Temps (K)	277.679	277.309	278.825	277.339	
Ra	4.78898e+7	4.89227e+7	4.46927e+7	4.884e+7	
Nu	51.053	55.8912	44.708	21.1933	

Relative Hum.= .3

Table D.31. Reduced Data from Shelf Run 6

Test #	6	Left Wall	Right Wall	Rear Wall	Floor
Avg. HTC's (W/m <sup>2</sup> -K)	4.01239	4.18513	3.77413	1.63642	
Avg. Temps (K)	276.913	276.458	277.913	276.31	
Ra	4.86823e+7	4.99669e+7	4.58591e+7	5.03844e+7	
Nu	46.9215	48.9416	44.1353	19.1366	

Relative Hum.= .3

Table D.32. Reduced Data from Shelf Run 7

Test #	7	Left Wall	Right Wall	Rear Wall	Floor
Avg. HTC's (W/m <sup>2</sup> -K)	4.1929	4.12603	4.06052	2.07529	
Avg. Temps (K)	278.053	277.655	278.754	277.14	
Ra	4.62907e+7	4.74055e+7	4.43279e+7	4.88483e+7	
Nu	48.9633	48.1824	47.4174	24.2346	

Relative Hum.= .3

Table D.33. Reduced Data for Shelf Unit: All Runs

Shelf data

Test #	Avg. HTC	Nu	Ra
1	2.96428	34.4732	4.62134e+7
2	2.42065	28.1409	5.79708e+7
3	3.88851	45.3904	5.07656e+7
4	4.11140	48.0298	4.74722e+7
5	3.78756	44.1987	5.26642e+7
6	3.26330	38.1616	5.38460e+7
7	2.96551	34.6303	5.16174e+7